BNWL-1524
UC-80

Battelle
Pacific Northwest Laboratories
Richland, Washington 99352

AEC Research and Development Report

COOLANT BLOWDOWN STUDIES OF A REACTOR SIMULATOR VESSEL CONTAINING A SIMULATED REACTOR CORE

R.T. ALLEMANN, J.C. GUSTAFSON,
A.S. NEULS, W.C. TOWNSEND,
N.P. WILBURN, M.E. WITHERSPOON

June 1971

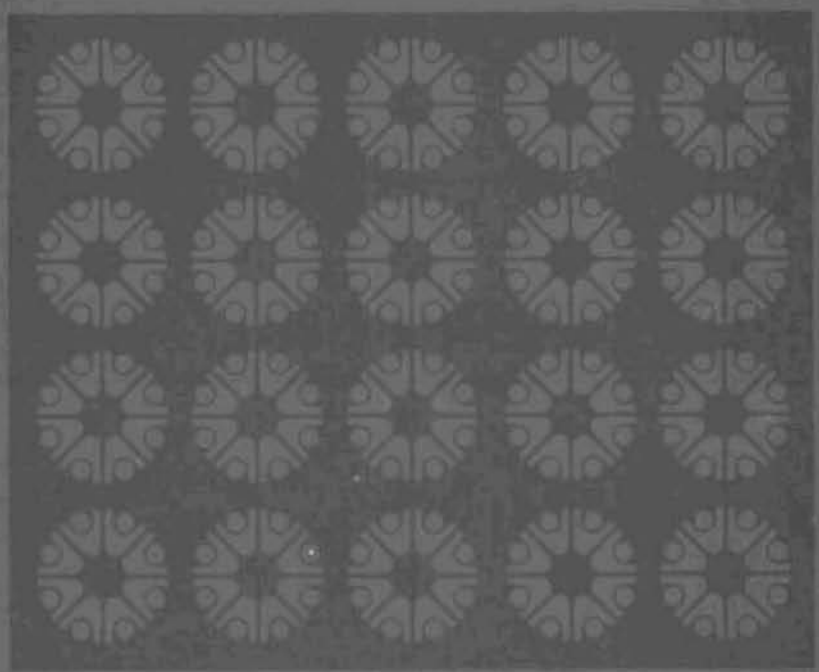

BNWL-1524

PACIFIC NORTHWEST LABORATORY
operated by
BATTELLE MEMORIAL INSTITUTE
for the
U. S. ATOMIC ENERGY COMMISSION
Under Contract AT(45-1) 1830

BNWL-1524

UC-80, Reactor
Technology

COOLANT BLOWDOWN STUDIES OF A REACTOR SIMULATOR VESSEL CONTAINING A SIMULATED REACTOR CORE

by

R. T. Allemann
J. C. Gustafson
A. S. Neuls
W. C. Townsend
N. P. Wilburn
M. E. Witherspoon

June 1971

BATTELLE
PACIFIC NORTHWEST LABORATORIES
RICHLAND, WASHINGTON 99352

Printed in the United States of America
Available from
National Technical Information Service
National Bureau of Standards, U.S. Department of Commerce
Springfield, Virginia 22151
Price: Printed Copy $3.00; Microfiche $0.95

COOLANT BLOWDOWN STUDIES OF A REACTOR SIMULATOR VESSEL CONTAINING A SIMULATED REACTOR CORE

R. T. Allemann
J. C. Gustafson
A. S. Neuls
W. C. Townsend
N. P. Wilburn
M. E. Witherspoon

ABSTRACT

Blowdown experiments were made with a 150 ft^3 vessel containing a simulated reactor core consisting of 4' long tubes. High pressure water (up to 2100 psi, 500 °F) was exhausted suddenly from the annular zone of the vessel through orifices of 1.69, 3.44, and 5.2" diameter. Temperature, pressure liquid level, pressure differential, and core movement were measured during the transient fluid flow period and much of the data is given. The forces measured during subcooled decompression were less than predicted, liquid remaining was less than after blowdown without a core structure although pressure histories were about the same. Development of a differential-pressure transducer is described.

CONTENTS

LIST OF FIGURES

LIST OF TABLES

COOLANT BLOWDOWN STUDIES OF A REACTOR SIMULATOR VESSEL CONTAINING A SIMULATED REACTOR CORE

PURPOSE AND SCOPE

This report describes the experiments made as part of the water reactor safety program to study loss-of-coolant accidents. The overall objective of these experiments was to obtain data from blowdown tests using a large reactor-simulator vessel and to make comparisons with the results of analytical prediction methods. The results are given for blowdown experiments which were made using different initial water conditions and different size blowdown orifices in the exit pipe section attached to the annulus region of the simulated reactor. These tests continued those made with the same vessel with no internal parts, which were reported in BNWL-1411 and BNWL-1470, and with a sieve plate which were reported in BNWL-1463. This report discusses the experimental layout and the main conclusions which resulted from a partial reduction of the data. Data are presented in the discussion and in the Appendix.

CONTAINMENT SYSTEM EXPERIMENT

The containment system experiment (CSE) at Battelle-Northwest was a large scale program to evaluate the effectiveness of containment vessels and other engineered safeguard systems in reducing the release of radioactive fission products resulting from a serious accident in a nuclear electric power plant. The main objective of the CSE program was to obtain experimental information for use in testing calculational models and for developing improved models. The following specific program objectives were identified as a basis for development of engineering tests and related research and development, and this report is concerned with work pertaining to the last objective on this list.

1) Determination of the effect of natural processes, such as agglomeration and settling, diffusional deposition, and condensation of water vapor, on reduction of airborne fission product concentration

in containment systems; and application of experimental data to the evaluation of available analytical models.

2) Determination of the effectiveness of both active and passive engineered safeguard systems in reducing fission product concentration in the containment atmosphere. Active safeguard systems employ water sprays and air filtration methods, whereas a passive system might achieve pressure suppression by means of a containment water pool. Measured values were compared with those calculated from analytical models.
3) Evaluation of the effectiveness of different methods of pressure reduction in containment vessels. Methods include water pool pressure suppression, cooling the contained atmosphere, and heat transfer to low temperature materials inside containment and through the containment membrane to the atmosphere.
4) Determination of the amount of leakage of fission product activity from containment under a range of postaccident conditions and comparison of these values with those calculated from both low and high temperature air leakage rate tests and fission product concentration in the containment vessel.
5) Determination of (both inside and outside a reactor vessel) the transient and dynamic pressures, temperatures, stresses, coolant flow rates, and hydraulic forces resulting from the sudden rupture of a high temperature water system. Measured values were compared with those calculated from analytical models.

The results furnish a better technical basis for reactor site evaluation and for those aspects of reactor plant design affecting public safety.

The results of Tasks 1, 2 & 4 are reported elsewhere. Task 3 was not undertaken as the result of early termination of the program.

Blowdown Program

Background

The blowdown program is designed around a vessel built to simulate

a water-moderated reactor inside the CSE containment vessel. Originally, only a small amount of blowdown transient experimental work was proposed for CSE, primarily because of the interference between aerosol and blowdown transient tests inside the containment vessels, along with space limitations and resulting low test frequency. To increase both the frequency of tests and extent of data gathered, a special test stand for the simulator vessel was built close to the containment vessel so that common facilities, personnel, and power could be used.

The reactor simulator vessel tests outside containment have provided both a better environment for the experimental instrumentation and greatly improved access to the vessel and its instrumentation for repair of sensors and for experimental modifications. In addition, there has been an increased interest in the acquisition of large scale experimental data which would permit the testing of analytical techniques intended to provide detailed and sophisticated analyses of both the thermal and mechanical or structural effects on the reactor vessel internals during the blowdown transient. Aspects of particular interest include mechanical damage to the core or to the emergency cooling system which might adversely affect or prevent adequate functioning of this emergency cooling system in the event of a major loss-of-coolant accident.

Problem Areas

The two principal problem areas to be investigated consisted of the mechanical and structural aspects and the thermal aspects. The mechanical and structural aspects primarily include the hydraulic resistance effects of the core structure and of the typical reactor vessel internal parts, such as thermal shields, core barrels, and flow baffles, on the discharge rate of coolant during the blowdown transient. Forces resulting from sudden coolant system rupture must be known in order to evaluate the tendency to dislodge or deform reactor vessel internals. Such relative movements between parts may compound the effects of the coolant loss. Deformation, for example, by preventing control rod entry or by causing movement of fuel elements relative to the rods, might produce a reactivity excursion. Motion of core internals could block the normal or emergency coolant

paths, damage the emergency cooling system, or so change the core geometry as to impair the required effectiveness of the emergency cooling.

Forces of interest arise during the first few hundred milliseconds of the transient because of the passage and reflection of acoustic waves into the interior of the reactor vessel from the point of coolant system rupture. These waves relieve fluid compression until flashing begins. Longer term forces result from the friction forces accompanying rapid coolant outflow. Also, temperature differences between hot and cold portions of the coolant system create differences in saturation pressure of these water volumes when the subcooled blowdown is complete. With a break in one portion of the system, this difference may lead to an oscillation of flow and of flashing brought on by the saturation-pressure difference between the volumes. This postulated oscillation could continue until fluid and mechanical damping cause it to die out. All of the forces discussed herein have the potential for developing lateral loads as well as the symmetrical loads usually calculated with a one-dimensional treatment. The physical processes such as bubble and void formation, heat transfer, and liquid level swell occurring in the reactor vessel when the pressure is suddenly relieved have a bearing on the design of the reactor safeguards and of the reactor itself.

There are important effects external to the reactor, which include, for example, forces from the impact of the fluid jet, vessel reaction forces, and whiplash of piping between the reactor vessel and the point of the coolant system rupture.

Data needed for evaluating all of these effects can be obtained during blowdown transient tests through the use of a series of unheated dummy cores. The initial tests performed prior to those herein reported were conducted without dummy core parts or with a simple core plate in order to check blowdown theories against simple tests and/or to provide a check of the test instrumentation and data processing methods being developed.

Purpose of CSE Blowdown Tests

CSE blowdown tests were conducted to:

- Provide data with which to design models and to check modeling assumptions and calculations so that these can be applied to full scale reactor plants. The blowdown results are used as input to design calculations for stress, heat transfer, fission product distribution, emergency core cooling, and engineered safeguards.
- Perform blowdown tests at large enough scale to measure liquid level, void fraction, and thrust forces, and to observe effects of bubble formation and rise and the effects of geometry upon a full size reactor.
- Provide actual blowdown results for use in empirical formulations of blowdown rates and, in particular, to accurately predict blowdown times expected in the CSE containment vessel-reactor simulator, combined tests.
- Contribute to the knowledge of two-phase critical flow, liquid-vapor action, and thermal hydraulic effects in a water-cooled reactor and thus increase safety and reduce the expense of engineering, construction, and licensing.

Perhaps this knowledge will eventually allow the codification of rules to cover safety aspects of the loss-of-coolant accient. Until that time, detailed calculations must be made for each case, and confidence in the calculation methods can only come through comparisons with experiments.

SUMMARY AND CONCLUSIONS

Six blowdown tests modeling a loss-of-coolant accident of a nuclear power reactor were made with a 150 ft^3 vessel 17 feet tall containing a core barrel and a 4 feet long simulated core. The blowdowns were made from a nozzle connected to the annular region outside the core barrel at a level above the core. Breaking of a double rupture disk on the nozzle simulated an inlet break of a pressurized water reactor. Two tests were made with cold pressurized water, one with a steam dome as is present in a boiling water reactor and three with hot (500 °F) pressurized water (1000 - 2080 psig). Square edge orifices were used to establish break sizes from 1.5 to 5.18 inches diameter. Data were taken on pressure,

temperature, liquid level, pressure differential, liquid remaining, weight of water, strain on core support bolts and nozzle thrust. Some comparisons were made with previous runs of simpler geometry and with analytical predictions. The results show that,

- The presence of the core and annulus showed little effect on the pressure histories during the saturated portion of blowdown when compared to similar blowdown with a sieve plate.
- The transient liquid level in the core region during blowdown was lower than during similar blowdowns without the core and annulus. This results from the generally downward core flow in these tests indicating the importance of properly assessing flow direction in LOCA calculations of core heat-up.
- The liquid remaining in the vessel after blowdown was less than with similar blowdowns without cores.
- The subcooled decompression history pattern was approximated by calculations with a one-dimensional code but the magnitudes of measured pressure oscillations and forces were less than predicted.

EXPERIMENTAL FACILITY AND EQUIPMENT

CSE BLOWDOWN FACILITY

Description

The full description of the CSE facility is contained in Reference 1. The CSE reactor simulator vessel (Figure 1) was fabricated and accepted in accordance with Section III of the ASME Pressure Vessel and Boiler Code. Design temperature and pressure is 650 °F and 2750 psig, respectively, and volume is 150 ft^3.

The reactor simulator vessel was mounted within a supporting frame (Figure 2). The weight of the vessel and simulator support frame were suspended from a vertical load cell. Thrust forces generated during the blowdown experiment were restrained by a thrust support system which include upper and lower thrust support members and load cells.

A simulated core was installed in the vessel. This core was built to be attached to a perforated core plate which was used for earlier experi-

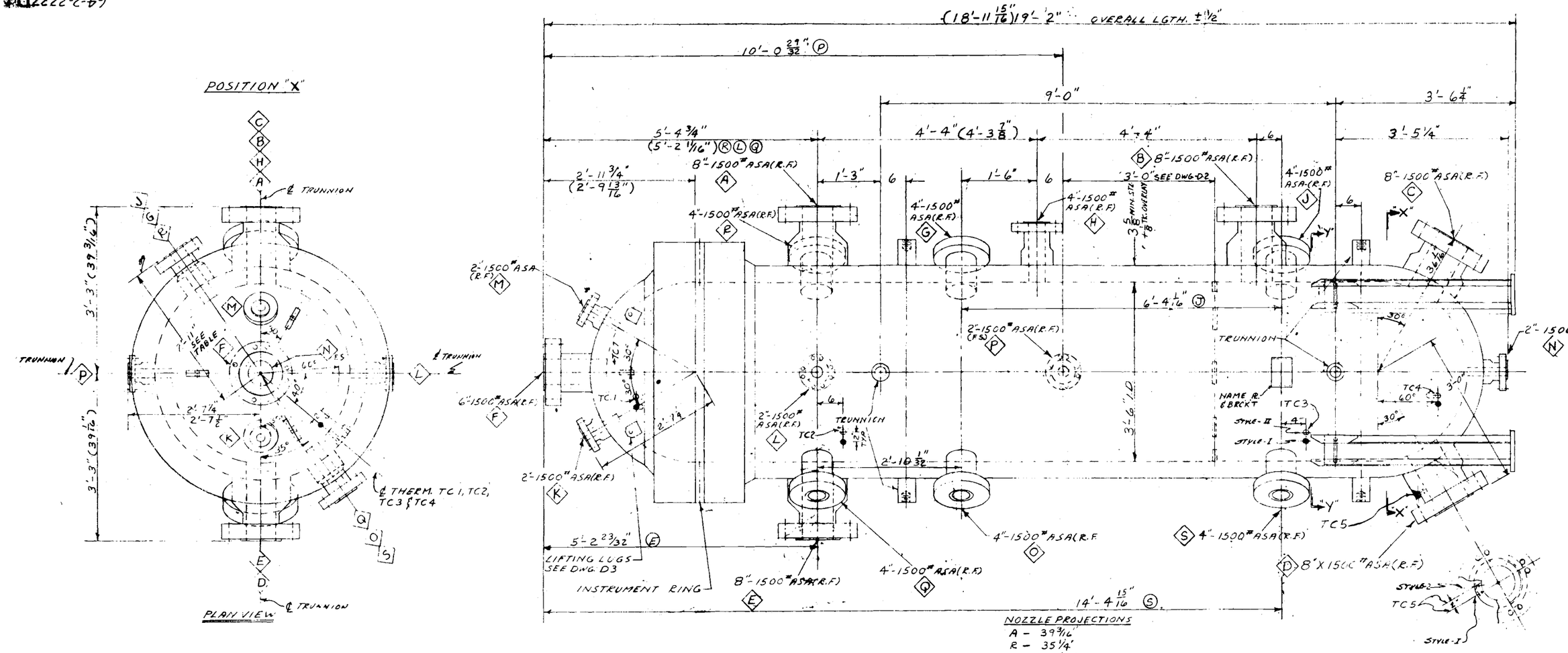

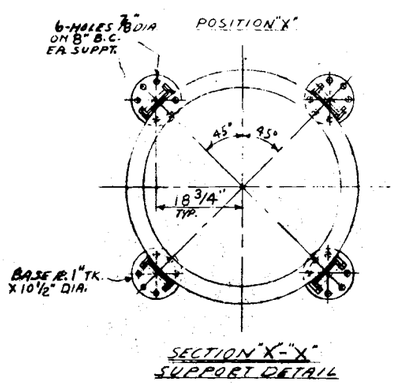

SECTION "X"-"X"
SUPPORT DETAIL

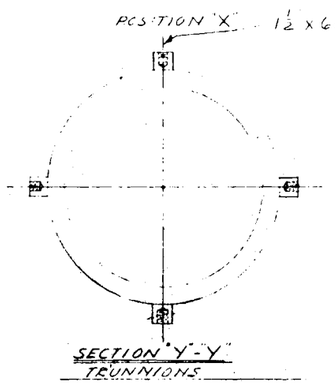

SECTION "Y"-"Y"
TRUNNIONS

NOZZLE PROJECTIONS

A –	39 9/16"
R –	35 1/4"
E –	39 1/16"
Q –	35 1/16"
L –	31 1/2"
G –	35 5/32"
O –	35 1/16"
H –	39 1/32
P –	31 7/16"
B –	39 5/32"
J –	35 7/32"
S –	35 1/8"
C –	36 1/16"
D –	36"
N	31 1/4"

NOTE

1) ALL NOZZLE GASKET SURFACE 80 R.M.S. OR BETTER
2) BOLT HOLES OF ALL NOZZLE FLANGES TO STRADDLE ℄'S
3) (DELETED)
4) THERMOWELL CONNECTIONS 3/4-16 UNF 3B (STYLE-1 (●) FULL DEPTH & STYLE-2 (○) HALF DEPTH.)
5) INSTRUMENT RING TO HAVE 1/2" N.P.T. CONNECTIONS.

P.O. JAI-44342 C.V.I.
FHB 1967 16674
SBH BDG 1 OF 221-T. EP 221-T. V-3

AS BUILT

FIGURE 1. Vessel Setting Plan (print)

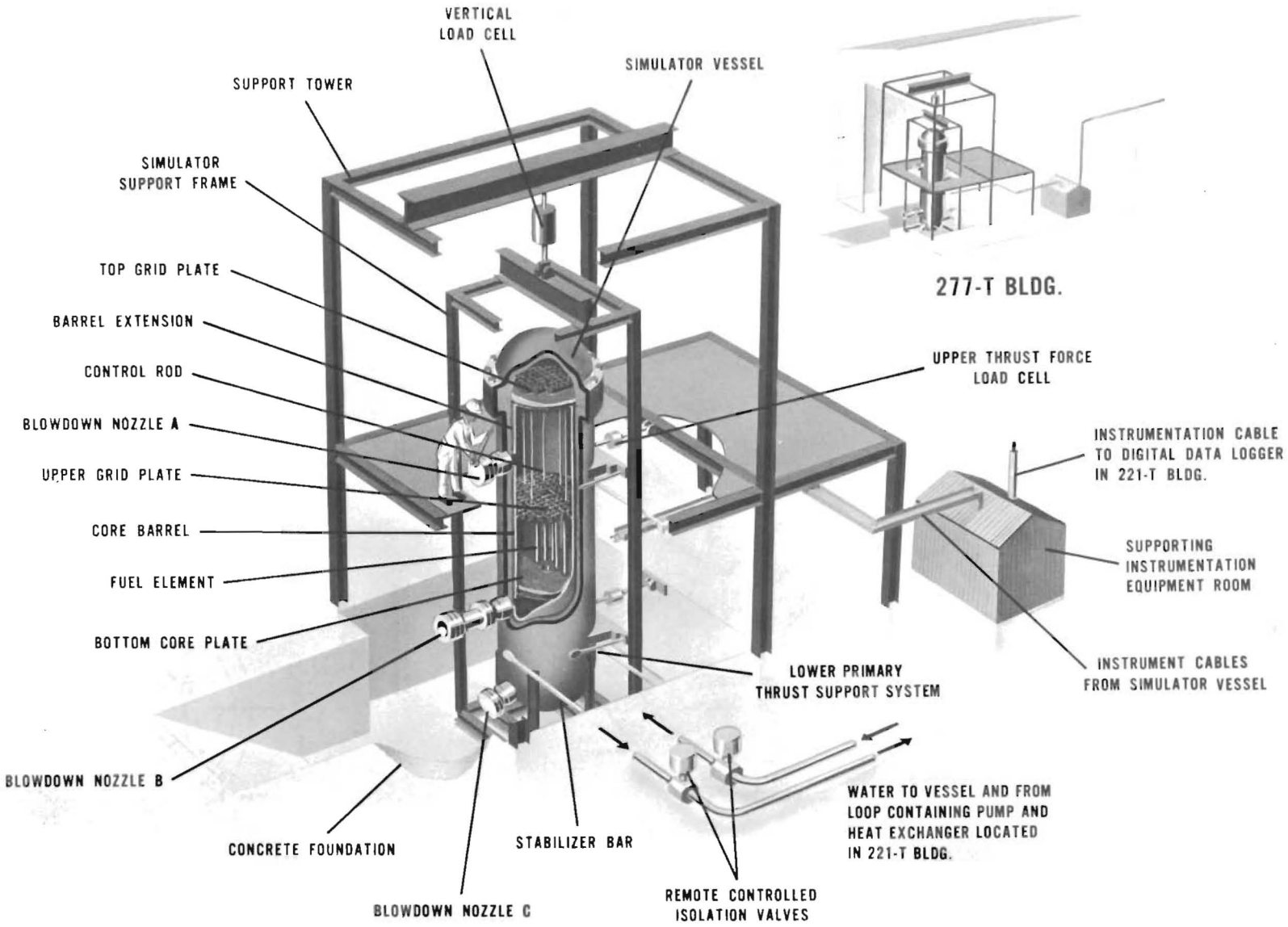

FIGURE 2. Reactor Simulator Vessel in Blowdown Framework

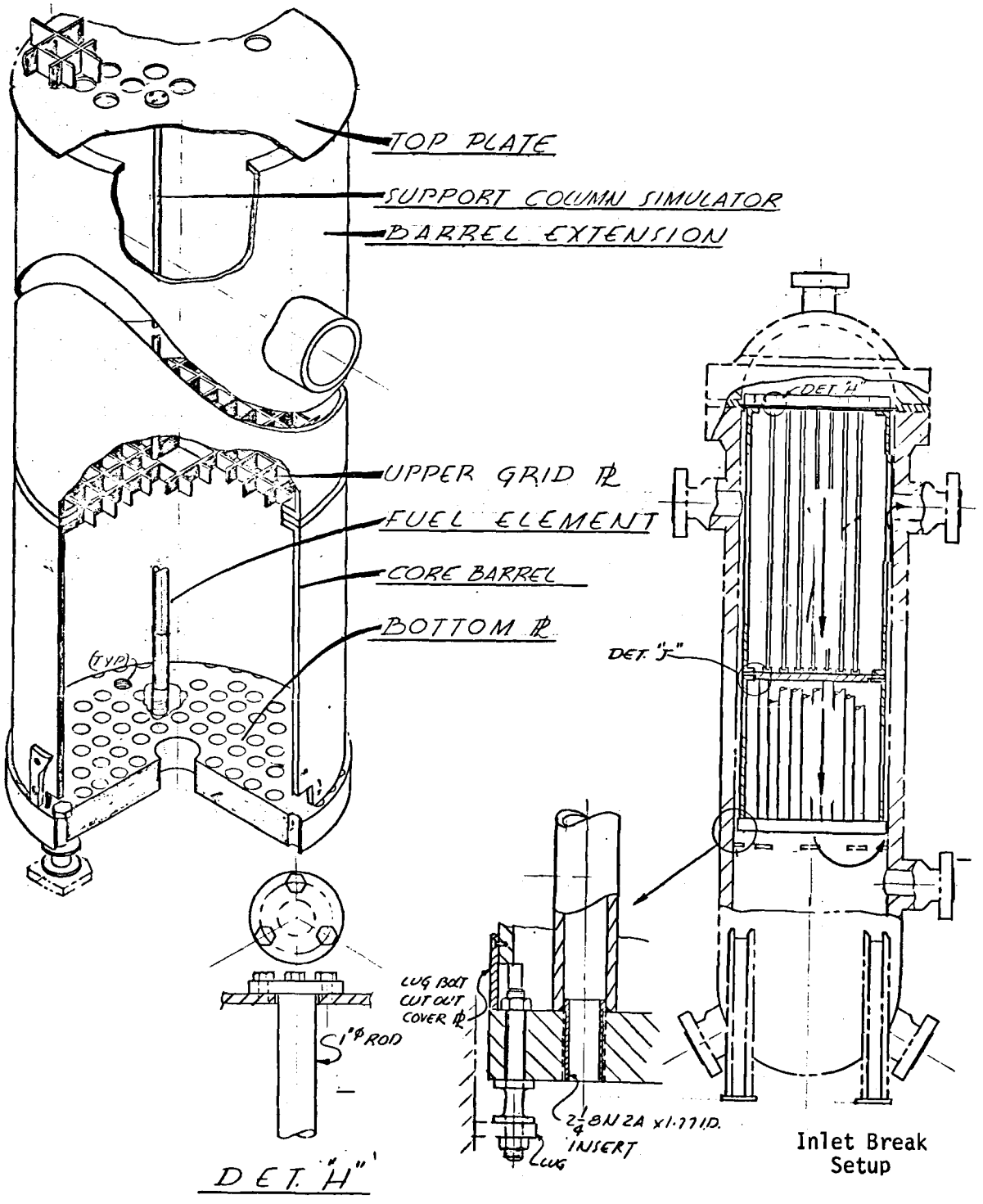

FIGURE 3. Dummy Core for PWR Tests

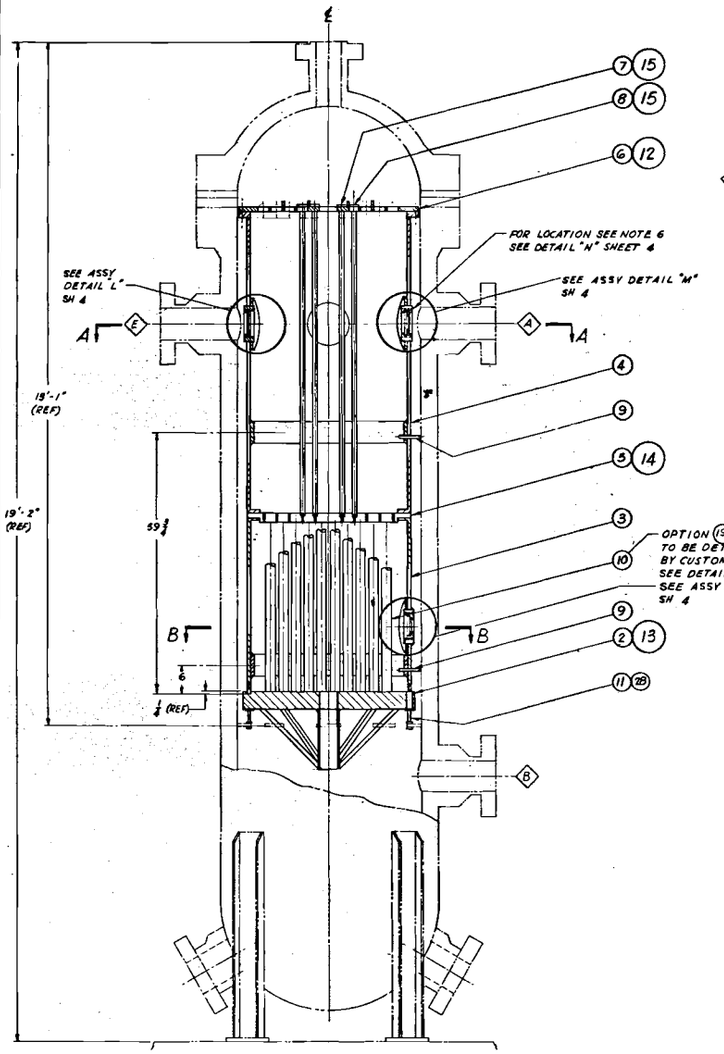

(1) ASSY

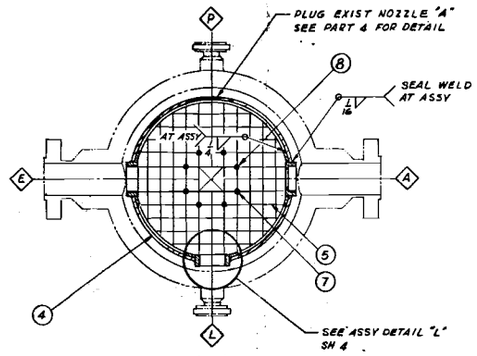

SECTION "A-A"

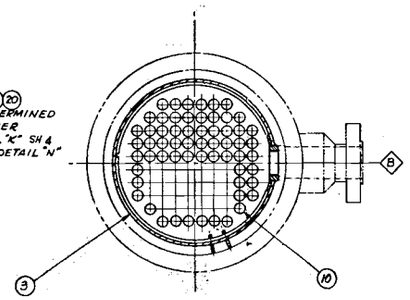

SECTION "B-B"

	QTY	NO	DESCRIPTION	SH NO & MATL
		1	ASSY	
*	1	2	PLATE, BOTTOM	SH 2
*	1	3	SHELL, LOWER	
*	1	4	SHELL, UPPER	
*	1	5	GRID	
*	1	6	PLATE, TOP	
*	5	7	SIMULATED CONTROL ROD	SH 3
*	5	8	SIMULATED CONTROL ROD	
	64	9	STUD	
*	84	10	CORE, TUBES	SH 4
*	8	11	STRAIN BOLTS	SH 5
18	16	12	SCR, 1/2-13 UNC-2A x 2 1/2 LG SOC HD	ALLENOY ALLEN MFG CO NO SUBSTITUTE
18	16	13	SCR, 1/2-13 UNC-2A x 4 3/4 LG SOC HD	
	16	14	SCR, 1/2-13 UNC-2A x 4 LG, SOC HD CAP	
18	24	15	SCR, 1/2-20 UNC-2A x 1 1/4 LG SOC HD	
*	1	16	SEAL,	SH 5
~~18~~	~~22~~	~~17~~	~~NOZZLE, (SEE NOTE 5)~~	
~~18~~	~~18~~	~~18~~	~~NOZZLE, (SEE NOTE 5)~~	
* 18	4	19	LOWER PLATE DP	SH 4
* 18	4	20	CONSTANT AREA PLUG	
*	3	21	WALL DP CASE	
*	1	22	NOZZLE DP CASE	
	8	23	SCREW, SOC HD SET, 1/4-20 UNC-2A x 1/2 LG, FLAT POINT	SST
*	1	24	DIAPHRAGM, NOZZLE DP 4.249/4.240 DIA x .187 THK	INCONEL X-750
*	3	25	DIAPHRAGM, WALL DP 4.496/4.492 DIA x .109 THK	INCONEL X-750
*	1	26	CAP, NOZZLE DP	SH 5
*	3	27	CAP, WALL DP	SH 5
*	32	28	NUT HEX, 1"-12 UNF-2B	INCONEL X-750

GENERAL NOTES:
(UNLESS OTHERWISE SPECIFIED)

1 TOLERANCES: FRACTIONAL ±1/32, DECIMAL ±.005, ANGULAR ±0°-30'

2 ALL MACHINED SURFACES (63) SURFACE TEXTURE SHALL BE IN ACCORDANCE WITH, USASI B46.1 (LATEST REV)

3 BREAK ALL SHARP EDGES AND REMOVE ALL BURRS.

4 ALL MATL SHALL BE AS SPECIFIED OR APPROVED EQUAL QUALITY.

~~5 USED ON BLOWDOWN EXPERIMENTS USING CORE PLATE PART ONLY.~~

6 SHELL NOZZLE INSTALLED DURING INSTALLATION OF CORE ASSY SO THAT ITS CENTERLINE COINCIDES WITH CENTERLINE OF NOZZLE (A) WHEN VESSEL SYSTEM IS AT 550° F. SEE M.F. DREHER OR W.C. TOWNSEND FOR INSTALLATION PROCEDURES.

7 DRILL AND TAP 1/4-20 UNC-2A x 3/8 DEEP BETWEEN JOINING THD (2) REQD @ 180° ANY LOCATION NOT CONFLICTING WITH BLIND HOLES IN CASE.

18 8 * TO BE FURNISHED

FIGURE 4. Dummy Core Details I

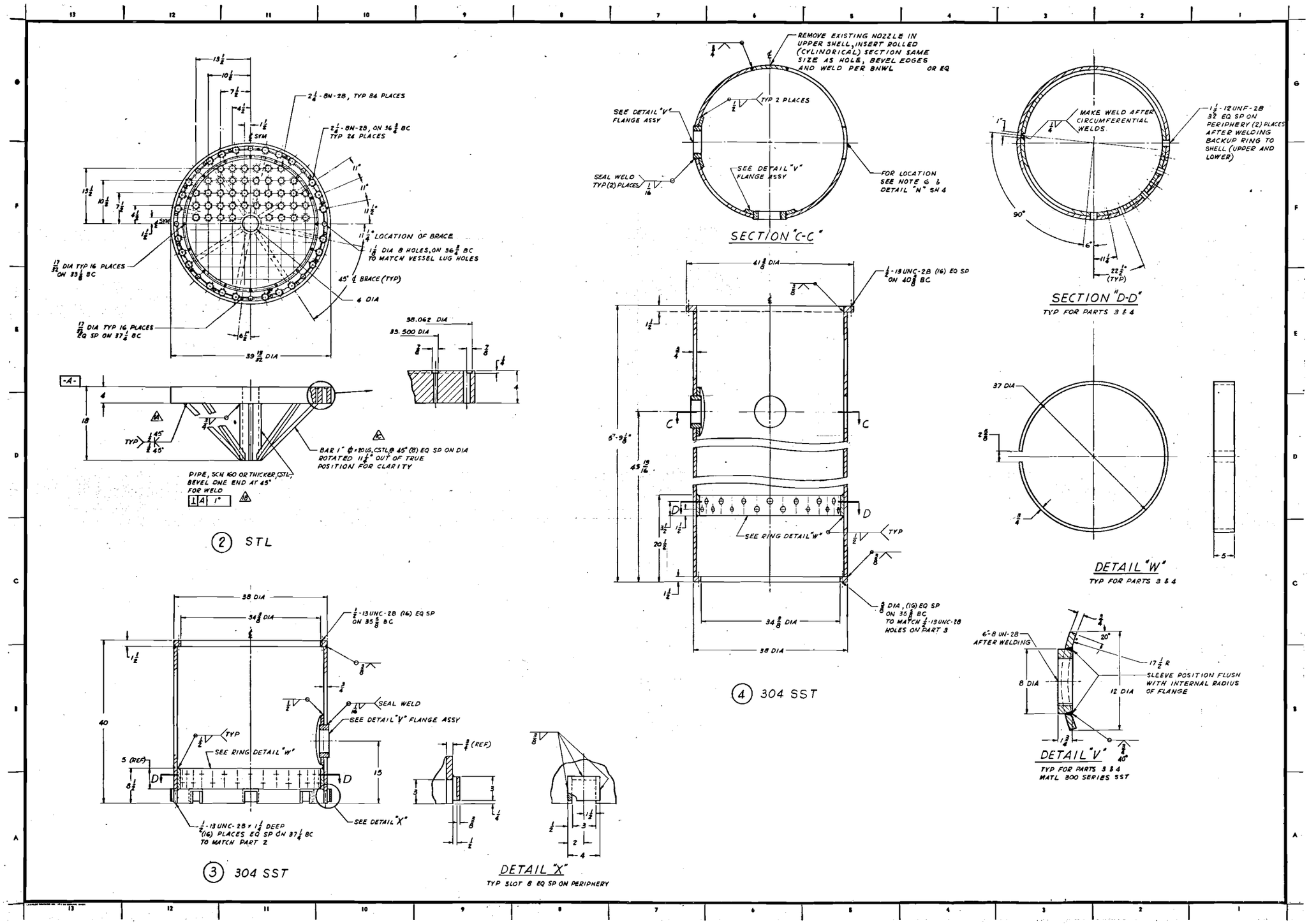

FIGURE 5. Dummy Core Details II

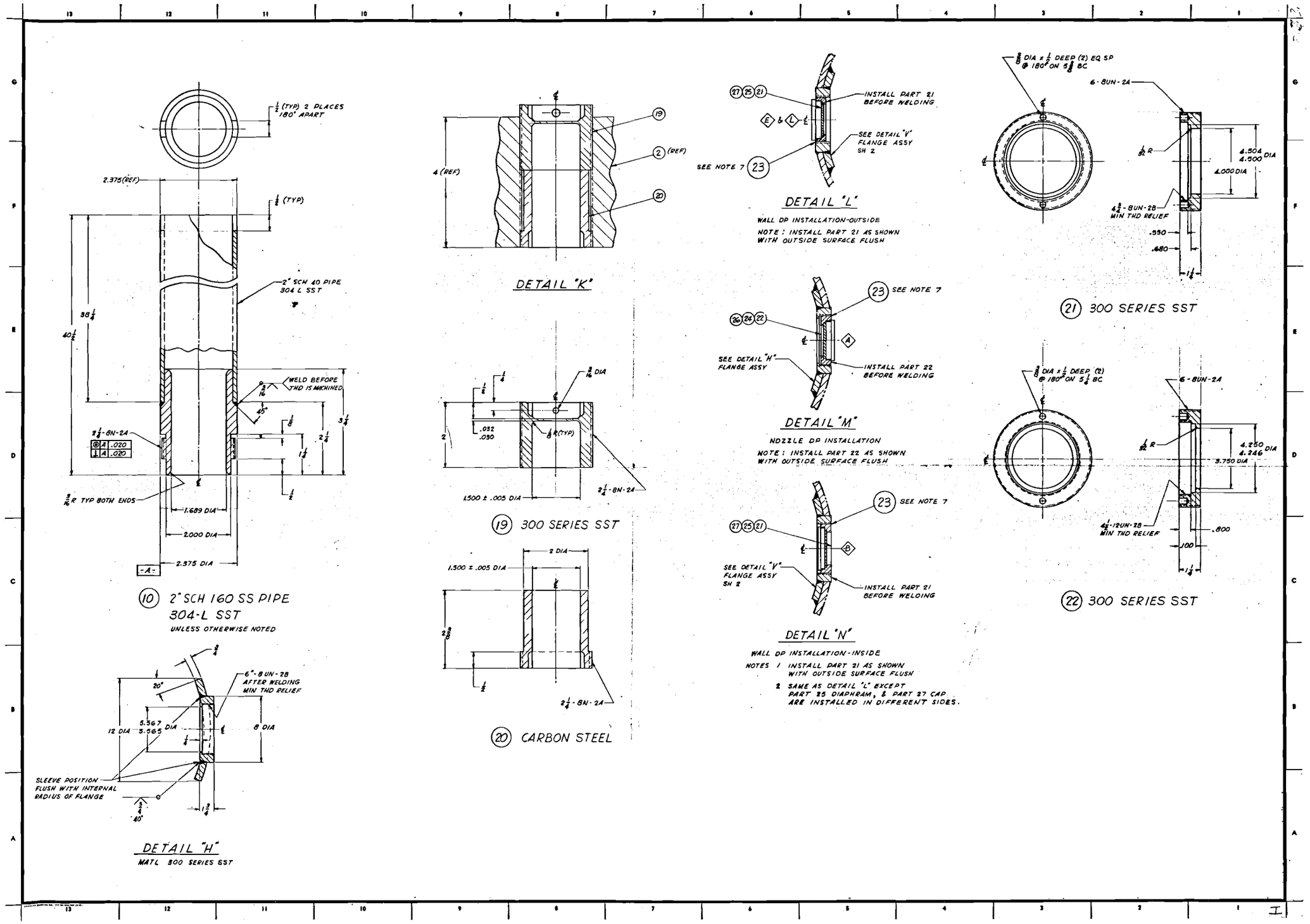

FIGURE 6. Dummy Core Details III

ments[2] and which was attached to the supporting lugs on the inside of the vessel with strain bolts. The dummy core (Figures 3, 4, 5, & 6) was designed following the criteria outlined in Reference 3. It had to fit into the existing vessel and was to have the capability of giving geometrical similarity to both BWR's and PWR's by appropriate changes in barrel size and flow restrictions. The design was an attempt to give typical scaled height positions of reactor piping for the blowdown nozzles. The core would probably be built differently if based on present insite. A longer core would probably be worthwhile, but at the time the proposed LOFT core length of four feet made this seem an appropriate value to use.

Subsequent to the initial design, calculations which took into account the results of experiments in progress showed that the lugs (eight) on the vessel wall designed to support the core might not be adequate, so bracing gussets were added. Similarly, the diagonal braces (Figure 4) were added to the main support plate (used as a simple plate in the sieve plate experiments[2]) to stiffen it. A few simulated control rods were designed with the idea of placing them to investigate side loads on structures of this type. Side loads might occur when fluid flow was out of a broken nozzle at the same level. The core barrel was modified to give it more strength, without significantly reducing flow areas by putting stud bolts through the shell to touch the walls of the vessel. For similar reasons, shear pins and compression pads were added to the top grid plate flanges.

Operation

Operation procedure of the blowdown experiments was started by filling the vessel with water. The water was then circulated through an external loop containing a heater and pressurizer until the fluid in the vessel was at the prescribed experimental conditions. The water level was held in a level pot above the vessel so that the vessel remained full during the entire heating period (except in the case of a BWR simulation when a steam plenum was required). Excess volume due to thermal expansion was bled off continuously through an outlet on the nozzle extension (Fig. 5). This procedure prevented the pressurizing gas (nitrogen) from dissolving in the water and prevented the outlet duct from becoming a cool stagnant

zone. During the heating period, the pressure in the cavity between the rupture discs was maintained at a fraction of the vessel pressure. After the desired conditions were established, the vessel was isolated (by valving off the circulation loop) and the rupture discs were broken by injecting nitrogen in the cavity between the two rupture discs until breakage occurred.

Control of the facility was switched to the on-line PDP-7 digital computer at a prescribed time (7 sec to 3 min) before the blowdown time. Nitrogen injection into the rupture disc cavity and data logging were triggered by the computer.

The blowdown facility was instrumented to measure pressure and temperature at selected locations, weight of water remaining, liquid level and thrust reaction force, and differential pressures.

INSTRUMENTATION ON THE CSE REACTOR SIMULATOR VESSEL

Several basic measurements were required to accomplish the objective of studying the fluid behavior during the simulated loss-of-coolant accident. Some of the measurements, such as pressure and temperature, could be made directly but others, such as mass flow rate or liquid level, required an indirect measurement because of inadequacies in state-of-the-art instrumentation or the general difficulties associated with basic measurement of two-phase flow. The nozzle extension detail is shown in Figure 7, and associated instrumentation for the simulator vessel in Figures 8, 9 and 10. Tables 1 and 2 summarize the instrumentation types, the intended measurements and locations, and list of the manufacturers. Details concerning

Notation Glossary

S	Strain gage	DRAG	Drag Disc Sensor
T	Temperature sensor	SBI#	Strain bolt inner gage #
P	Pressure sensor	SBO#	Strain bolt outer gage #
DP	Differential pressure	TIFZ#	Temperature inside fault zone
LC	Loadcell	TOFZ#	Temperature outside fault zone
LG	Level gage	SCBH#	Control rod in barrel extension probe
		TL#	Temperature on level gage

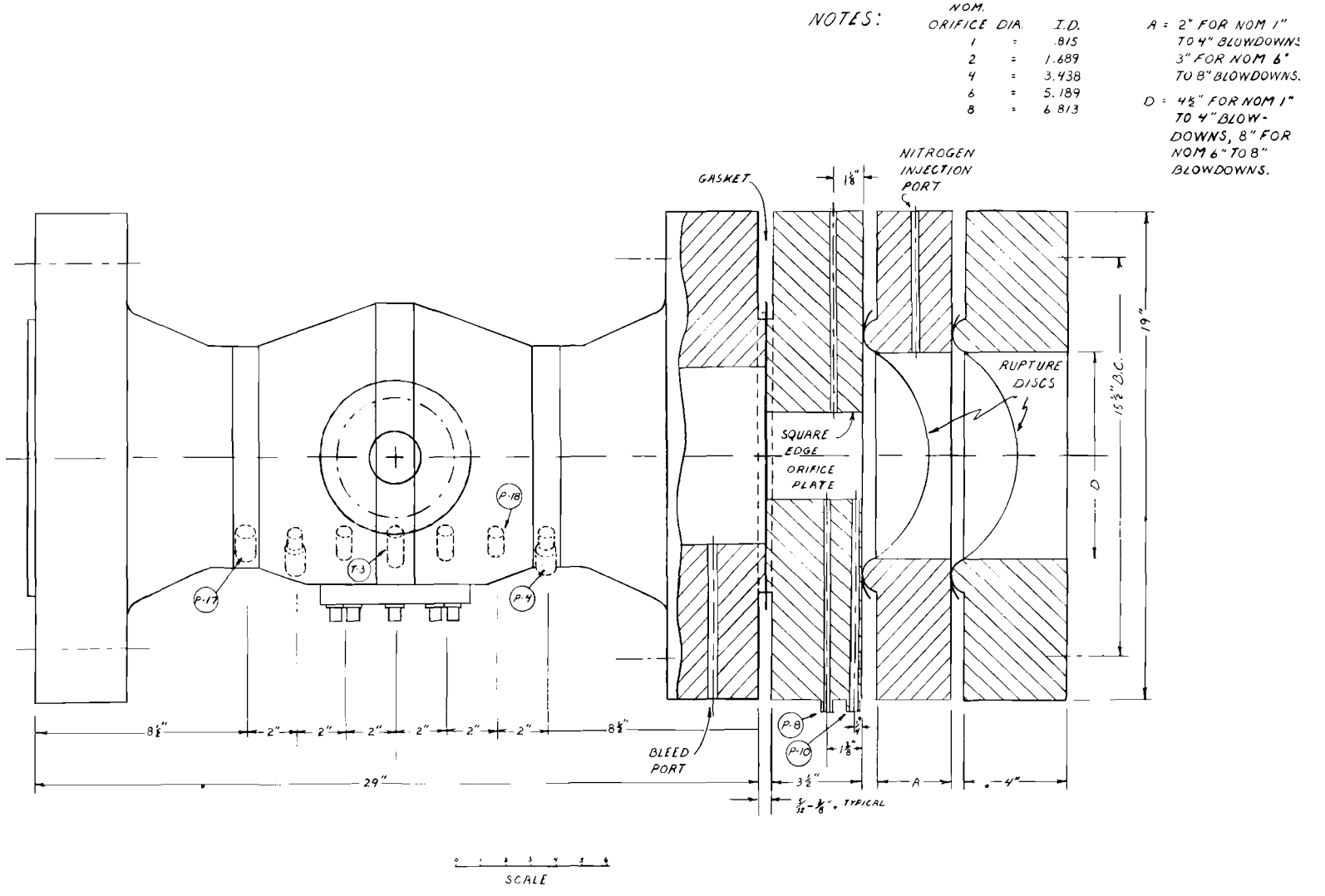

Neg 701424-2

FIGURE 7. Blowdown Nozzle Extension - Test Section

TABLE 1. Core Series Sensor Designations & Locations

Sensor Number	Type* (See Table 2)	Location	Measurement
LC-1	Toroid (2)	Top of vessel	Weight of vessel contents
LC-2	Strainsert (3)	Upper strongback	Thrust
LC-4	"	Lower " "	Thrust
LG-1	TDR (1)	Centerline vessel	Liquid level
LG-2	TDR (1)	Below core plate	Liquid level
P-1	Norwood (4)	Nozzle R	Pressure state of fluid
P-4	"	Nozzle ext.	" " "
P-6	"	Nozzle Q	" " "
P-7	"	Nozzle H	" " "
P-8	"	Nozzle extension	" " "
P-10	"	Nozzle extension	" " "
P-12	"	Nozzle C	" " "
P-13	"	Nozzle S } pressure probe	" " "
P-14	"	Nozzle S }	" " "
P-15	"	Instrument ring	" " "
*Plug 7	Standard Controls	Lug 7 below plate	" " "
P-20	Standard Controls	Outer plenum, core barrel, Nozzle A side	Pressure state inside vessel
P-21	"	Outer plenum, core barrel opposite nozzle A	" " "
P-22	"	Center of core assembly	" " "
P-23	"	Top of control rod support	" " "
SCR 4A	Microdot	On control rod in barrel ext. piece	Strain, control rod 4
SCR 4B	"	" " "	" " "
Drag 1	Ramapo	Discharge nozzle	ρu^2 of discharge fluid
T-1	.040" CHR-CON	Nozzle R	Temperature of fluid
T-2	" " "	" "	" " "
T-4	" " "	Nozzle extension	" " "
T-6	" " "	Nozzle Q	" " "
T-7	" " "	Nozzle H	" " "
T-12	" " "	Nozzle C	" " "
T-15	" " "	Inst. ring	" " "
TL-1	.040" CHR-CON	TDR	Temperature of fluid
TL-3	" " "	"	" " "
TL-4	" " "	"	" " "
TL-5	" " "	"	" " "
TL-6	" " "	"	" " "
TLUG 7	.040 C/A	Lug 7	" " "
TIFZ 3	.040 (stripped)C/A	Bottom head inside	Temperature of metal skin
TBI 2	"	"	" " "
TBI 9	"	"	" " "
TBI Ø	.060 C/A	"	" " "
TBI 6	.040 (stripped)C/A	"	" " fluid
TBI 12	"	"	" " fluid
CPDP-1	Microdot	Inserted in core plate	Differential pressure across plate
CPDP-2	"	" " " "	" " " "
CPDP-3	"	" " " "	" " " "
CPDP-4	"	" " " "	" " " "
NDP	"	Flanged in barrel blowdown nozzle	Differential pressure on barrel
CBDP-1	"	Flanged, in lower barrel	" " " "
CBDP-2	"	Flanged, in upper barrel	" " " "
CBDP-3	"	" " "	Diff. pressure on core barrel
SB1I	"	Lug Support bolts	Strain in lug bolt
SB1Ø	"	" " "	" " " "
SB2I	"	" " "	" " " "
SB3I	"	" " "	" " " "
SB4I	"	" " "	" " " "
SB5I	"	" " "	" " " "
SB5Q	"	" " "	" " " "
SB6I	"	" " "	" " " "
SB6Q	"	" " "	" " " "
SB7I	"	" " "	" " " "
SB8I	"	" " "	" " " "
SB8Q	"	" " "	" " " "
SCR 8A	Microdot	On control rod barrel extension	Strain on control rod 8
SCR 8B	"	" " " "	" " " "
SCR 8C	"	" " " "	" " " "
SCR 6A	"	" " " "	Strain on control rod 6
SCR 6B	"	" " " "	" " " "

TABLE 2. Manufacturers, Models, and Nominal Specifications of Instrumentation

	Manufacturer and Model	No.	Description	Range	Static Accuracy
1	Hewlett-Packard 14DA	1	Sampling Oscilloscope Coupled with Time Domain Reflectometer	N/A	N/A
2	Toroid Model 35-132 DDG	1	Strain Gage Load Cell	0-100,000 lb	0.1% FS
3	Strainsert Model FLY-50SF2.5	2	Strain Gage Load Cell	0-50,000 lb	0.1% FS
	Strainsert Model FLY-100SG2.5	2	Strain Gage Load Cell	0-100,000 lb	
4	American Standard-Norwood Model 110-2-3000G	8	Water Cooled Strain Gage Pressure Sensor	0-3000 psig	0.1% FS
5	NANMAC Models A and G	7	Chromel-Constantan Thermocouple Probes	0-600 °F	1.0% FS
6	Microdot Model SG 122	2	Quarter Bridge Weldable Strain Gage	0-6000 micro-strain	5.0% FS
7	FASTAX Camera		2000-9000 Frames/sec	400 ft/film	millisecond timer
8	Standard Controls model 420	2	Uncooled High Temperature Strain Gage Pressure Sensor	0-3000 psig	0.1% FS

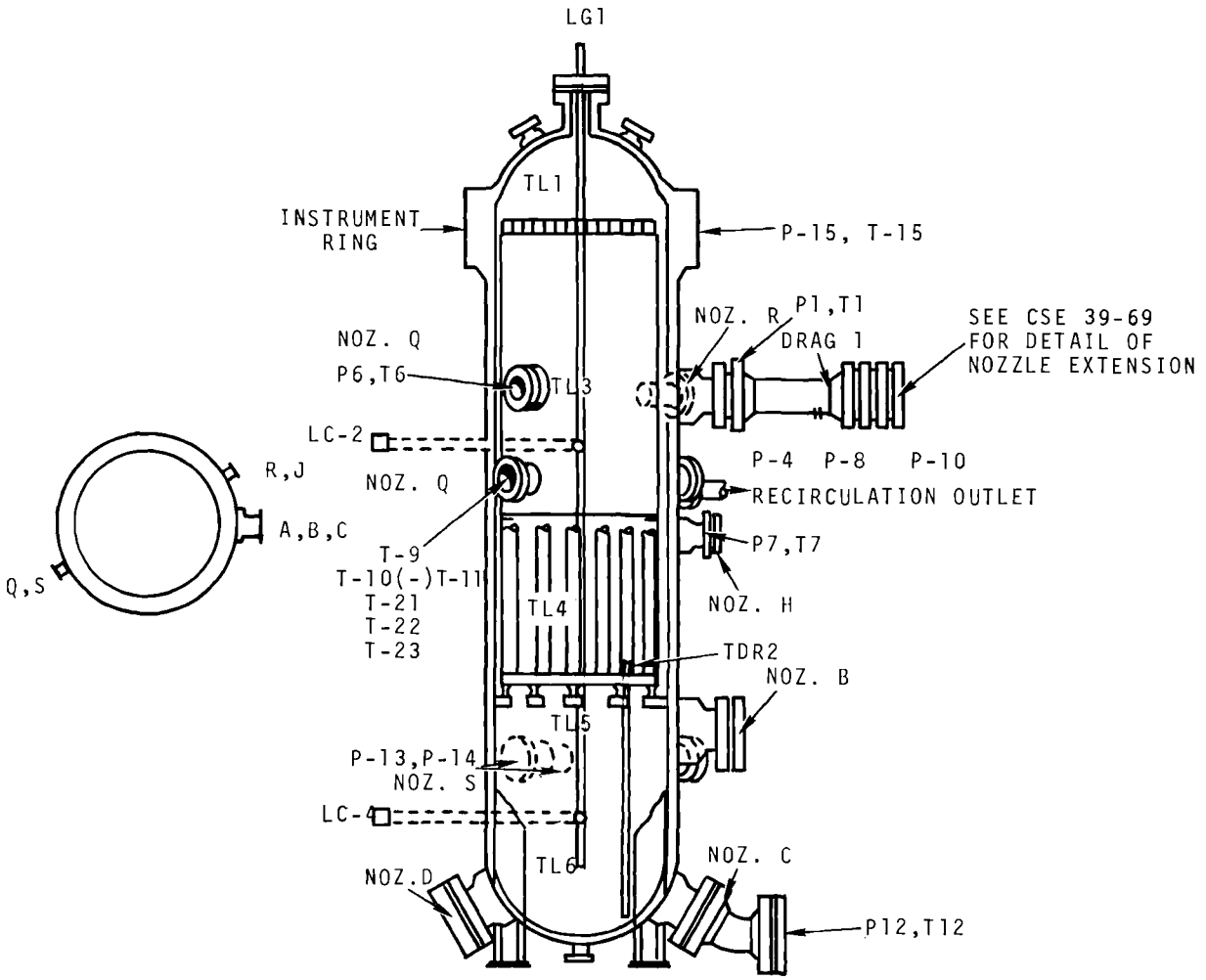

NOTE: SOME DETAILS OF THE UNDER CORE PLATE STRUCTURE OMITTED. SEE FIG. 3 & 4.

FIGURE 8. Location of Sensors, PWR Run Series - External Sensors

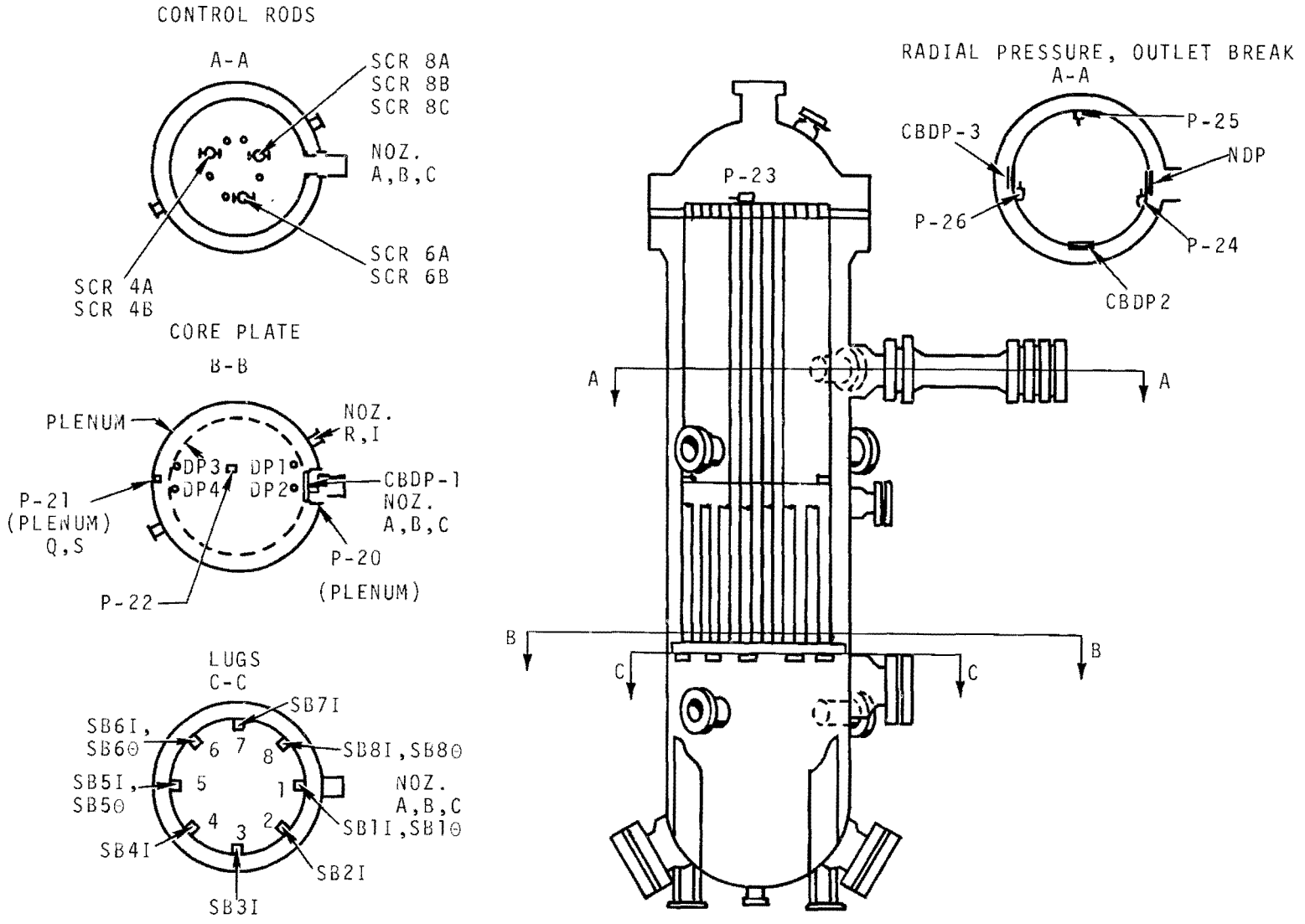

FIGURE 9. Location of Sensors, PWR Run Series - Internal Sensors

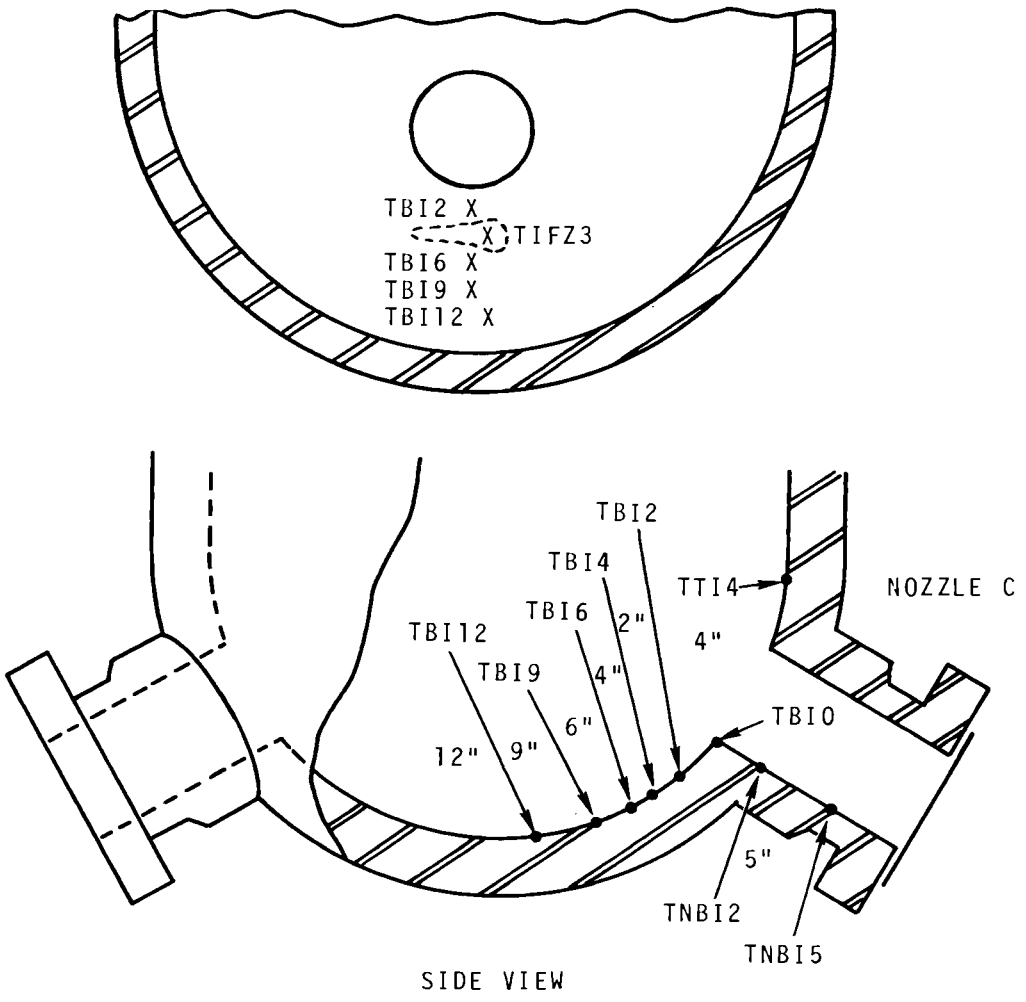

SPECIAL CONFIGURATION #1
FLUID TEMPERATURE;

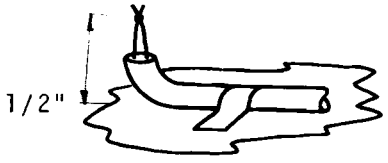

TYPICAL,
TBI6
TBI12

SPECIAL CONFIGURATION #2
METAL SKIN TEMPERATURE;

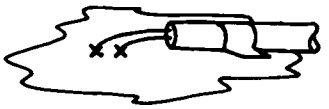

TYPICAL,
TBI2
TBI9
TIFZ3

FIGURE 10. Thermocouples for Bottom Head Heat Transfer

the time domain reflectometer may be found in Reference 5. The camera arrangement is discussed in Reference 6.

Experimental instrumentation was similar to that used previously[2] except that additional instruments were added in the core and barrel regions.

Figures 8, 9 and 10 show the general location of the sensors which were logged by computer.

INSTRUMENTATION DEVELOPMENT

Three additions were made to the instrumentation of this experimental series that were not reported previously. These include the fully submerged TDR probe (Fig. 8), the diaphragm type differential pressure transducer (Fig. 6), and the drag disc flow velocity transducer. All of these devices were developmental and were not reliable enough to give results on every test. However, the results which were obtained are reported.

Fully Submerged Time Domain Reflectometer Probe

The results of blowdown tests made with a sieve plate[2] indicated that under certain blowdown conditions a steam dome could form beneath the sieve plate. Because the central TDR probe which was used in those tests sensed only the top surface of the liquid, the liquid level in the lower plenum could not actually be detected until the upper plenum was dry. For this series of runs with the reactor core, a second probe was added which detected the level of the fluid in the lower plenum only. This sensor could give level information in the lower plenum throughout the blowdown and be corroborated at the end of the run by the central TDR which also extended into the lower plenum. The basic method of operation of the lower plenum TDR was exactly the same as the other[5]. The main problem with its design (and operation) was the sealed feedthrough for the high frequency electrical signals. The method used was to encase the signal lead in a nitrogen pressurized conduit and feedthrough (Figure 11). Occasional electrical short circuits and discontinuities still occurred because inadequate nitrogen pressure control resulted in leakage of water through the sealing packing. These difficulties resulted in useable level

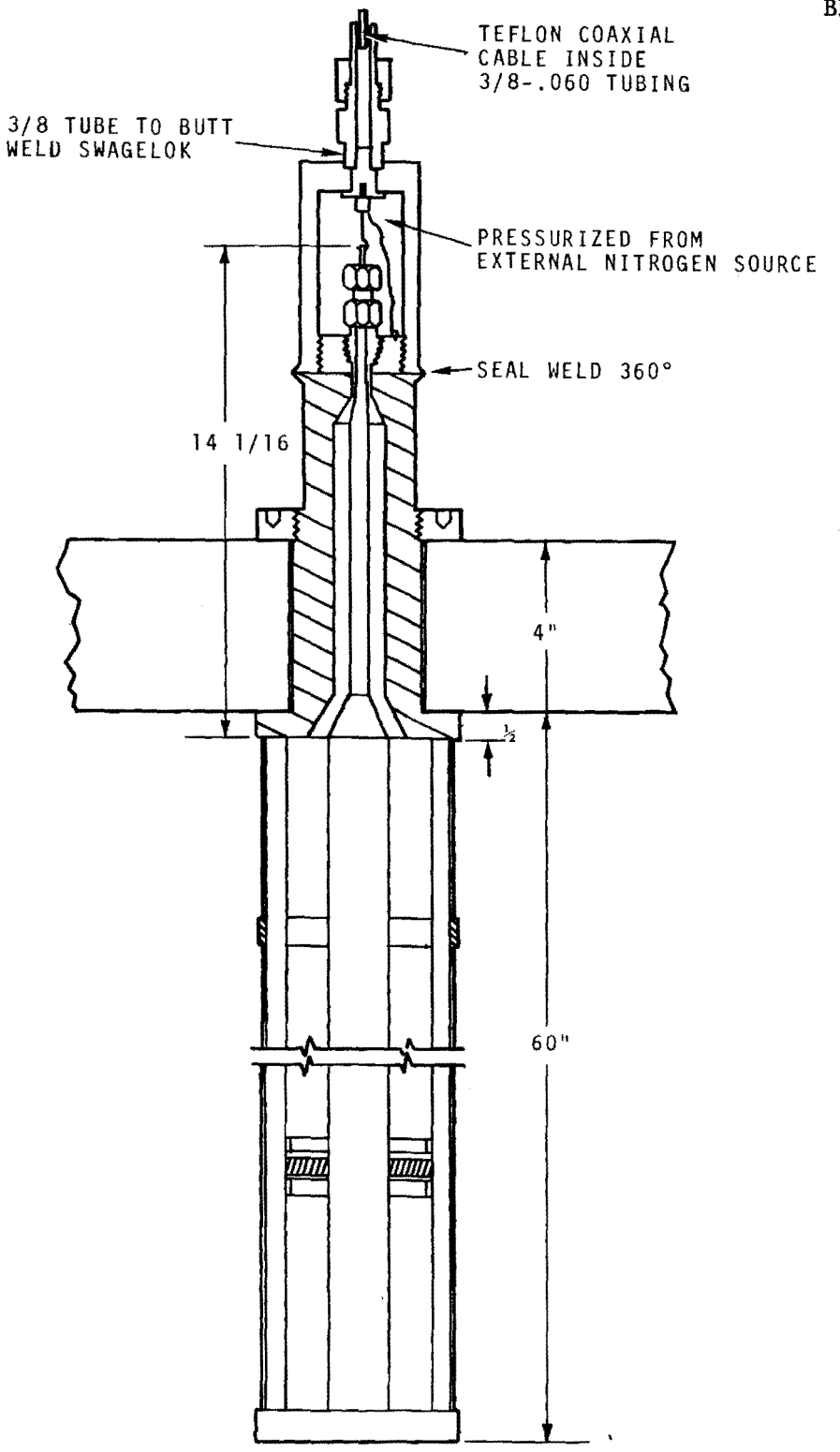

FIGURE 11. Time Domain Reflectometer Probe Below Core Plate

data from the lower plenum only for run B75.

Diaphragm Type Differential Pressure Transducer

Experience with several commercial high speed pressure transducers had shown that they could not give differential pressures under the wet high temperature and rapid transient conditions of the blowdown. The success of the sealed, weldable strain gages suggested their use in a differential pressure transducer which operated on the principle of deflection of a thin diaphragm of metal. Two types were eventually developed. One was used for the differential pressure across the core plate (Figure 6, Part 19). It was machined from a solid piece of steel to preclude hysteresis and slipping at the edges. These problems were not serious on a larger type which used a thin sheet of Inconel clamped between rings. The larger type (Figure 6, Part 21) was used for measuring pressure differential across the core barrel. On both types a weldable strain gage was attached to the diaphragm radially as near as feasible to the region of maximum strain caused by uniform differential pressure across the diaphragm. These differential pressure transducers were calibrated before being installed in the reactor simulator vessel and were found to be linear ($\pm$4%) in the region of operation and they could withstand considerable overpressure. Appendix A contains developmental notes concerning these transducers.

RESULTS AND DISCUSSION

EXPERIMENTAL CONDITIONS

The initial conditions used for the core-in-vessel blowdown test are shown in Table 3. The series was designed in order to work up from small forces and to allow safe extrapolation to larger breaks and higher pressures. Only an inlet break condition was simulated for the PWR because budget limitations caused a sharp curtailment of the series. The parameters were initial temperature, pressure and break size. One run was made with a partly full vessel to simulate a steam line break of a BWR.

The objectives of the complete run series (Table 4) as outlined in the operation run plan were to simulate the blowdown of a power reactor

TABLE 3. Summary of Blowdown Runs Performed

Run No.	Date 1970	Pressure Psig	Approx. Initial Temp. °F	Nominal Orifice Diam., in.	Initial Water Volume, Ft^2	Initial Water Mass lb_m
B 60	4-7	2086	75	2	140	8700
B 73	4-9	1285	75	2	140	8700
B 63	4-17	2081	500	2	140	full
B 74	4-24	1283	500	4	140	full
B 66	5-1	952	535	4	107	steam line
B 75	5-14	1000	500	6	140	full

Nominal Orifice Size, in.	I.D. in.	Area, ft^2
2	1.689	.0156
4	3.438	.0643
6	5.189	.146

TABLE 4. Proposed Run Conditions

Run No.	Type	Nozz. Nom. Diam.	Press (psia)	Temp. (°F)	Over Press.	Nom. Vessel Volume	Area Break Free Area of Core
B60	PWR/Inlet	A2"	2100	70		Full	.00838
B61	"	A4"	1700	"		Full	.00345
B62	"	A6"	1300	"		Full	.136
B63	"	A2"	2100	500	1420	Full	.00838
B64	"	A4"	1700	500	1020	Full	.0345
B65	"	A6"	1300	500	620	Full	.136
B66	BWR/Recirc	B4"	1000	545	0	3/4 Full	.0345
B67	PWR/Outlet	A2"	2100	500	1420	Full	.00838
B68	"	A4"	1700	500	1020	Full	.0345
B69	"	A8"	1300	500	620	Full	.136
B70	BWR/steam	A4"	1000	545	0	3/4 Full	.0345
B71	"	A4"	1000	545 top/500 bot.	0	3/4 Full	.0345
B72	PWR/outlet similar to B-64, but for high N_2 content effect						

using a PWR dummy core to study the effects of complex geometry, break size, and break locations or blowdown and on the comparison with analytical results.

Specific Objectives

1. To obtain subcooled decompression data in the several internal volume zones in the simulated reactor core.
2. To obtain saturated blowdown rates as a function of break size.
3. To measure the forces during decompression and blowdown on an internal vessel structure, including support members, core barrel, and simulated control rods.
4. To measure the operational vertical temperature gradient in the fluid filling the vessel.
5. To measure the heat-transfer coefficient from the vessel walls to fluid during and after blowdown.
6. To measure liquid level remaining shortly after blowdown.
7. To measure additional temperature, liquid levels, pressures, and forces as required to determine the state of the fluid during blowdown.
8. To obtain the pressure history in the vessel during decompression after saturation has been reached.
9. To obtain the effect of flow restrictions and a multizone volume distribution on the decompression pattern in the vessel and subsequent saturated blowdown.
10. To monitor the defect in the bottom head.
11. To obtain BWR blowdown data with vertical temperature rise from 500 °F to 545 °F, (bottom to top of liquid level respectively).

SUBCOOLED DECOMPRESSION

As has been described elsewhere[1,2,5,6,7], the rupture of a water leg of a hot pressurized water system results in a rapid pressure decrease to a pressure below saturation with subsequent recovery to the saturation

pressure and formation of two phase conditions as the water flashes to steam. The time for the depressurization to saturation is very short (less than 100 milliseconds in these experiments) because the low compressibility of water requires very little volume change (i.e., flow out the break) to reduce the pressure. The pattern of reduction of pressure is dominated by the conservation of mass and momentum and by the equation of state of the water which are manifested in an acoustic propagation velocity. Although the propagation velocity is high, since the decompression pattern starts from the break point, temporal and spatial imbalances of pressure are set up in the fluid system. Decompression patterns are observed in which pipe lengths and locations and chamber position have important effects.

The use of a one-dimensional analysis such as WHAM[8] to model the actual system has been found to be reasonably successful for simple pipe-vessel systems[2,6,7]. It is valuable to know whether this type of analysis can be extended to the more complicated case with vessel internals (such as annulus, baffles, core tubes, etc.). Although most data of subcooled pressure history are available in Appendix B for comparison, only a few features will be discussed here. Comparisons were made with a computer solution obtained from WHAM[8]. A schematic layout of the nodal input to WHAM is shown in Figure 12. The figure shows the rather complicated layout suggested to model the core system. A few comparisons of the WHAM predictions with data from 2", 4", and 6" PWR blowdowns (the sizes given are nominal diameters for runs B-63, B-74, and B-75, respectively) are shown in Figures 13, 14, and 15. The WHAM predictions used the outlet pressure history from the run as a boundary condition, obtained by the techniques described in Reference 2. The data for pressure gage P-10 appears to have calibration errors on most runs because P-4 generally agrees well with WHAM for the first 10-15 msec. The structure and magnitude of the WHAM calculations begin to deviate beyond this point perhaps because of incorrect modeling of the pipe to annulus transition. WHAM predictions of the vessel pressure show too large an amplitude of fluctuation, and some phasing error late in the calculation. The measured core

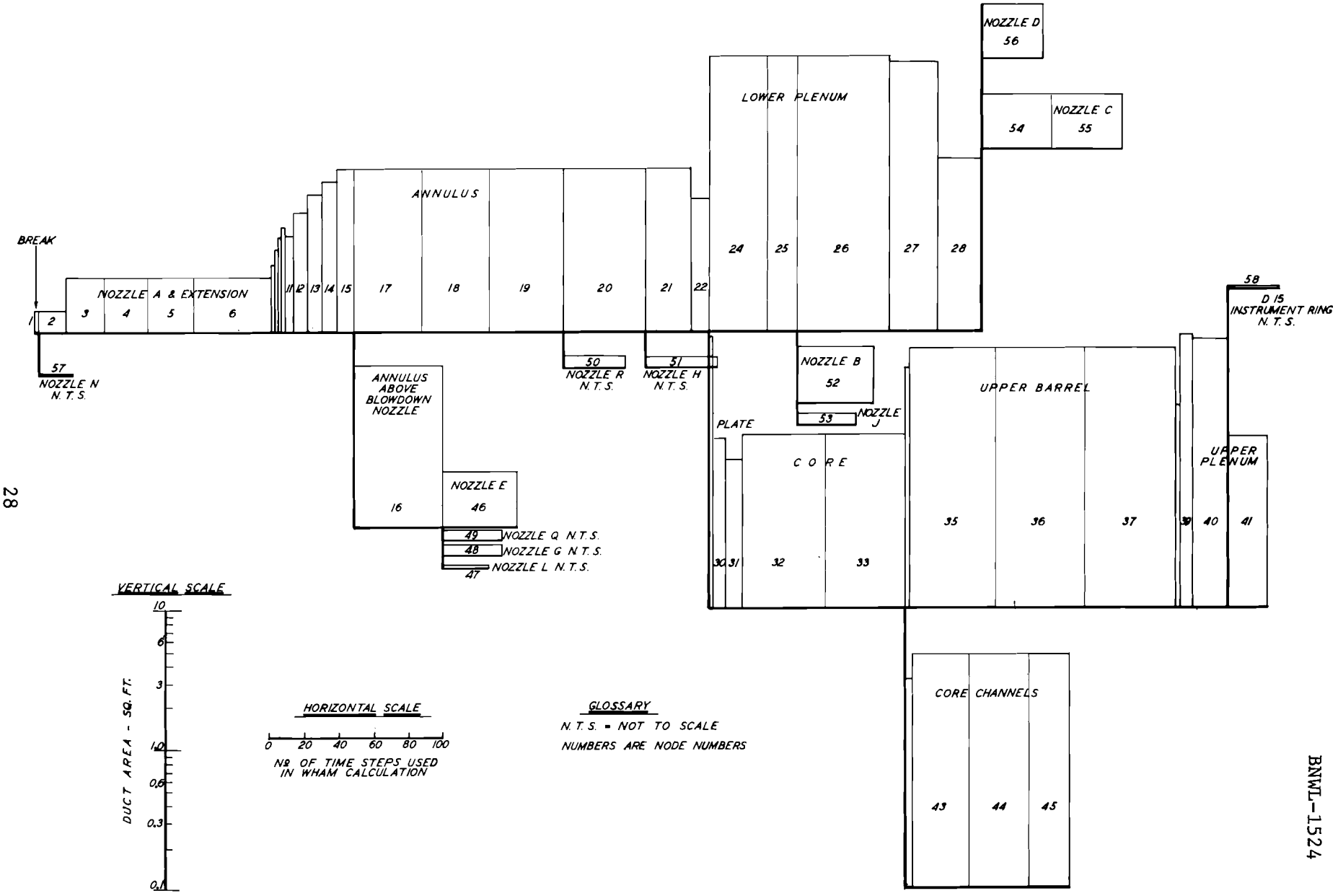

FIGURE 12. Schematic Diagram of Nodes Used for WHAM Calculations

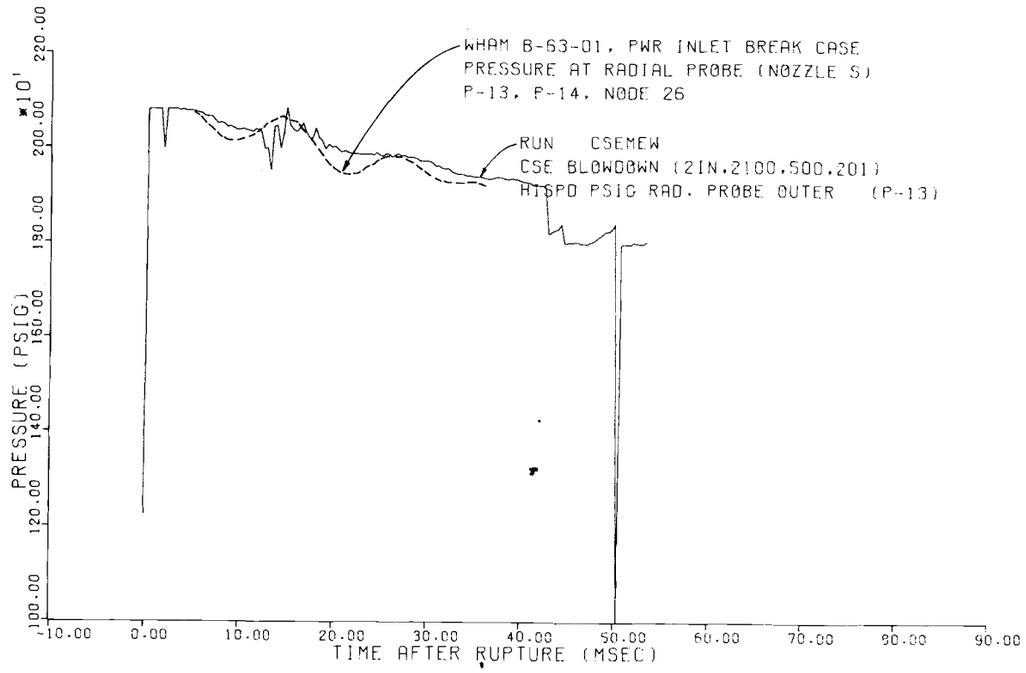

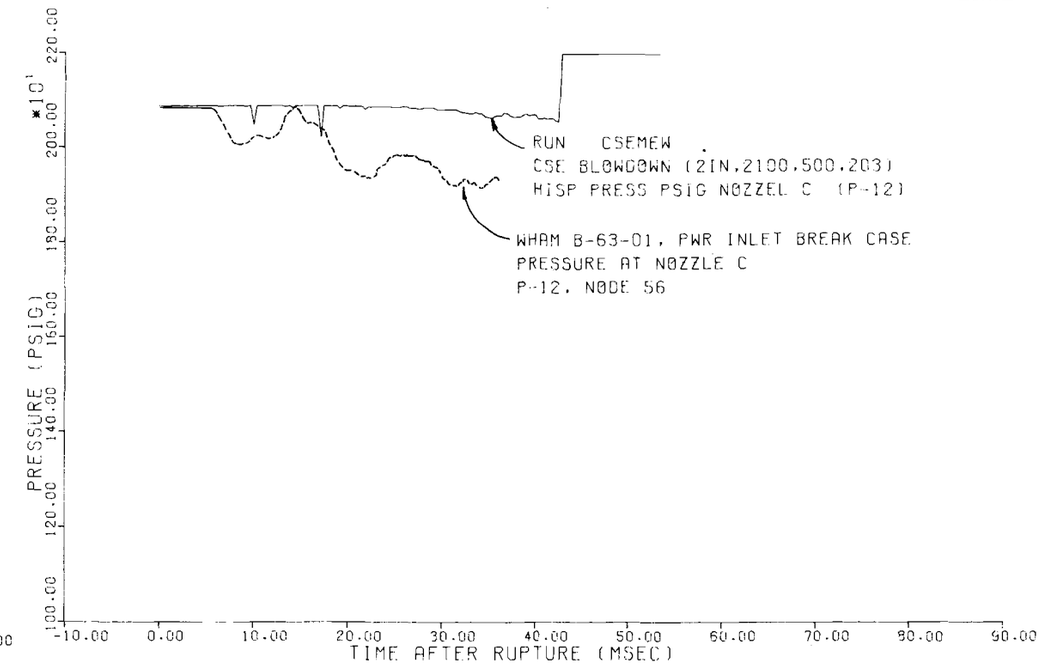

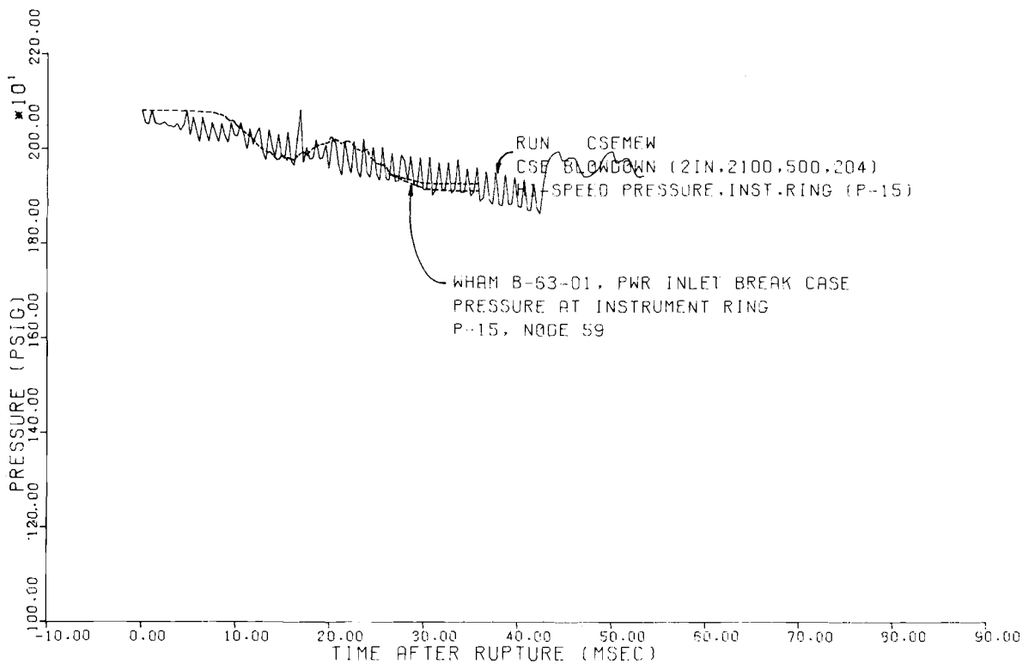

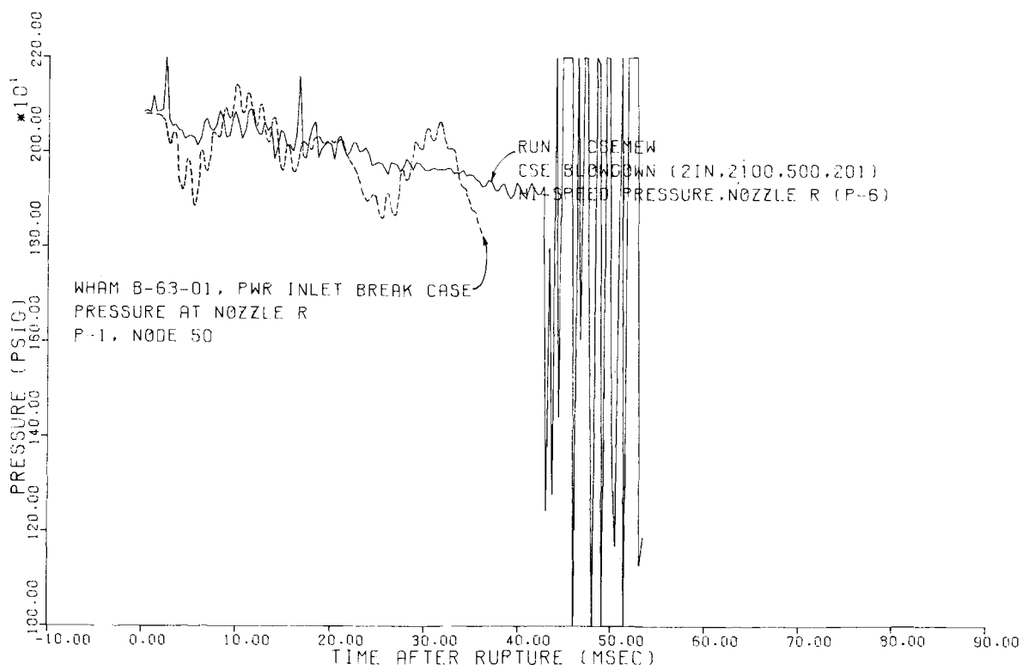

FIGURE 13. Comparison of WHAM with 2" Data

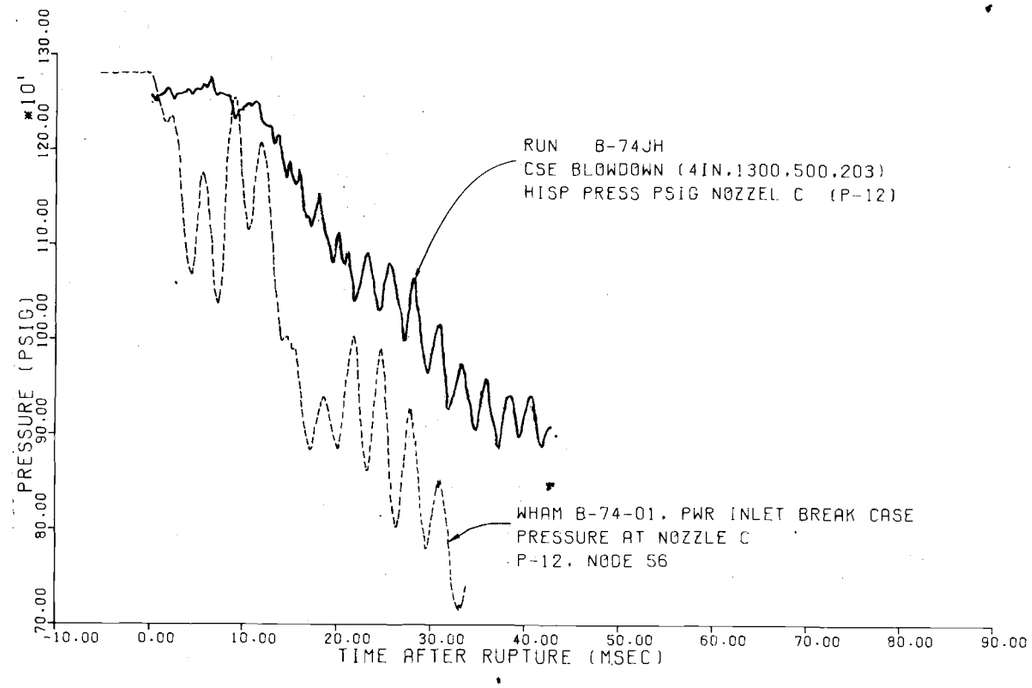

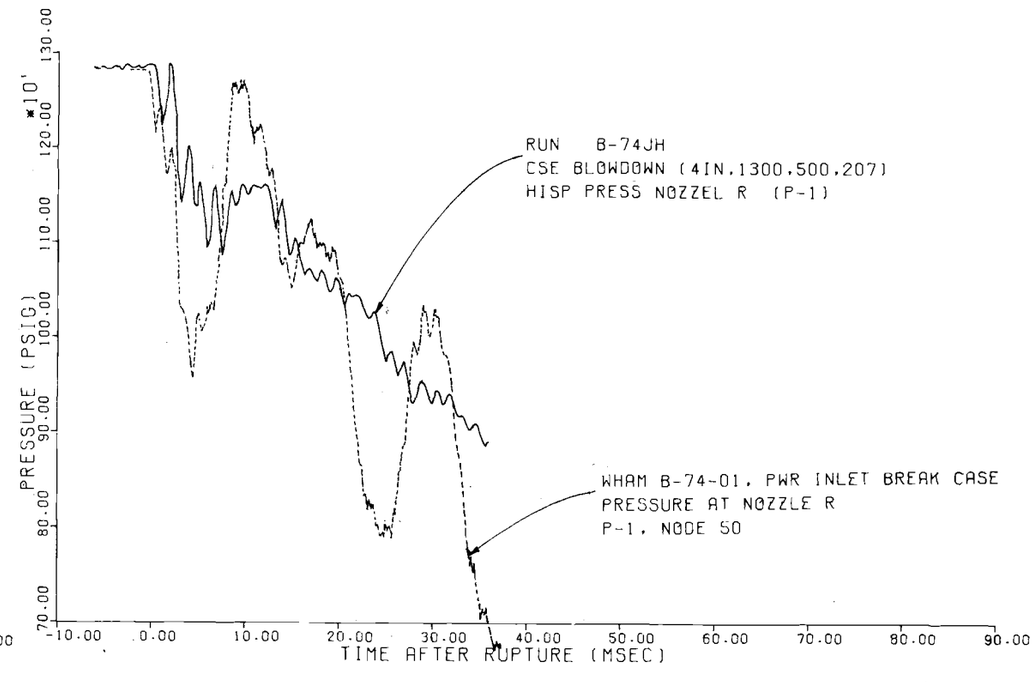

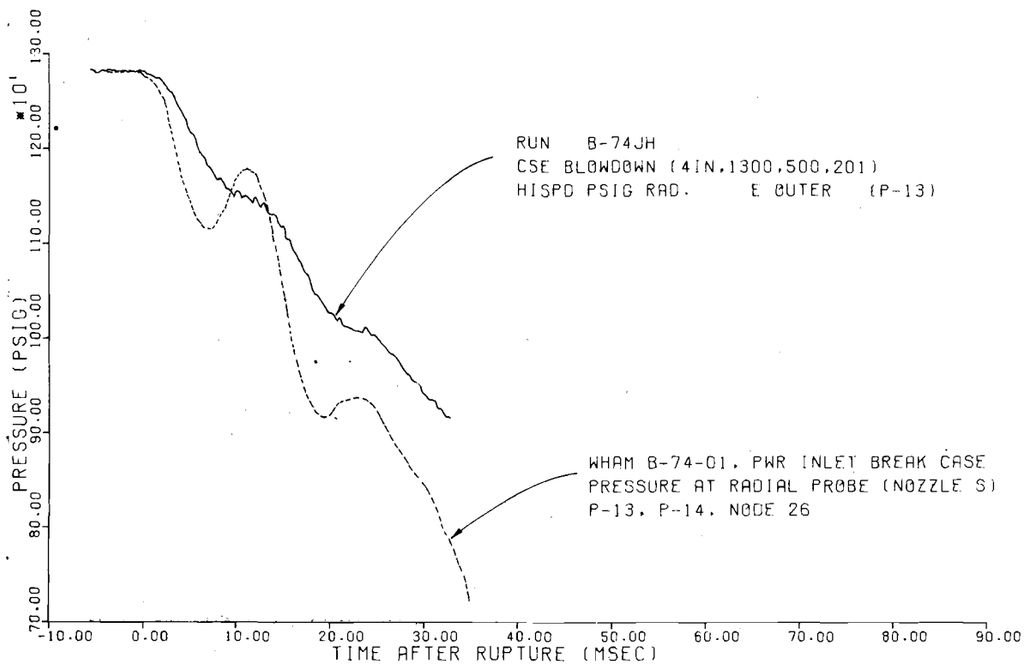

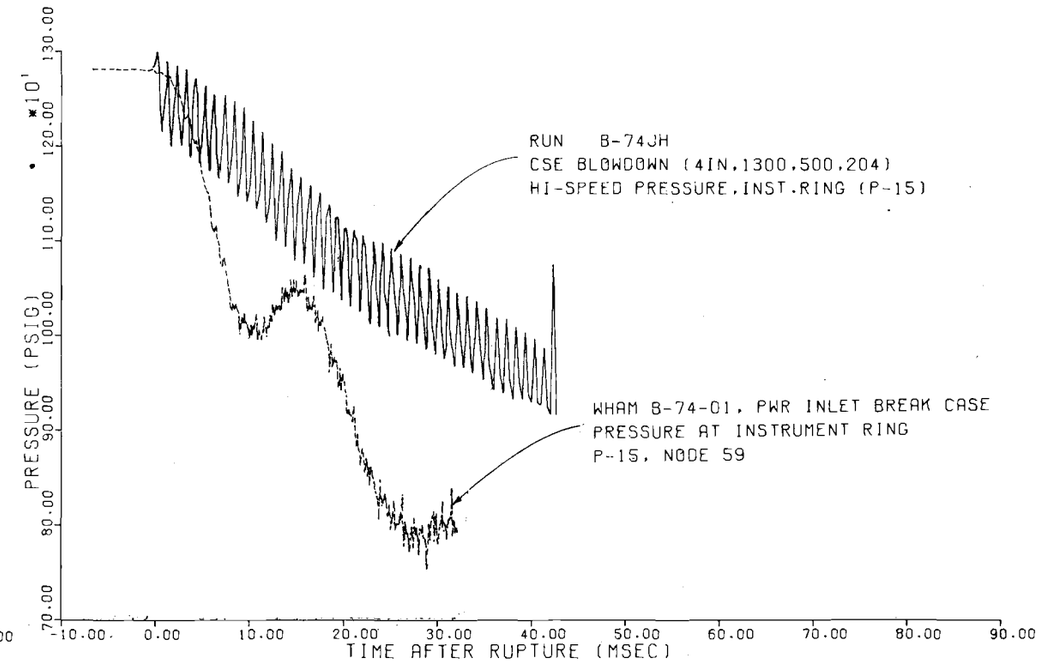

FIGURE 14. Comparison of WHAM With 4" Data

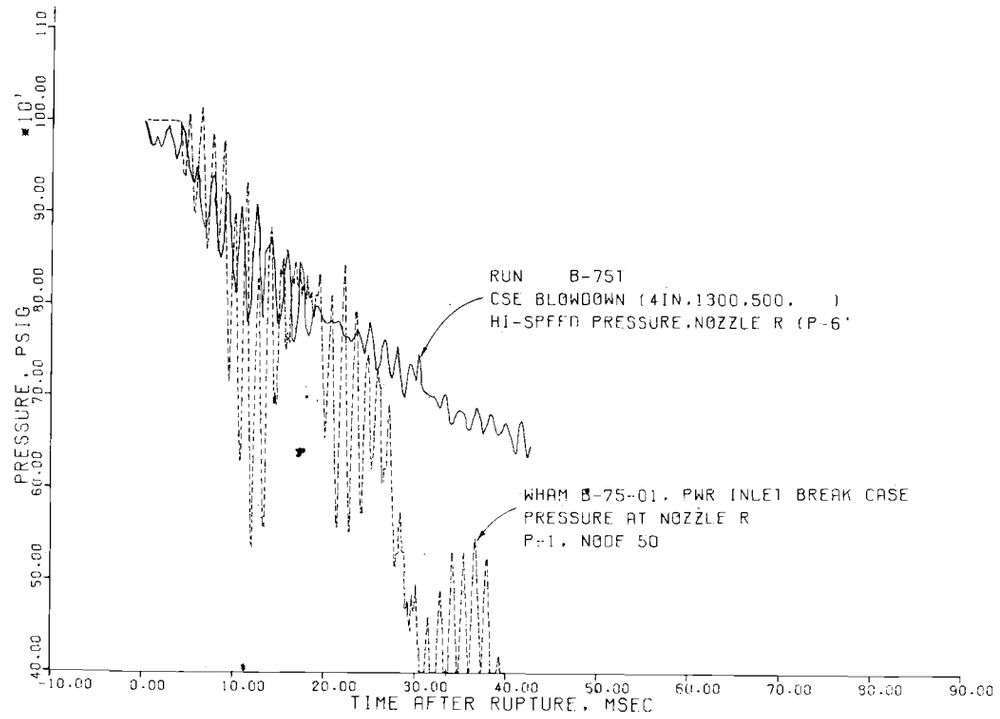

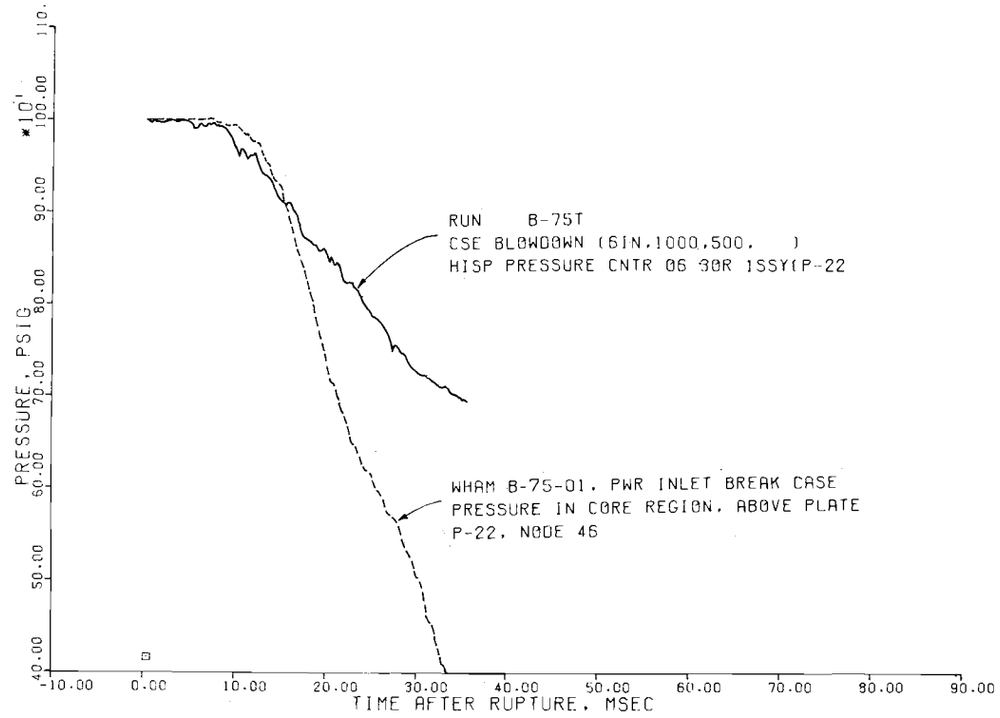

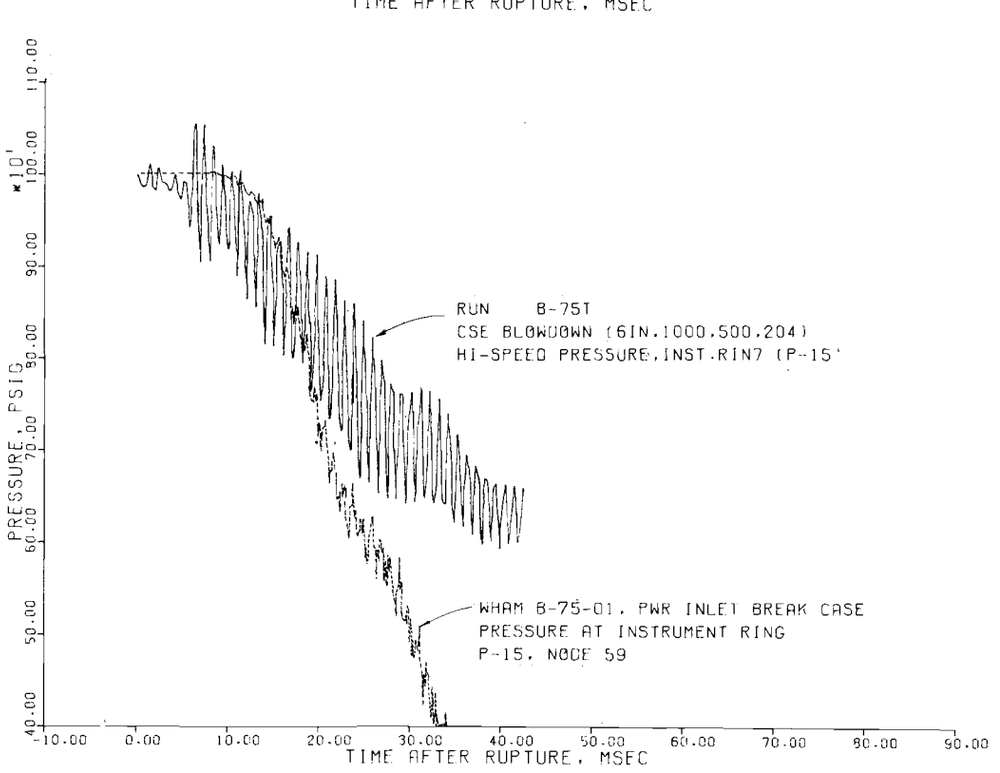

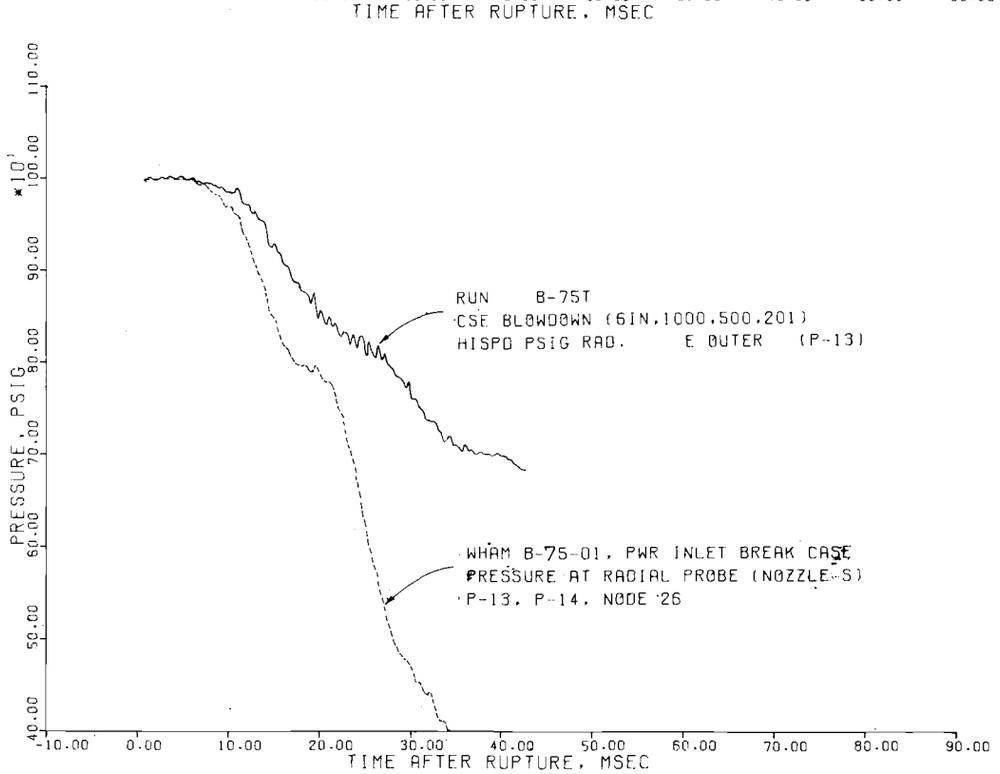

FIGURE 15. Comparison of WHAM With 6" Data

and barrel differential pressures are less than predicted and there are some phase errors. The core plate forces show some super position of a lateral force on the vertical force. No terms for losses were included in the WHAM predictions. The WHAM results show the general trend of the pressure reduction but seems to overpredict the rate of reduction and the size of the oscillations. There is considerable smoothing compared to WHAM of the major oscillations at the top of the vessel at the instrument ring. It is possible that some of this smoothing is due to leakage past the seal at the top of the core barrel but smoothing is also evident in the lower regions as well. The agreement is better for the larger break sizes. The pressure drop across the core barrel (shown in Figures 16, 17 and 18) or the supporting plate were less than the predicted values.

Since generally better agreement was obtained with WHAM for the simpler piping arrangements[2][6] than in these tests, one could say that the increased complexity or the less perfectly defined geometry of the core-in-vessel case causes a wider spread between prediction and measurement. If the measurements are to be believed, then WHAM (that is, one-dimensional analysis) shows itself to be a powerful, but not assuredly accurate, method of prediction in the form used here. Further development of the method might hinge on establishing loss factors and standard methods of treating area changes in plenums, core entrances, etc.

The results from WHAM predict the main features of the blowdown patterns even when applied in this relatively simple manner. In general, the "no loss" calculations have predicted pressure histories that are more severe than measured. A few minor frequencies that appear more prominent in the measured pressure differential (Figures 13 and 15) may be associated with the instrumentation. It appears that WHAM can be used to calculate order of magnitude (usually conservative) pressures and therefore impulses on major internal parts; but to use the WHAM results as input to calculations of dynamic response may not be successful because of slight frequency mismatches, non linear response, and possible dynamic-hydraulic interaction.

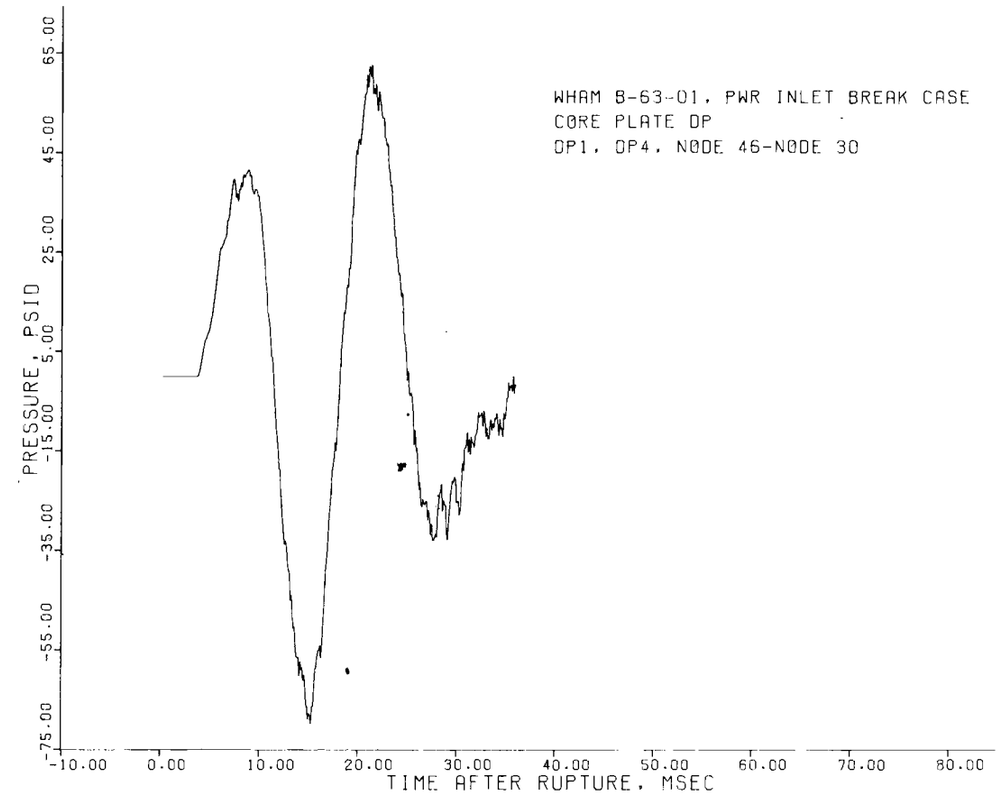

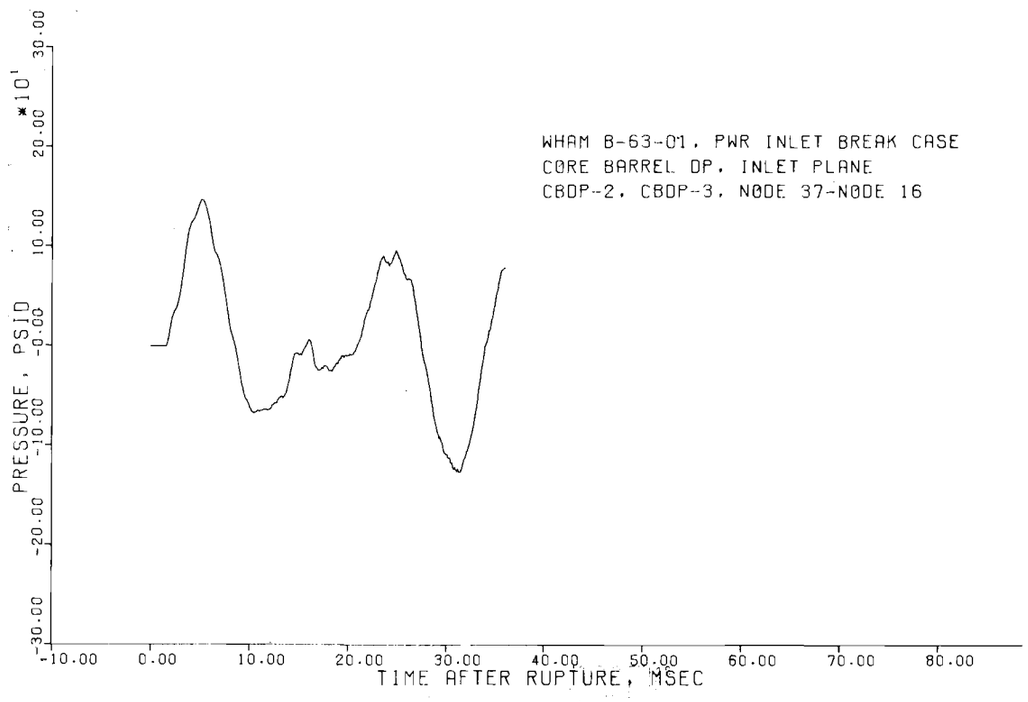

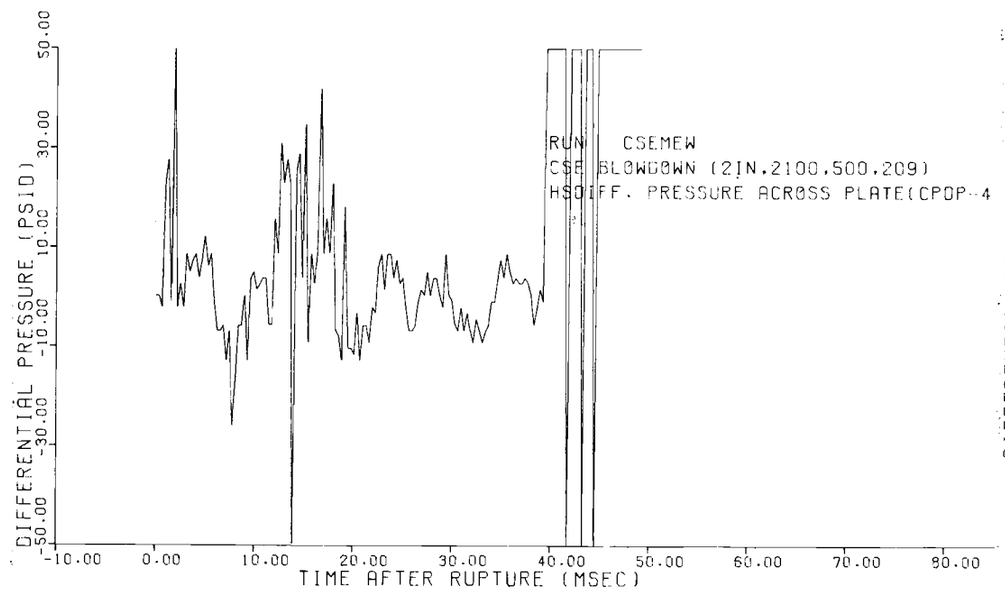

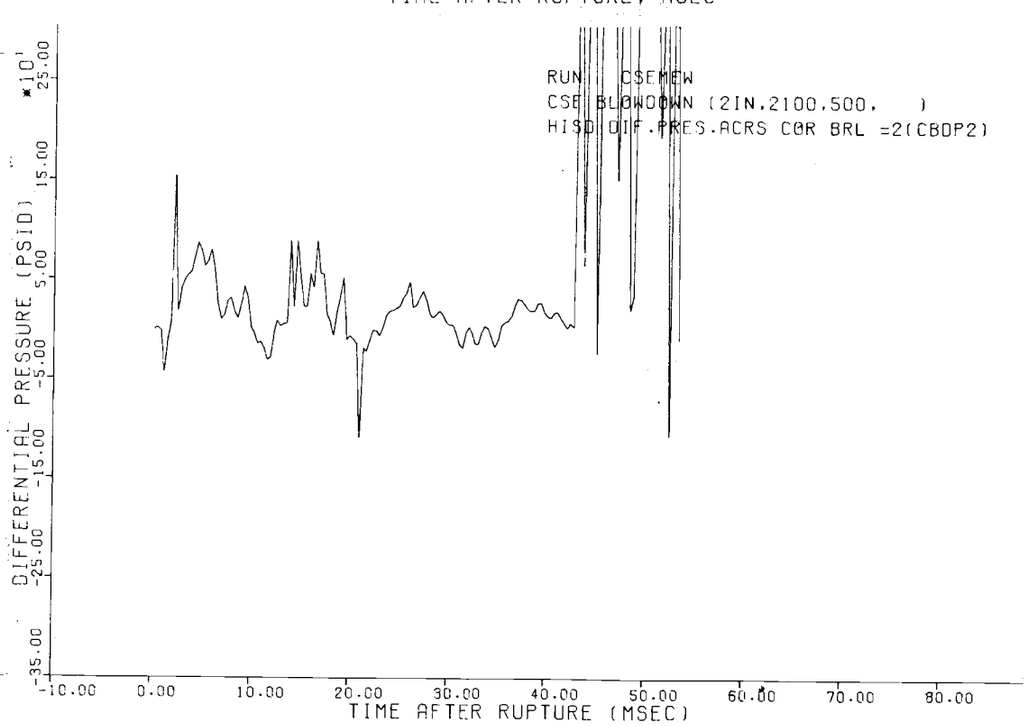

FIGURE 16. Comparison of WHAM Differential Pressure With 2" Data

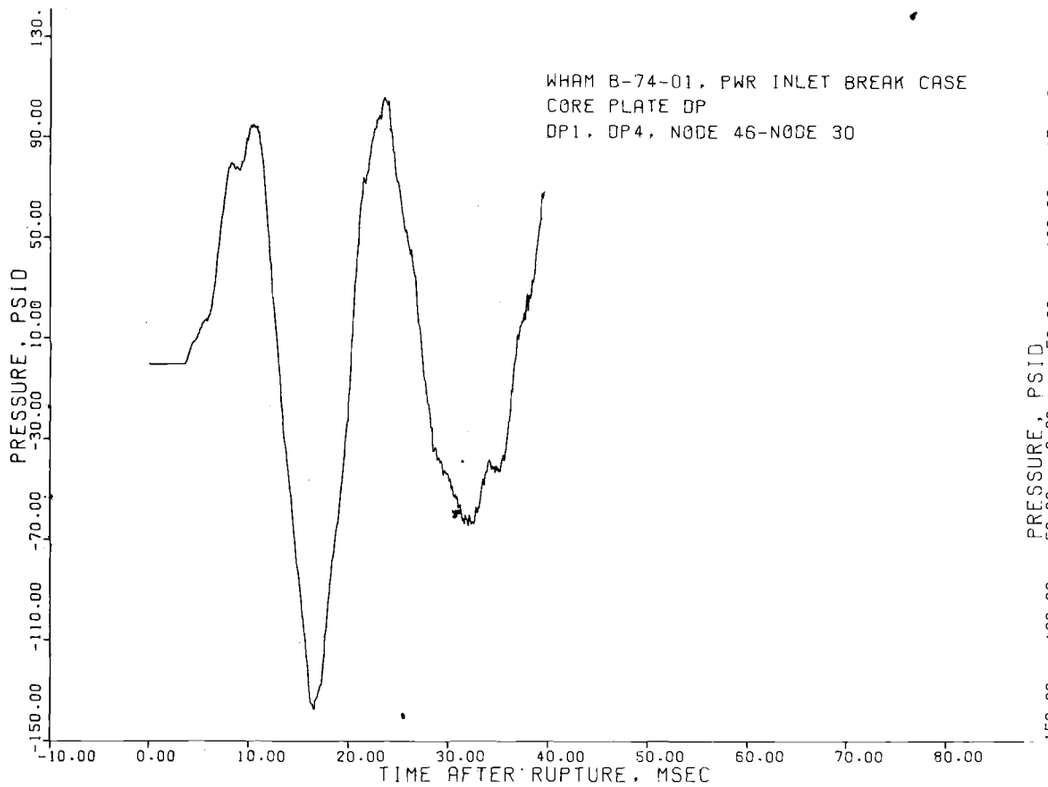

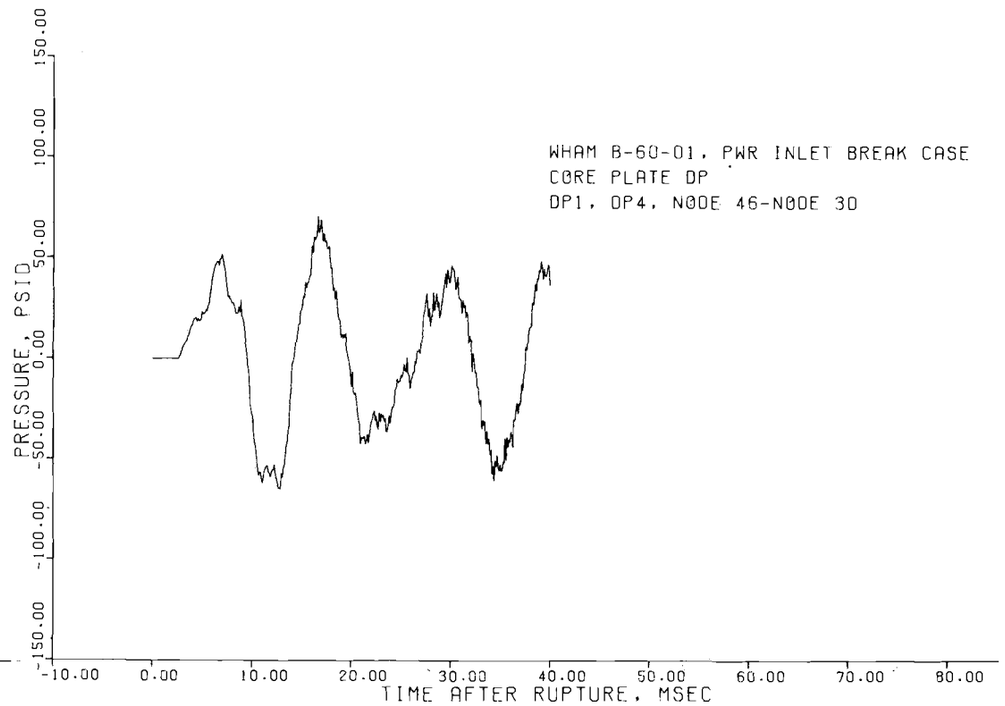

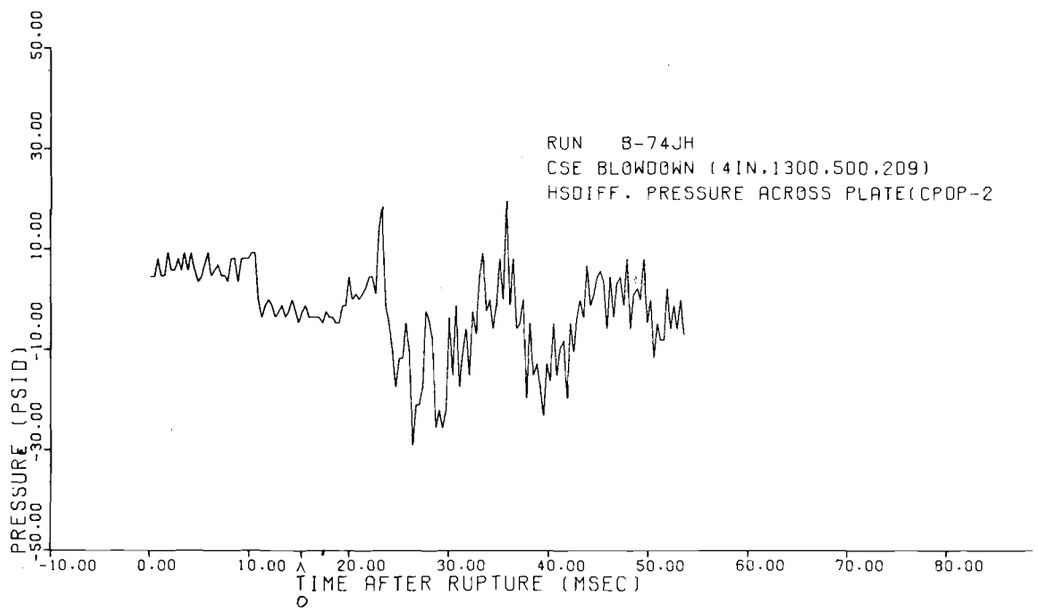

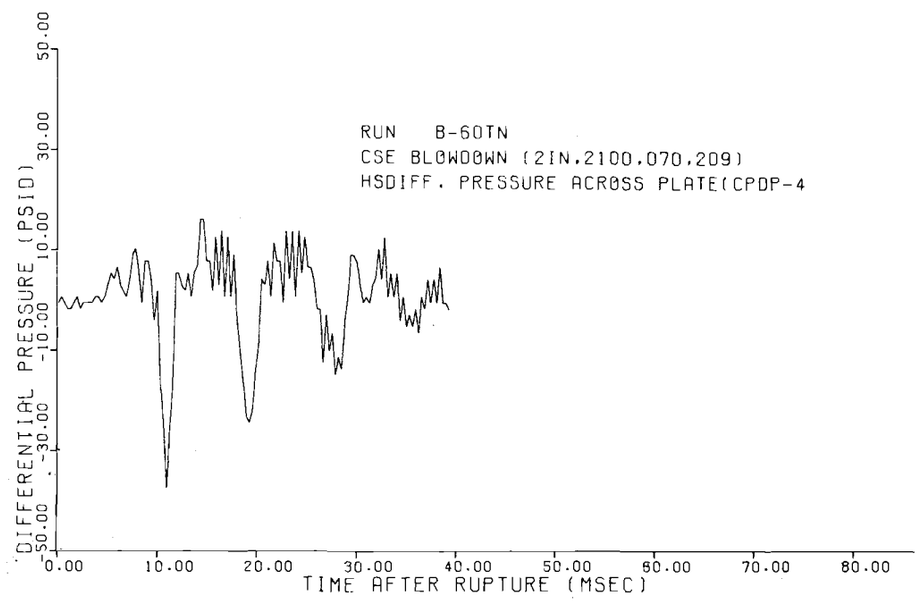

FIGURE 17. Comparison of WHAM Differential Pressure With 4" and Cold 2" Data

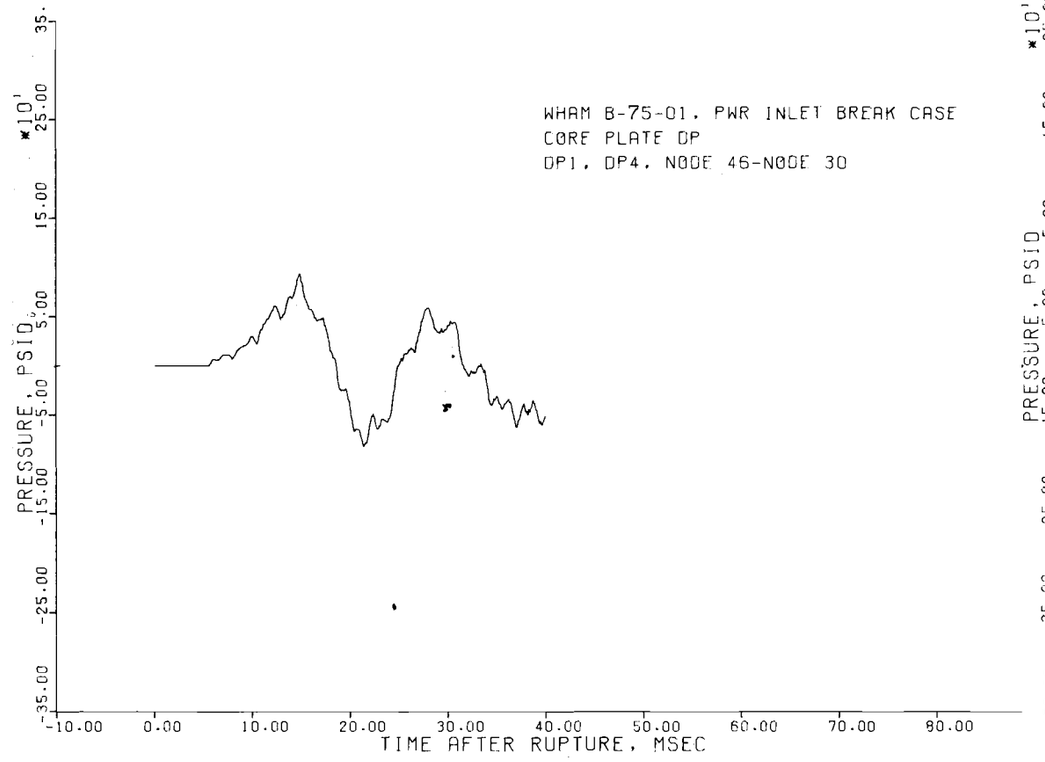

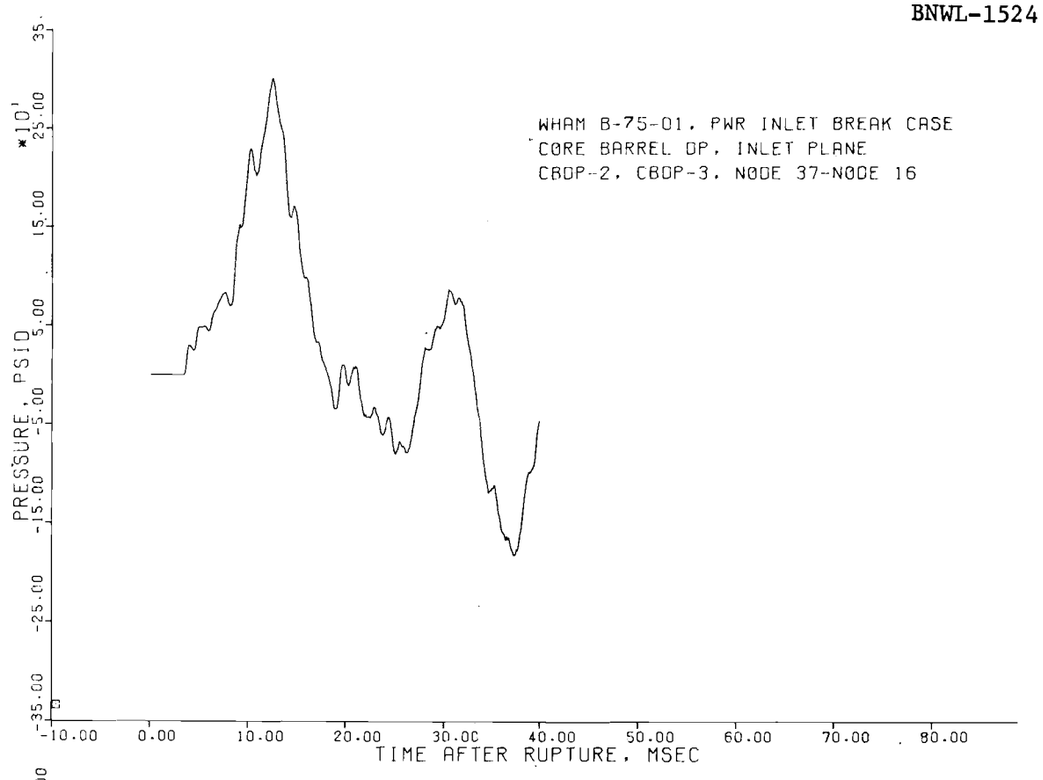

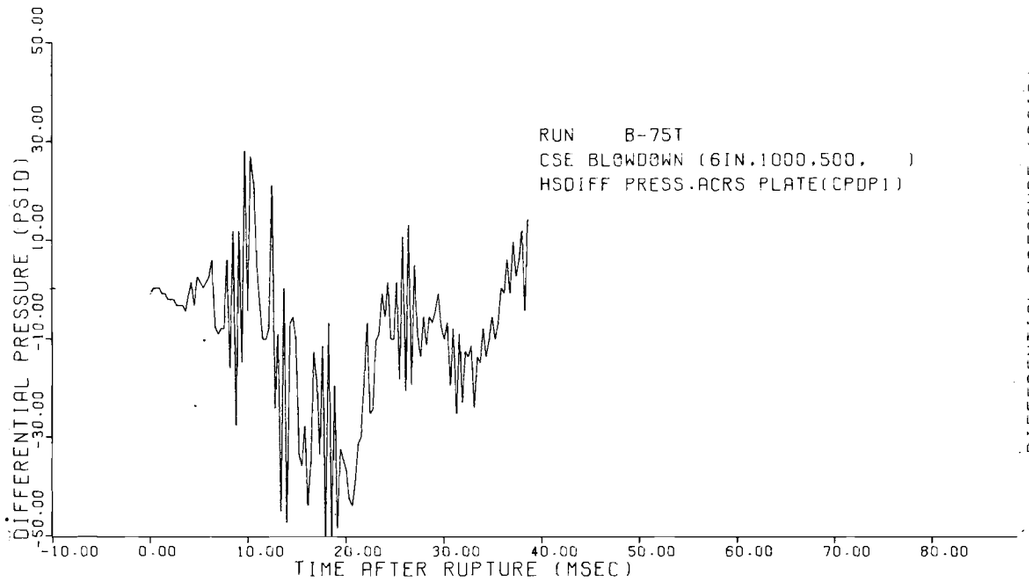

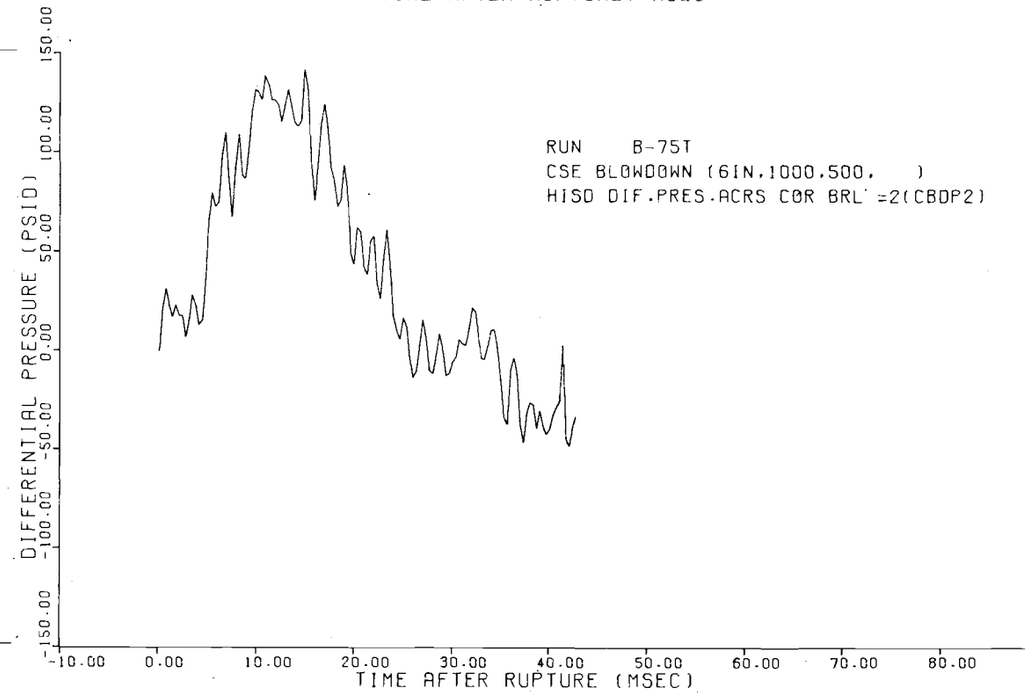

FIGURE 18. Comparison of WHAM Differential Pressure with 6" Data

TWO-DIMENSIONAL EFFECTS

An example of an effect which is not predicted by a straightforward calculation using WHAM is the non-uniformity of the forces on the supporting plate. Figure 19 shows the forces as measured by the plate supporting "strain bolts." The initial pulse on the bolts on the side of the barrel away from the break, bolts 5 and 6 (refer to Figure 18), was in tension while the bolts on the near side (bolts 1 and 8) were in compression. This was probably the result of the unequalized lateral foce on the barrel causing a tilting moment toward the break. Within 15-30 ms, however, the force had equalized and the bolts were receiving the up and down pulses in unison. The WHAM calculations were based on the layout assumption of a series of legs shaped as concentric rings at the outlet position of the annulus. The area of the rings were increased until the annulus cross sectional area was achieved. The lateral force on the barrel was taken equivalent to the unbalanced force across the barrel (pressure x area) for these ring shaped legs. The moment generated by this lateral force would be taken up by the bolts and the contact of the barrel with the vessel wall. The WHAM calculated lateral force shows some agreement early in time with the forces on the strain bolts but the data does not extend far enough to show whether the moment dies out or continues* as a condition of flow.

AMBIENT TESTS

The cold runs B-60 and B-73 were made to explore the subcooled decompression phenomenon by a relatively easy method not requiring heat-up. The results were nearly as comparable with WHAM calculations as were the high temperature blowdowns made later. For example, Figure 17 shows the pressure history and prediction for a location in 2" blowdown tests at 75°C and Figure 16 shows the same location results at 500 °C. The similarities outweigh the differences. The success of this method suggests that simple checks of the analytical treatments can be made for the full scale reactor

* During steady flow there may be a moment on the barrel caused by the Bernoulli pressure loss in the region of the outlet. It may be of interest to explore these aspects further.

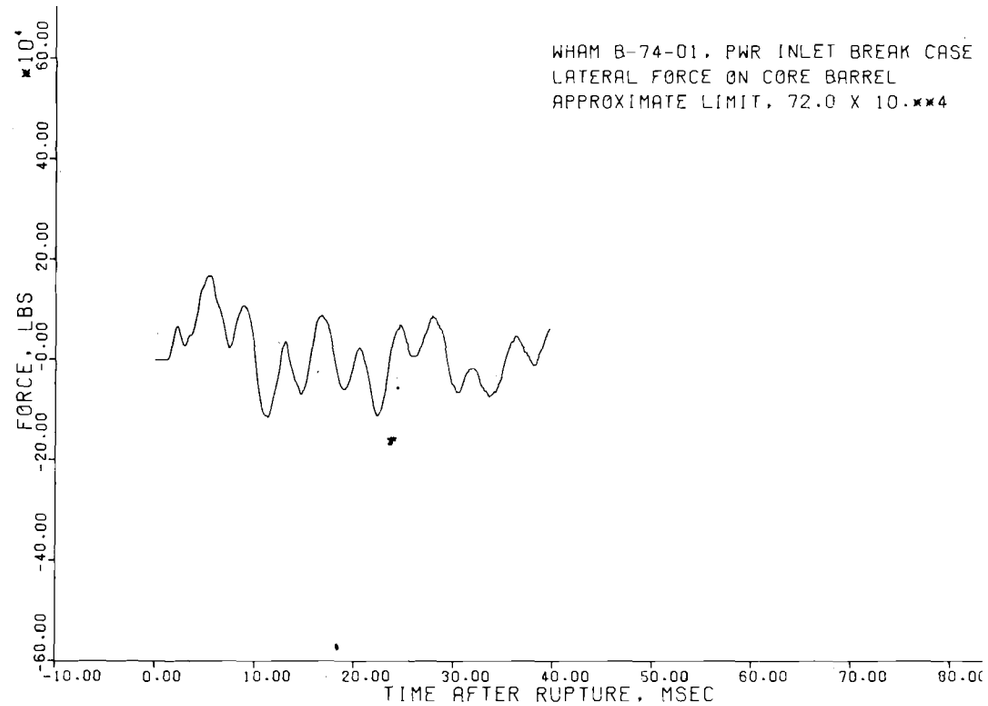

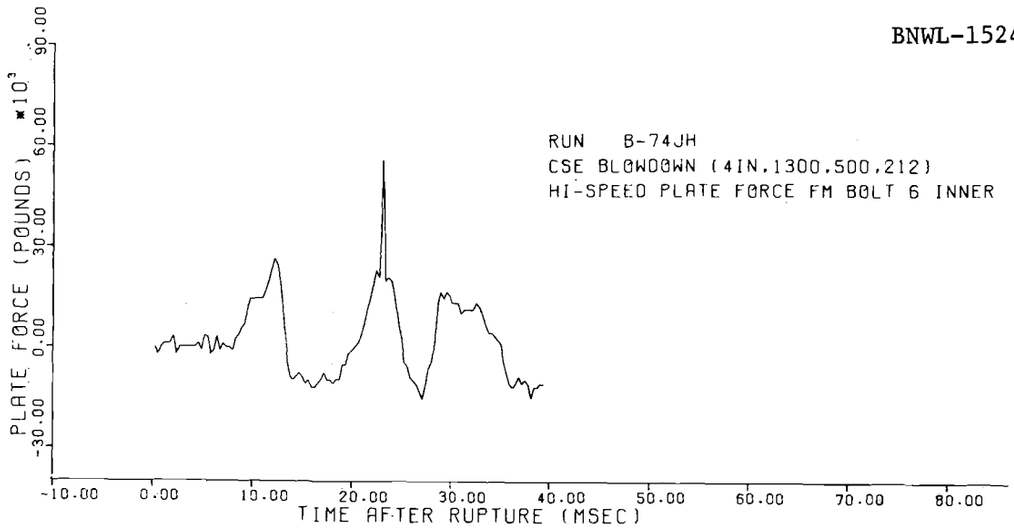

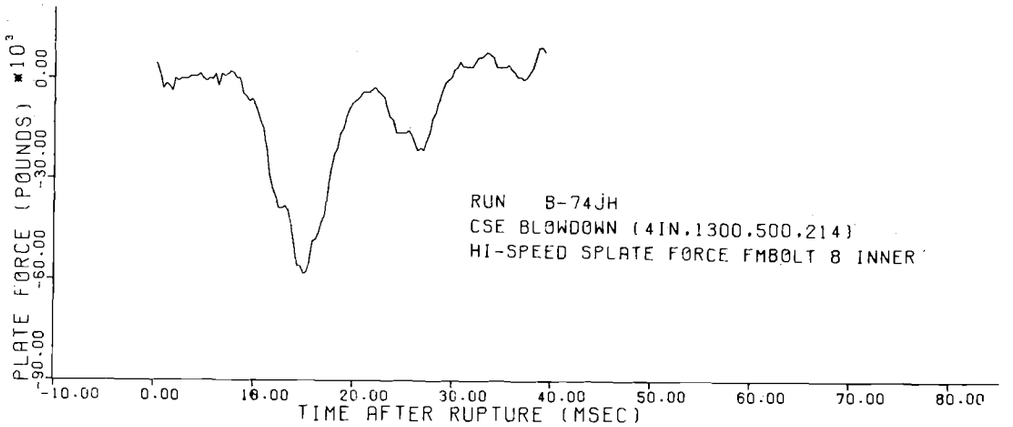

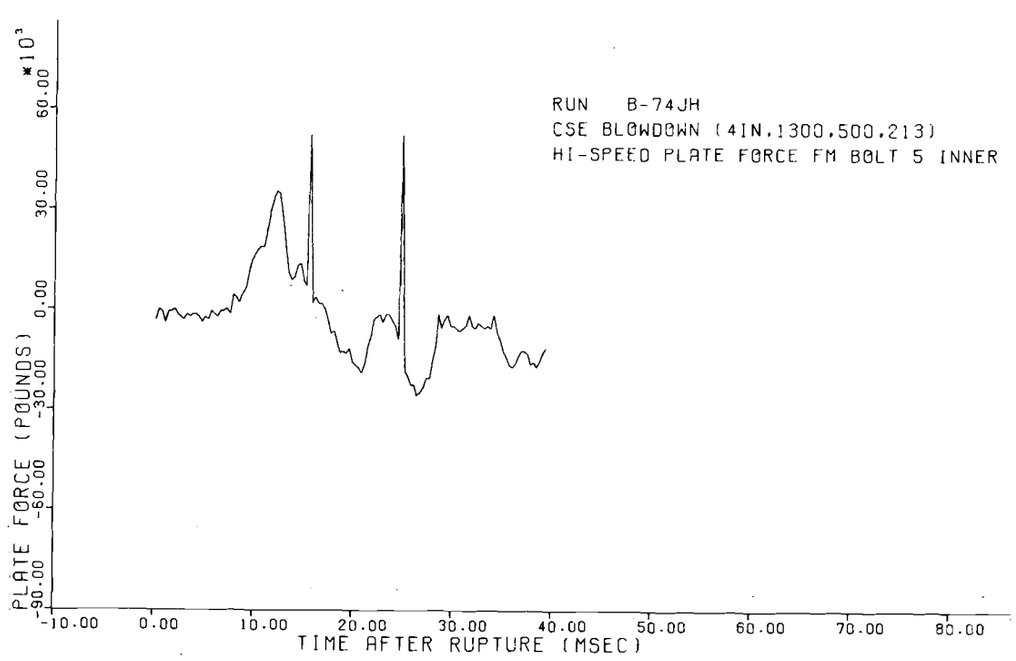

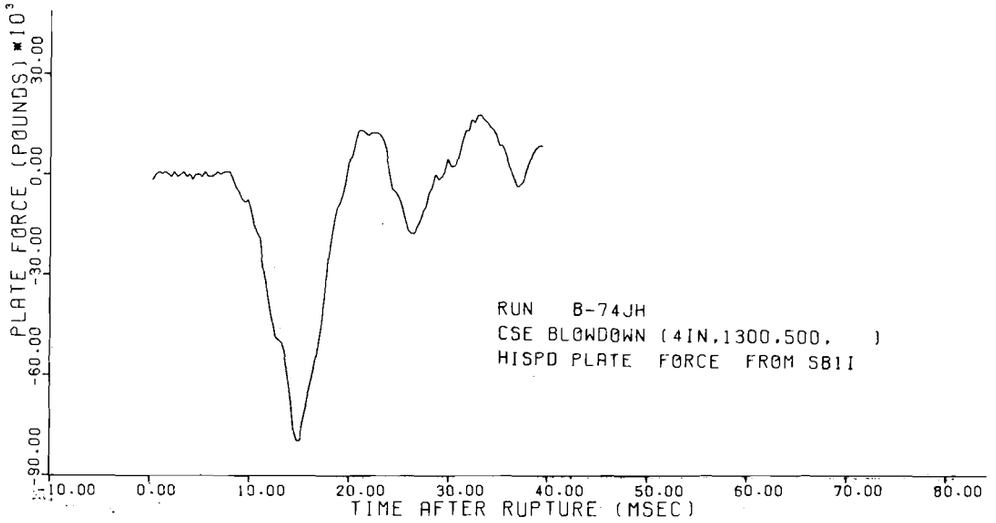

FIGURE 19. Comparison of WHAM Lateral Force With Bolt Loads

system by rupture disc testing of the pressurized system when filled with cold water. Subsequent recalculation using the propagation velocities at operating temperatures would then give a semi-verified prediction of the accident case.

SATURATED PORTION OF BLOWDOWN

After decompression to saturation is accomplished, the pressure history in the hot water filled system becomes a function of the equation of state of the fluid as it flashes to a vapor and of the critical two-phase flow condition at the break. Previous reports[2][5] deal extensively with this part of the blowdown. The most important questions to be answered by the experiments with the core in the vessel concerned the effect of the core on the rate of flow from the vessel, the liquid level during the blowdown and the liquid level remaining after the blowdown.

Rate of Flow

The results show that times required for blowdown are about the same with or without the core, but that slightly more liquid is actually removed in the core case; hence the actual flow rate might be slightly higher. The mass flux is probably a strong function of the break size.

A typical result of the CSE blowdown experiments has been that the mass flux as predicted by the Moody maximum flow slip model[9] has not been achieved in practice. However, the mass flow rate that was achieved could be predicted by using Moody's calculation and multiplying the break area by a factor. The factor was dependent on the size of the break. A "homogeneous", that is a non-slip, thermal equilibrium, model has also been used to predict mass flux of water from a broken pipe. This model predicts less flow than the Moody slip model roughly as shown by the ratio plot in Figure 20. Also, shown on the ordinate are typical coefficients for the different break orifices used in the CSE experiments. Although at first it might seem that the CSE coefficients are merely the manifestation of the homogeneous flow condition, this is not the case as evidenced by the typical range of enthalpies used in the CSE experiments. If the flow followed the homogeneous model, the experimental coefficients of all

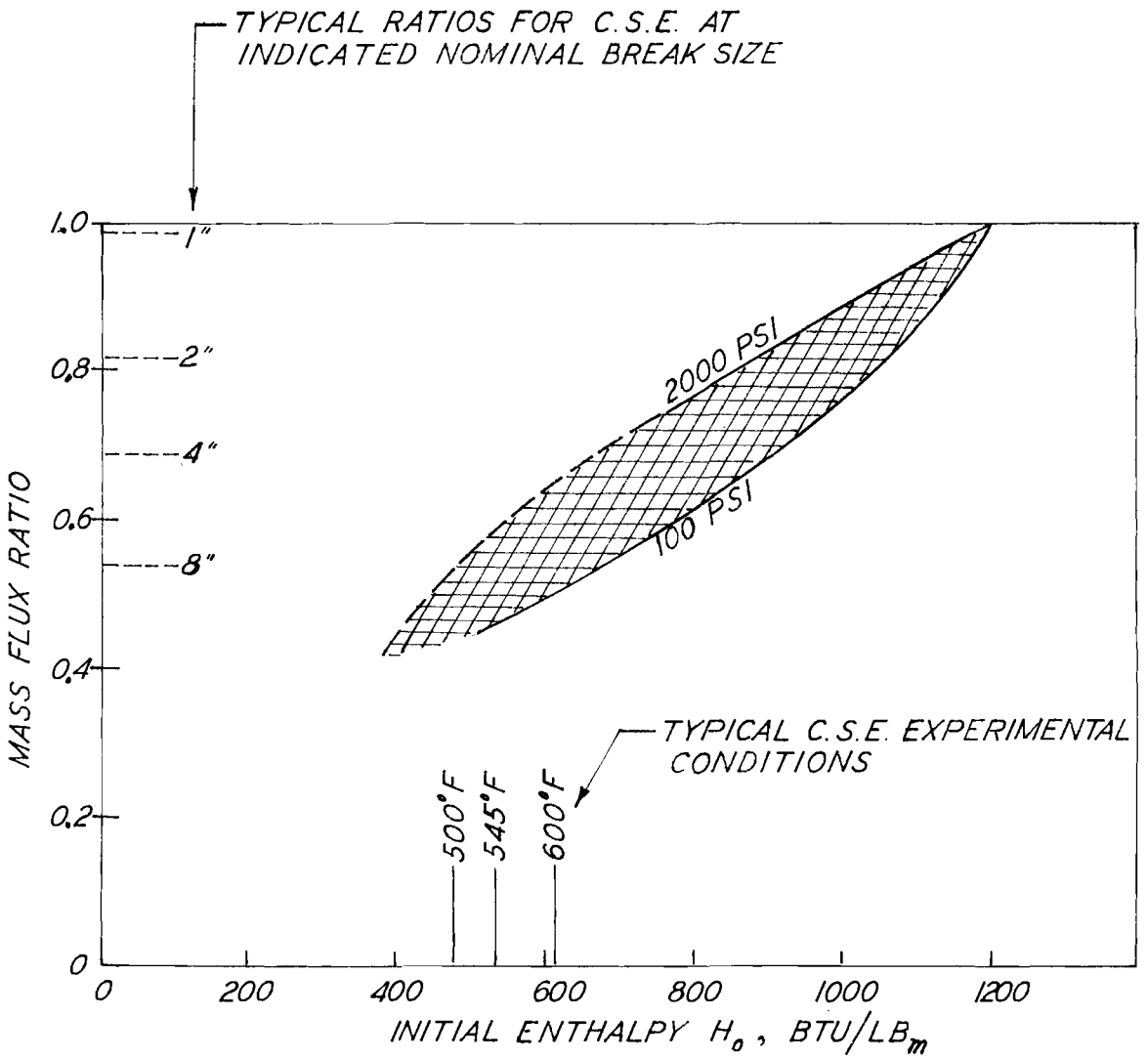

FIGURE 20. Ratio of Mass Flux (Homogeneous/Moody)

nozzle sizes should have been below 0.6. However, some coefficients are greater than this. The evidence gathered so far suggests that the flow is "metastable", i.e. non equilibrium flow. That is, not all the steam has been formed that would ultimately form at the pressure conditions of the exit duct. This allows the flow rate to be higher than for the "homogeneous" equilibrium, non-slip condition. The deviation from equilibrium seems to be influended by the size of the break, showing less metastability (and closer to homogeneous equilibrium flow) for the larger breaks. It is a matter of interest how phenomena seen for these sizes might be extrapolated to the pipe sizes involved in design basis accidents of nuclear power plants.

The influence of the core on the blowdown rate was small. A comparison of the results with a core and with a sieve plate can be made by referring to results of blowdowns made from the same nozzle and the same initial temperature. The latter were reported in Reference 2 (see Table 5 for comparable runs).

TABLE 5. Comparable Blowdowns
(Core Series and Sieve Plate Series)

Core Series Run No.	Sieve Plate Series Run No.	Nozzle Size Inches	Temperatures °F
B63	B50	2	500
B74	B51	4	500
B75	B52	6	500

For example, the pressure histories were not much affected by the presence of the core as can be seen in the comparison of 6" blowdown results in Figure 21.

LIQUID LEVEL

The liquid level history, however, was affected by the presence of the core (Figure 22). The effect is caused by the presence of the annular path of the fluid to the break. In the core case, the flow was

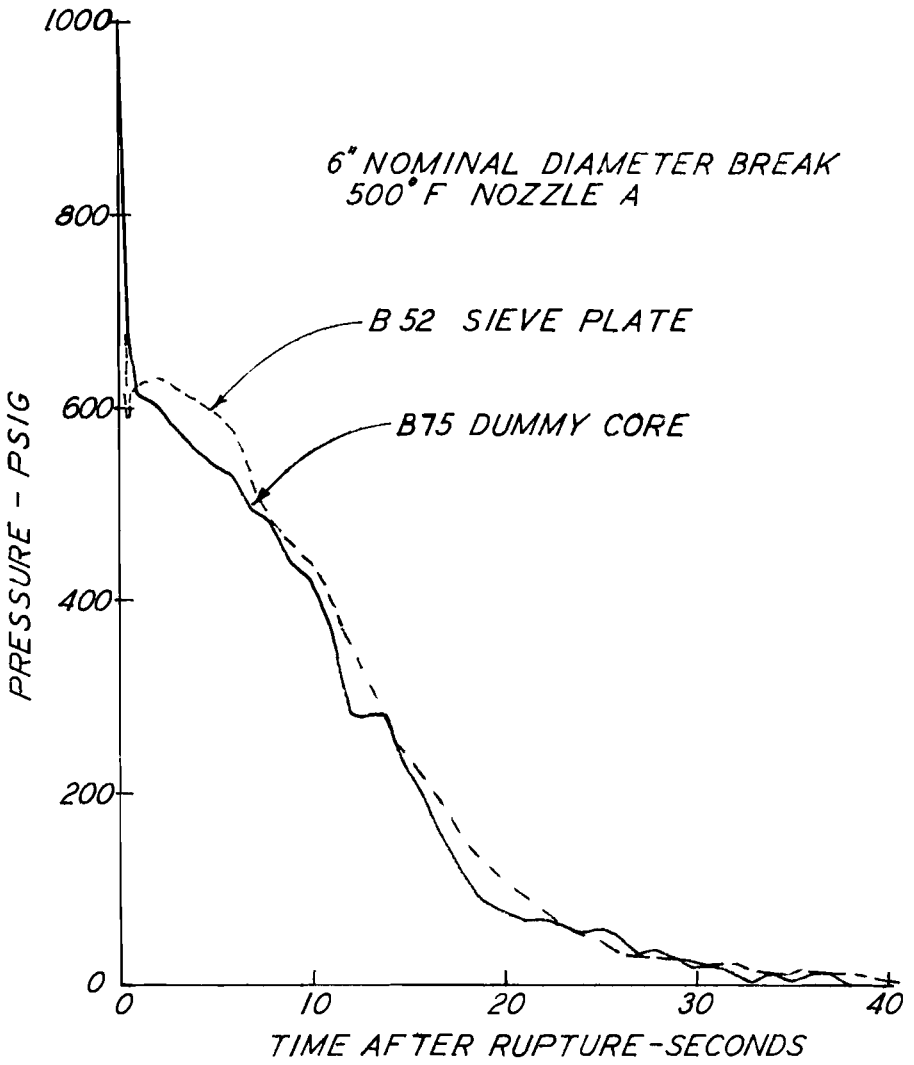

FIGURE 21. Comparison of Pressure Histories With and Without Core

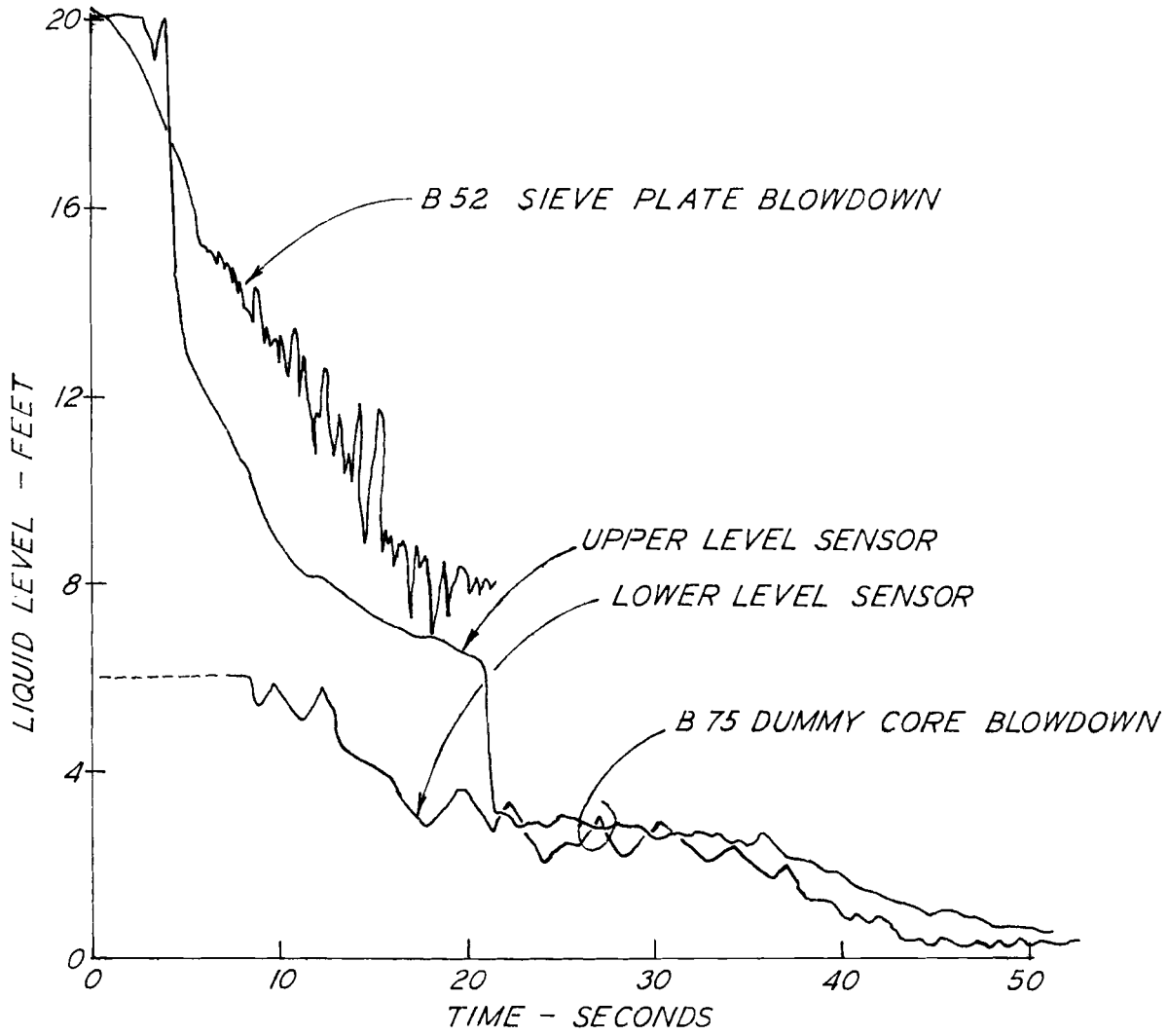

FIGURE 22. Level of Fluid in Vessel

generally downward toward the lower plenum and then upward in the annulus to the break. In the sieve plate case (Run B52) the flow was generally upwards toward the break for most of the flow from the vessel. The upward flow tended to hold the level up near the break but with the core the liquid level seemed to show a drop in the lower plenum even before the liquid was cleared out of the space below the core. This was probably caused by the liquid level dropping below the top of the core tubes, such that insufficient liquid came from above to make up that being lost from the lower plenum. Subsequent reduction in level in the core region was due to flashing and slow flow through the small leakage path through the plate at TDR probe seal. The downward path through the core results in an earlier uncovering of the core than would result from an upward path. Hence, an accurate assessment of the flow path in the reactor core during a design basis accident may be important to proper determination of the core heat-up rate.

LIQUID REMAINING AFTER BLOWDOWN

The core had the effect of reducing the amount of liquid remaining in the vessel after blowdown to a value similar to that which probably would have remained if the break were at the bottom of the core (i.e., at the core to annulus restriction). Figure 23 shows a comparison of several blowdowns made with and without core from the top nozzle. The figure also shows the differences in the amount remaining as a result of changing the height of the break. The top nozzle is about 12 ft above the bottom of the vessel, the middle nozzle about 4 ft, and the core plate about 6 ft above the bottom. The presence of the core apparently reduces the amount of liquid remaining for the same break nozzle position. The mass remaining is only a little greater than for the case of the middle nozzle break. Although the fraction remaining is slight and the mass differences small, the effect may be important when full scale reactors are considered in which the height differences are larger. Analysis should be used to properly account for these effects for scaling to the full size reactor rather than using the ratios given in Figure 23 for direct application.

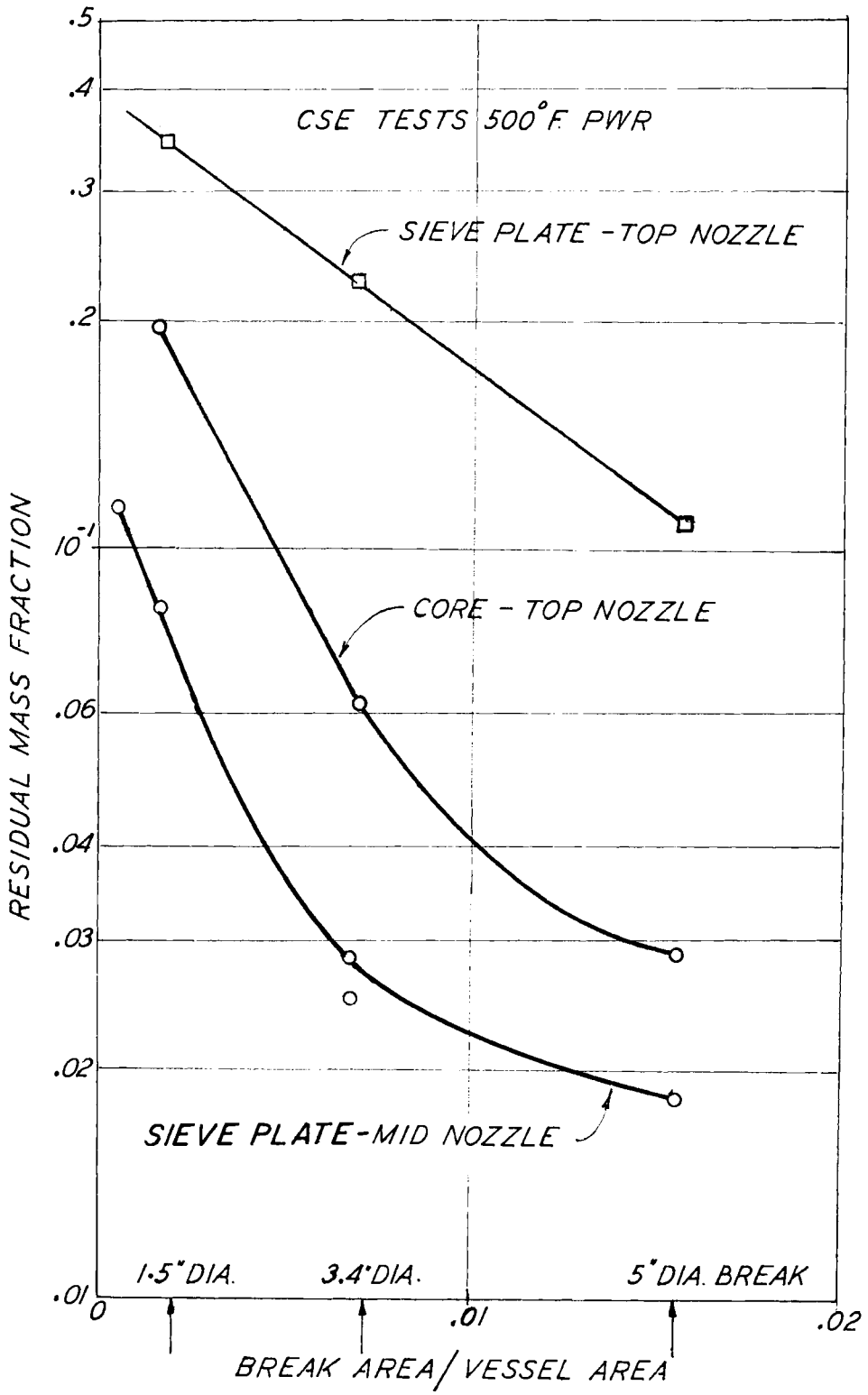

FIGURE 23. Liquid Remaining

REFERENCES

1. C.E. Linderoth, Containment Systems Experiment, Description of Experimental Facilities, BNWL-456, Richland, Wash., Feb. 1970.

2. R.T. Allemann, et al, Coolant Blowdown Studies of a Reactor Simulator Vessel Containing a Perforated Sieve Plate Separator, BNWL-1463 (1971).

3. C.H. Henager and J.M. Smith, Design Criteria for Phase II Dummy Hydraulic Core for Containment Systems Experiment Reactor Simulator, BNWL-CC-816, Oct. 1966.

4. LOFT and STEP Program Quarterly Reports and Program Document Series, Phillips Petroleum Company, Idaho Nuclear Company, Idaho Falls, Idaho, 1964-1969.

5. R.T. Allemann, et al., Experimental High-Enthalpy Water Blowdown from a Simple Vessel Through a Bottom Outlet, BNWL-1411, 1970.

6. R.T. Allemann, et al, High-Enthalpy-Water Blowdown Tests from a Simple Vessel Through a Side Outlet, BNWL-1470 (1971)

7. G.E. Gruen, WHAM Prediction of Semi Scale Results, IN-1431, Oct. 1970.

8. S. Fabic, Computer Program WHAM for Calculation of Transients in Liquid Filled Piping Networks, Argonne Code Center Reference Material Abstract 278, Nov. 1967.

9. F.J. Moody, "Maximum Flow Rate of a Single Component, Two-Phase Mixture, Trans ASME J. of Heat Transfer, Vol. 87-C, p. 134, 1965.

10. Micro-Measurements, Tech. Notes-129, August 1968.

APPENDIX A

NOTES ON THE DEVELOPMENT OF A DIFFERENTIAL PRESSURE TRANSDUCER

APPENDIX A

Notes on the Development of A Differential Pressure Transducer

A differential pressure transducer was designed which can measure the differential pressure across the core plate and survive the hostile environment of the fluid in the simulator vessel during blowdown. This same basic design of transducer was used to measure the differential pressure on the core barrel.

Two designs of an instrumented diaphragm differential pressure transducer were proposed and tested statically at ambient temperature. The design selected for use in the core plate of the CSE simulator vessel had the diaphragm as an integral part of the transducer case. The sensing element was a weldable uniaxial resistive strain gage mounted in the center of the diaphragm. The resultant transducer would function in a water environment to 600 °F if corrections were made to relate to the ambient temperature calibration of data obtained. Two corrections which had to be applied to calibration data at 70 °F involve the gage factor of the sensor and change in modulus of elasticity of the diaphragm material.

The transducer was calibrated to ±50 psid. The resultant measured strain vs. pressure was linear and the maximum static calibration errors were ±3.7% of the applied differential pressure or the error may be expressed as ±2.0% of the peak differential pressure applied. The natural frequency was calculated to be greater than 4800 Hz.

The second design consisted of a 12 mil Inconel X-750 diaphragm clamped in a stainless steel case. This thin diaphragm did not produce an acceptable transducer; however, for larger thickness, this design was thought to be sufficient. Further discussion of this design is given in the text which follows.

DESIGN AND CALIBRATION

The completed differential pressure transducer had to be installed in an existing 2 1/4" - 8 threaded hole in the core plate. The required

differential pressure range was $\pm$50 psid. The environment in which the transducer was to be used is 500 °F water with pressure pulses at nominal rates of 100 Hz. As with all transducers, maximum reasonable accuracy, sensitivity, and reliability were desired. To meet the above requirements, it was decided to design and construct a strain gage instrumented diaphragm ΔP transducer.

Weldable resistance strain gages were selected as the sensing elements. When properly hydro-tested, this gage has proven to be reliable in the harsh environment within the simulator vessel.

The analysis of the diaphragm is based on the following assumptions:

1. Uniform diaphragm thickness
2. Small deflections
3. Infinitely rigid clamping around the diaphragm periphery
4. Perfectly elastic behavior
5. The presence of the sensing element is negligible

With these assumptions, the radial strain is

$$\varepsilon_r = \frac{3 R_o^2 P\nu}{8 Et^2}\left[\left(\frac{3}{\nu} - 3\nu\right)\frac{r^2}{R_o^2} - \frac{1}{\nu} + \nu\right]$$

where

P = differential pressure

r = radius

R_o = diaphragm radius

ν = Poisson's ratio

t = diaphragm thickness

E = modulus of elasticity

A plot of this equation for radial strain is shown in Figure A-1. For interest, the tangential strain is also shown.

Maximum signal would be obtained if the point of maximum strain were instrumented ($r = R_o$). Because of physical contraints, the strain gage could not be located here. This maximum strain was the determining factor for the diaphragm dimensions. The second choice location, the center of

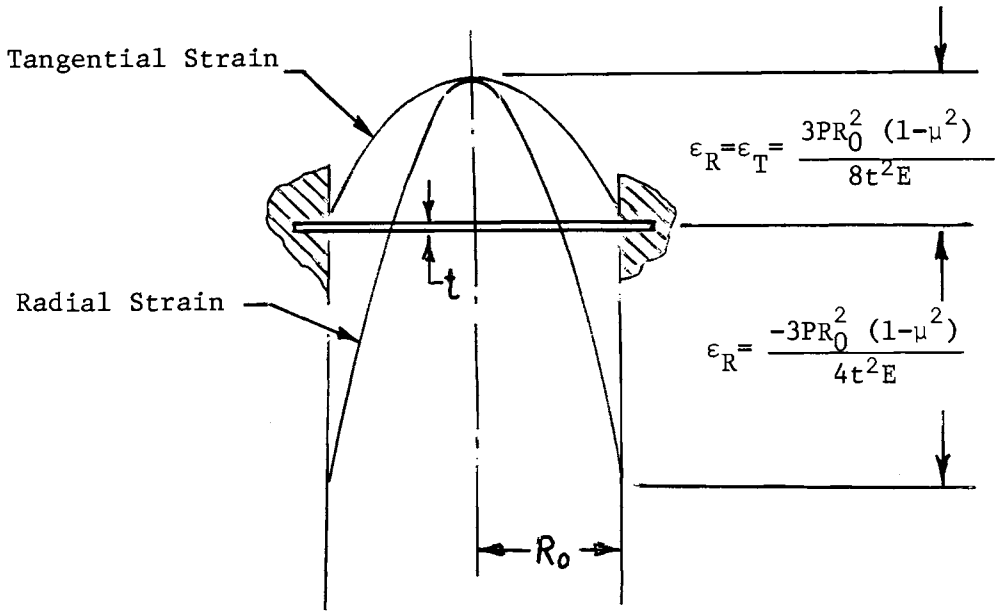

Figure A-1. Strain Distribution in Clamped Diaphragm

the diaphragm, was where the gage was located. The active element of the gage was to be as short as possible because the radial strain drops off rapidly (Figure A-1) and the signal from the gage is the integrated value over the gage length.

The resonant frequency of such a diaphragm is

$$f_n = \frac{9.26t}{R_o^2} \quad \frac{E}{\gamma(1-\nu^2)}$$

γ is the density of the diaphragm material.

The radial strain at $r = R_o$ is the maximum strain in the diaphragm and is

$$\varepsilon_r = \frac{3 R_o^2 P (1-\nu^2)}{4t^2 E}$$

This is twice the strain at r = o for the same differential pressure. The larger the magnitude of strain at $r = R_o$, the greater would be the transducer's response per psid applied. It is natural then, to make the diaphragm of a material with a high yield strength. Such a transducer was built using a 12 mils 1.25 inch diameter Inconel X-750 (E_{yd} > 3000 at 600 °F) diaphragm placed in a stainless steel case. The diaphragm was not clamped tight because of differences in the thermal expansions of the two materials. The radial clearance was 2 mils, and the axial clearance was 1/2 mil.

Static calibration of this differential pressure transducer resulted in errors of ±10 psid throughout the range of ±50 psid. The difficulty is thought to be related to minor imperfections in the case or small particles of dirt between the diaphragm and the case which tend to change the static of strain in the diaphragm. Particles of dirt may jam between the diaphragm and case which, when the pressure is removed, do not allow the diaphragm to return its free state. It is believed that with larger and thicker diaphragms, (where the presence of dirt would produce negligible effects) a "clamped" diaphragm of this type would produce a usable transducer. Such a transducer was built for use in the core barrel wall of the CSE simulator vessel.

Because of the difficulties encountered with the mechanical configuration of the Inconel diaphragm in the small differential pressure transducer, a unit construction design was built and tested.

This transducer was machined from stainless steel and is shown in Figure 3.5. This material has a yield strain of 730 με. The experimental strain measured for this differential pressure was 330 με, and the agreement is considered satisfactory.

Two additional factors had to be included before the data obtained from this transducer could be evaluated. The most significant was the change in modulus of elasticity of stainless steel with temperature. For stainless steel

$$E_{70°F} = 28 \times 10^6 \text{ psi}$$

$$E_{550°F} = 24.8 \times 10^6 \text{ psi}$$

At 550 °F, the με/psid value will be 1.129 the value of 70 °F (static calibration value) because of this decrease in modulus. The second temperature correction was the gage factor of the weldable strain gage. The gage factor is approximately 5% lower at 550 °F than at 70 °F. The gage was connected in a 3-wire Wheatstone bridge. The net effect of the decrease in gage factor was a 5% decrease in voltage output for a given strain value.

The data recording system was calibrated using parallel calibration resistors. The overall indicated response (ΔP) produced by the calibration resistors was 12.9% (change in modulus) -5% (change in gage factor) or 7.9% higher at 550 °F than at 70 °F. That is, the MV/psid value at 550 °F were 1.079 times this value at 70 °F when all other parameters are unchanged. The needed calibration information is shown in Table A-1

Notes:

1. Calibration resistors to be ±1% or better.
2. Calibration must be performed at 70 °F.

TABLE A-1

CALIBRATION DATA

R_{cal} ohms	Indicated ΔP 70 °F - psid	Indicated ΔP 550 °F - psid
800K	14.39	13.34
600K	19.07	17.67
400K	28.42	26.34
200K	57.41	53.21
150K	76.67	71.06

CONCLUSIONS AND RECOMMENDATIONS

An accurate differential pressure transducer with sufficient sensitivity has been developed for ΔP measurements on the CSE simulator vessel core plate. This transucer will survive the 550 °F water environment of the simulator vessel.

It is recommended that high yield strength material be used in future construction of such ΔP transducers of this design since the potential signal which can be obtained from the transducer is directly dependent on this strength.

If such measurements of differential pressure are to be made in a less hostile environment, it is recommended that one consult Reference 10.

APPENDIX B

DATA PLOTS

APPENDIX B

Data Plots

This appendix contains some of the plots of raw data taken during the core series blowdown tests. Fiscal limitations did not allow all data to be correctly zero adjusted. Also available but not given here are other pressure and temperature histories of the fluid, force data, and the data of temperatures and strain in the bottom of the vessel.

TABLE B-1. Figure Numbers - Appendix B

T = See main body of report

	Run Number			
Low Speed Data	B-63	B-74	B-66	B-75
Weight of Water		B6	B12	B18
Nozzle Thrust Force		B6		B18
Level of Fluid Remaining	B1	B7		T
Pressure at Exit (P-10)	B1	"	B12	B18
Pressure at Exit Pipe (P-4)	B1	"	B12	B18
Pressure,Nozzle R (P-6)	B1	"	B12	B18
Pressure,Instrument Ring (P-15)	B1	"	B12	B18
Pressure, Radial Probe (P-13)	B1	"	B13	B19
Pressure,Nozzle C (P-12)	B1	B8	B13	B19
Pressure,Core, Side Near A (P-20)	B1	B8	B13	B19
Pressure,Core, Side Opposite A (P-21)	B2	B8	B13	B19
Pressure,Center of Core Assembly (P-22)	B2	B8	B13	B19
Temperature,Exit Pipe T-3	B2	B8	B13	B19
Temperature,Nozzle R T-1	B2	B8	B14	B20
Temperature,Nozzle J T 2	B2	B9	B14	B20
Temperature,Inst. Ring T-15	B2	B9	B14	B20
Temperature,Lower Plenum TWG 7	B2	B9	B14	B20
High Speed Pressure Data				
Exit Orifice (P-10)	B3		B15	B20
Exit Pipe (P-4)	B3		B15	B20
Nozzle R (P-1)	B3	T	B15	B20
Core Near A (P-20)	B3	B9	B15	B21
Core Opposite A (P-21)	B3	B9	B15	B21
Center of Core (P-22)	B4	B10	B15	
Radial Probe Outer (P-13)		T	B16	
Radial Probe Inner (P-14)		B10	B16	B21
Diff. across Plate CPDP-1	B4	B10	B16	B21
Diff. across Plate CPDP-4		B10	B16	B21
Diff. across Barrel CBDP-1	B4	B11	B16	B21
Diff. across Barrel CBDP-2		B11	B16	B22
Diff. across Barrel CBDP-3	B4	B11	B17	B22
Plate Force SB 1 I	B4		B17	B22
5 I	B4		B17	B22
6 θ	B5	B11	B17	B22
6 I	B5		B17	
8 I	B5		B17	

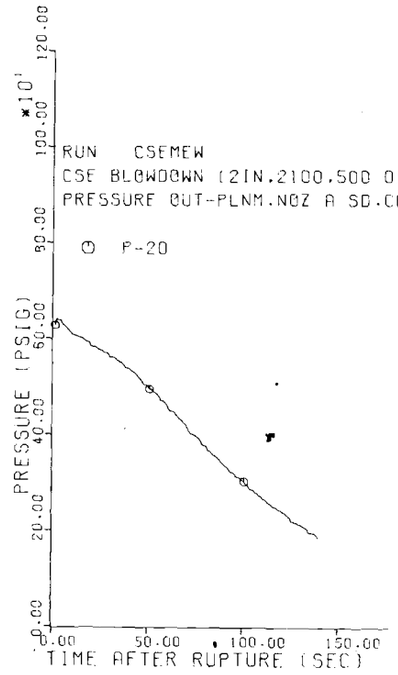
RUN CSEMEW
CSE BLOWDOWN (2IN.2100.500 013)
PRESSURE OUT-PLNM.NOZ A SD.CB (P-20)
P-20
PRESSURE (PSIG)
TIME AFTER RUPTURE (SEC)

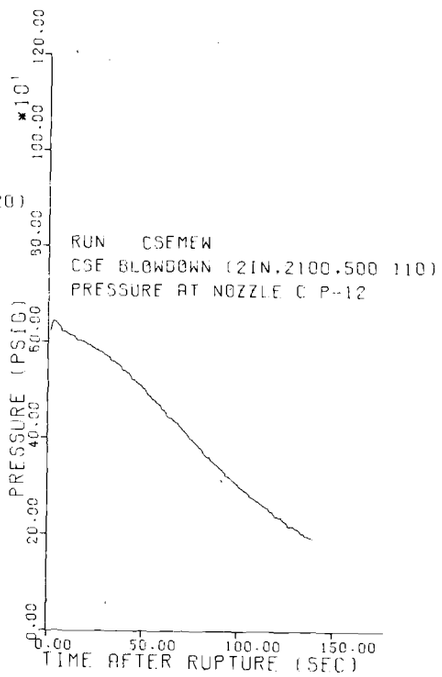
RUN CSEMEW
CSE BLOWDOWN (2IN.2100.500 110)
PRESSURE AT NOZZLE C P-12
PRESSURE (PSIG)
TIME AFTER RUPTURE (SEC)

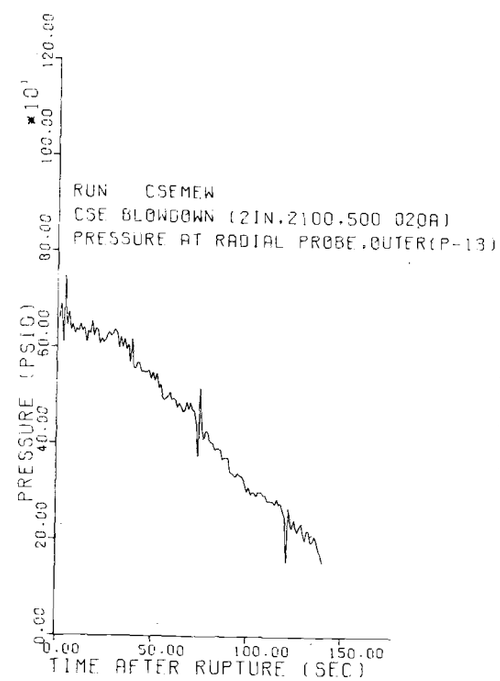
RUN CSEMEW
CSE BLOWDOWN (2IN.2100.500 020A)
PRESSURE AT RADIAL PROBE,OUTER(P-13)
PRESSURE (PSIG)
TIME AFTER RUPTURE (SEC)

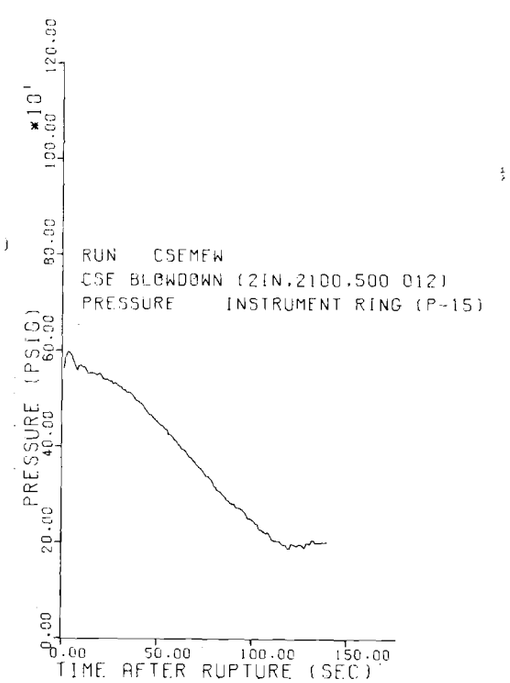
RUN CSEMEW
CSE BLOWDOWN (2IN.2100.500 012)
PRESSURE INSTRUMENT RING (P-15)
PRESSURE (PSIG)
TIME AFTER RUPTURE (SEC)

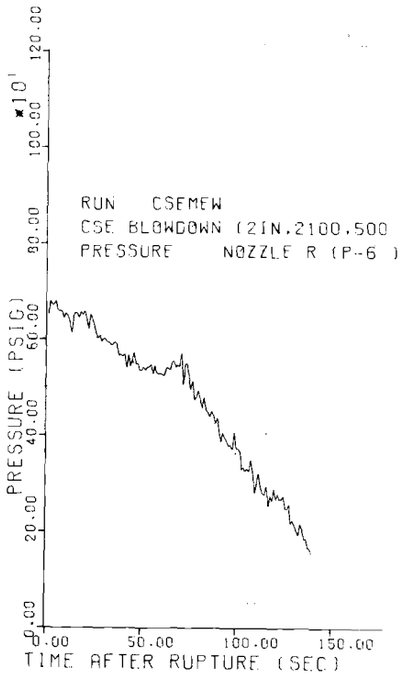
RUN CSEMEW
CSE BLOWDOWN (2IN.2100.500 009)
PRESSURE NOZZLE R (P-6)
PRESSURE (PSIG)
TIME AFTER RUPTURE (SEC)

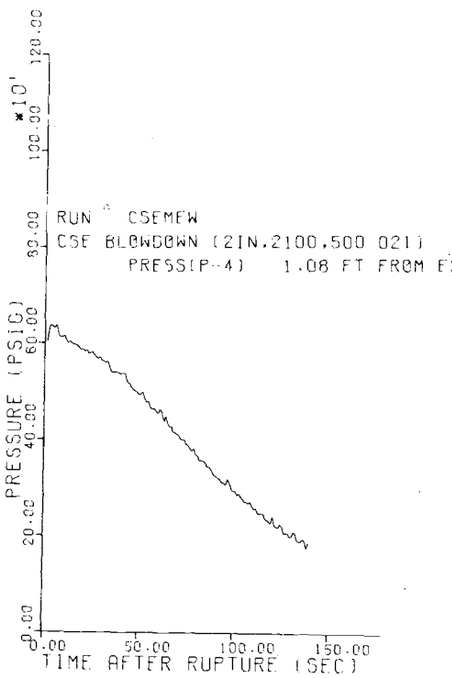
RUN CSEMEW
CSE BLOWDOWN (2IN.2100.500 021)
PRESS(P-4) 1.08 FT FROM EXIT
PRESSURE (PSIG)
TIME AFTER RUPTURE (SEC)

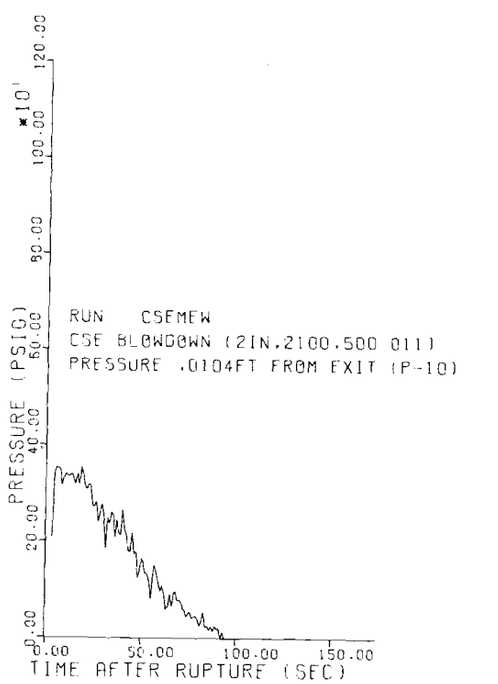
RUN CSEMEW
CSE BLOWDOWN (2IN.2100.500 011)
PRESSURE .0104FT FROM EXIT (P-10)
PRESSURE (PSIG)
TIME AFTER RUPTURE (SEC)

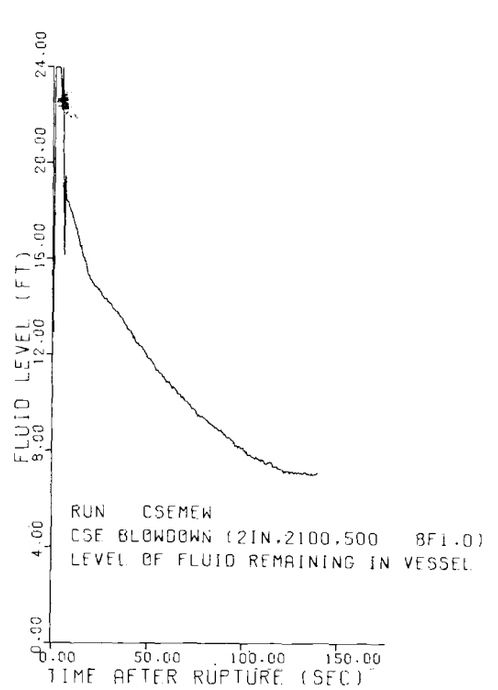
RUN CSEMEW
CSE BLOWDOWN (2IN.2100.500 BF1.0)
LEVEL OF FLUID REMAINING IN VESSEL
FLUID LEVEL (FT)
TIME AFTER RUPTURE (SEC)

FIGURE B-1.

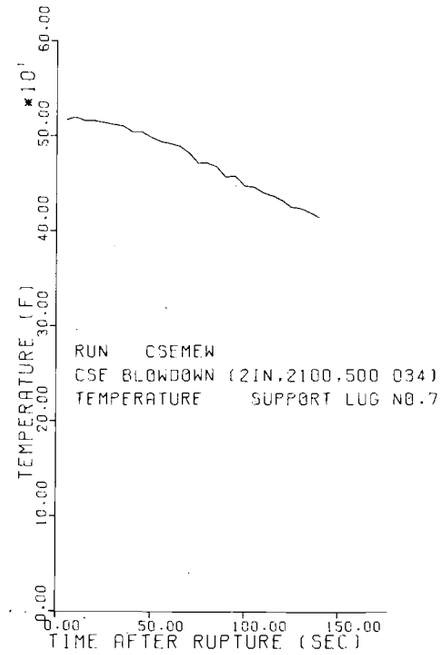
TEMPERATURE (F)
*10¹
60.00
50.00
40.00
30.00
20.00
10.00
0.00
0.00
50.00
100.00
150.00
TIME AFTER RUPTURE (SEC)
RUN CSEMEW
CSE BLOWDOWN (2IN,2100,500 034)
TEMPERATURE SUPPORT LUG NO.7

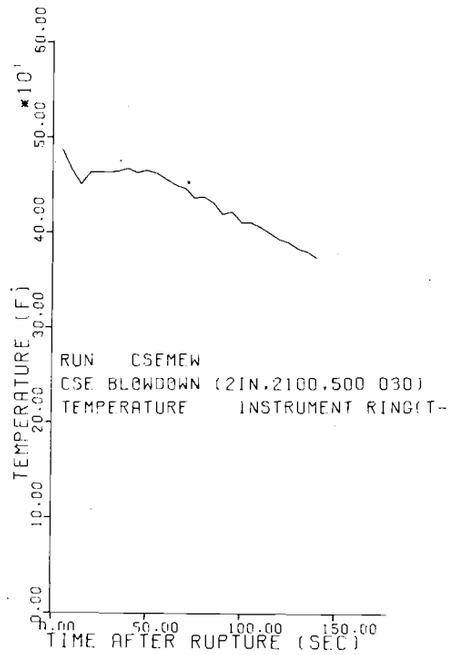
TEMPERATURE (F)
*10¹
60.00
50.00
40.00
30.00
20.00
10.00
0.00
0.00
50.00
100.00
150.00
TIME AFTER RUPTURE (SEC)
RUN CSEMEW
CSE BLOWDOWN (2IN,2100,500 030)
TEMPERATURE INSTRUMENT RING(T-15)

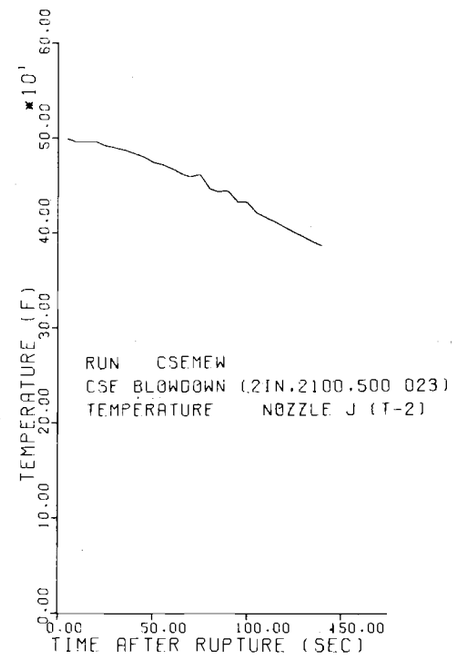
TEMPERATURE (F)
*10¹
60.00
50.00
40.00
30.00
20.00
10.00
0.00
0.00
50.00
100.00
150.00
TIME AFTER RUPTURE (SEC)
RUN CSEMEW
CSE BLOWDOWN (2IN,2100,500 023)
TEMPERATURE NOZZLE J (T-2)

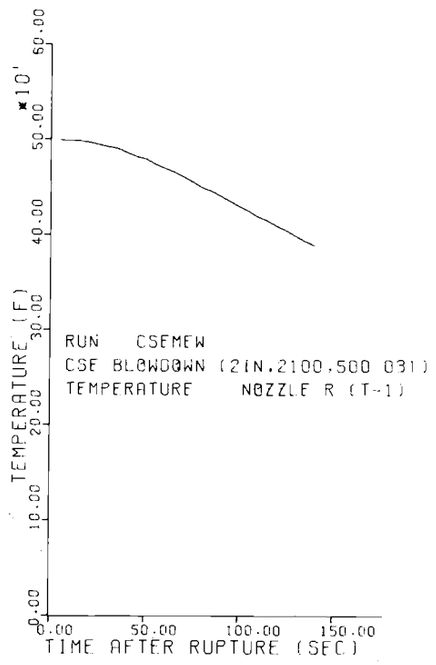
TEMPERATURE (F)
*10¹
60.00
50.00
40.00
30.00
20.00
10.00
0.00
0.00
50.00
100.00
150.00
TIME AFTER RUPTURE (SEC)
RUN CSEMEW
CSE BLOWDOWN (2IN,2100,500 031)
TEMPERATURE NOZZLE R (T-1)

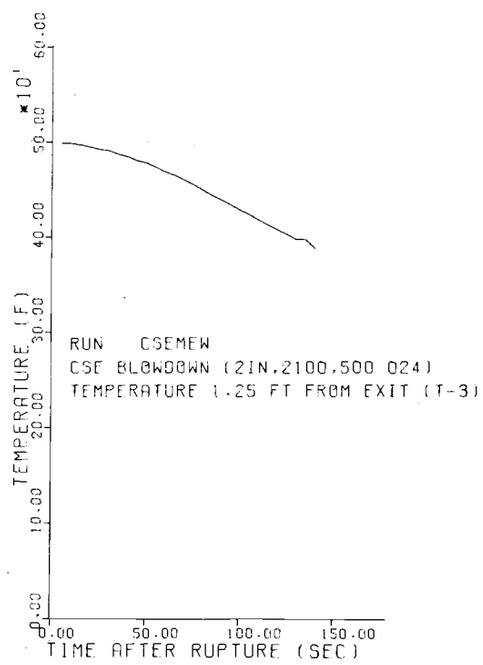
TEMPERATURE (F)
*10¹
60.00
50.00
40.00
30.00
20.00
10.00
0.00
0.00
50.00
100.00
150.00
TIME AFTER RUPTURE (SEC)
RUN CSEMEW
CSE BLOWDOWN (2IN,2100,500 024)
TEMPERATURE 1.25 FT FROM EXIT (T-3)

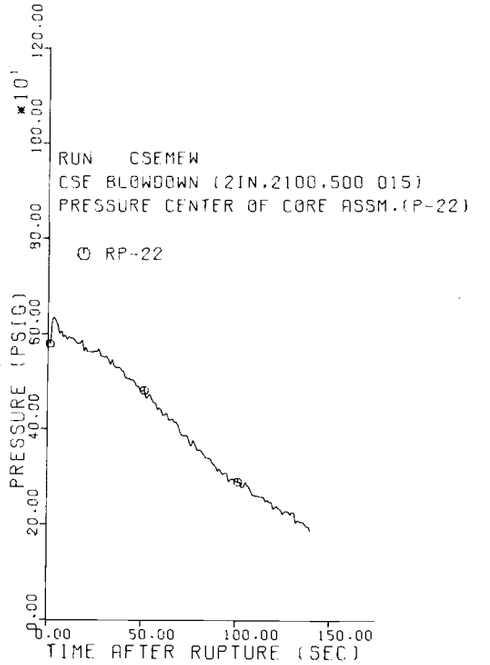
PRESSURE (PSIG)
*10¹
120.00
100.00
80.00
60.00
40.00
20.00
0.00
0.00
50.00
100.00
150.00
TIME AFTER RUPTURE (SEC)
RUN CSEMEW
CSE BLOWDOWN (2IN,2100,500 015)
PRESSURE CENTER OF CORE ASSM.(P-22)
RP-22

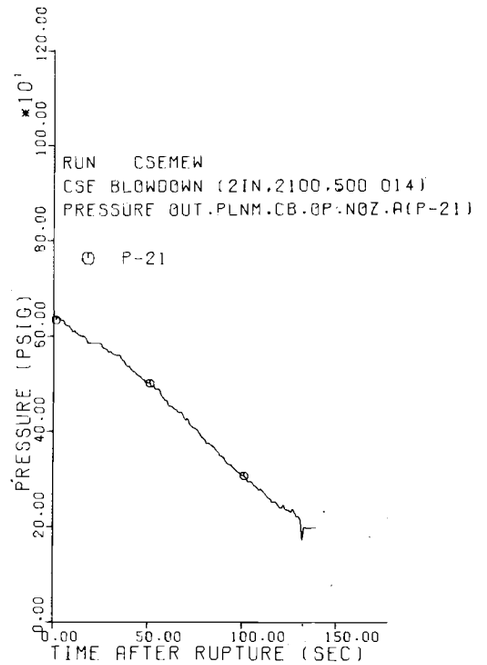
PRESSURE (PSIG)
*10¹
120.00
100.00
80.00
60.00
40.00
20.00
0.00
0.00
50.00
100.00
150.00
TIME AFTER RUPTURE (SEC)
RUN CSEMEW
CSE BLOWDOWN (2IN,2100,500 014)
PRESSURE OUT.PLNM.CB.OP.NOZ.A(P-21)
P-21

FIGURE B-2.

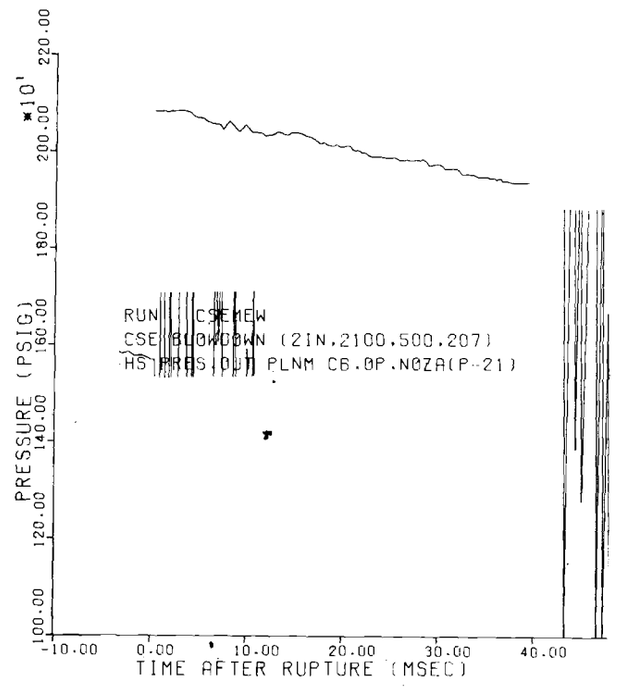
RUN CSEMEW
CSE BLOWDOWN (2IN,2100,500,207)
HS PRES.OUT.PLNM CB.0P.N0ZA(P-21)
PRESSURE (PSIG)
*10'
TIME AFTER RUPTURE (MSEC)

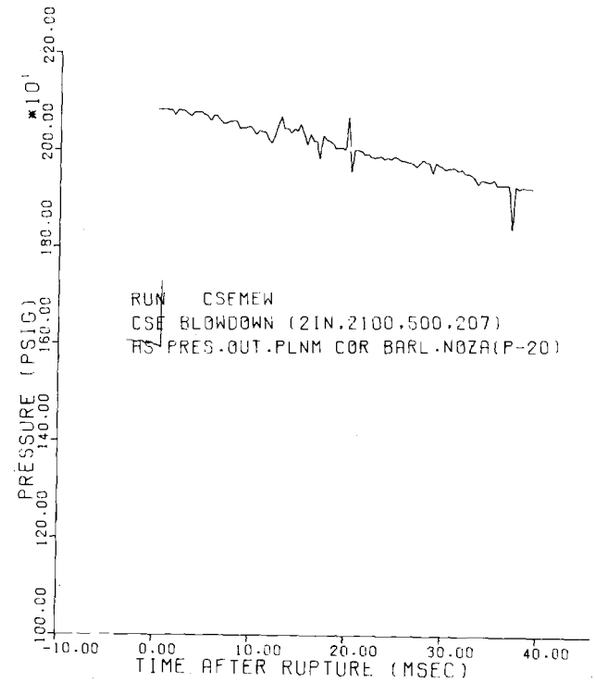
RUN CSEMEW
CSE BLOWDOWN (2IN,2100,500,207)
HS PRES.OUT.PLNM C0R BARL.N0ZA(P-20)
PRESSURE (PSIG)
*10'
TIME AFTER RUPTURE (MSEC)

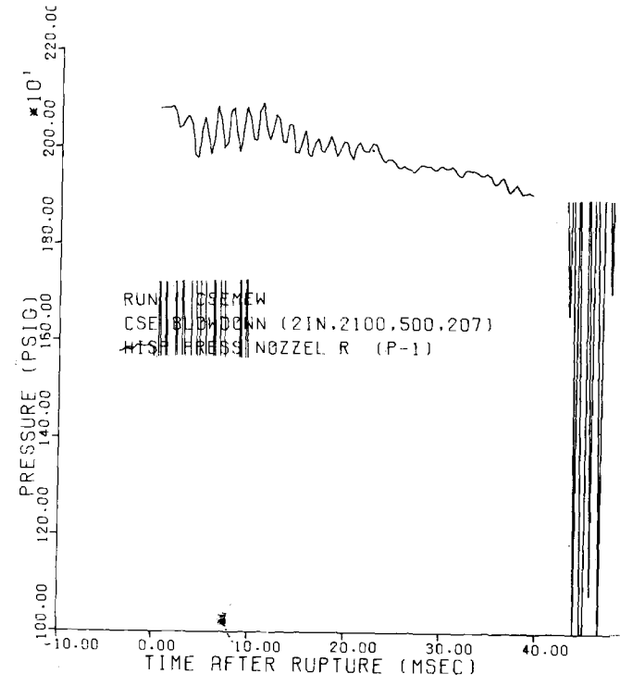
RUN CSEMEW
CSE BLOWDOWN (2IN,2100,500,207)
HISH PRESS N0ZZEL R (P-1)
PRESSURE (PSIG)
*10'
TIME AFTER RUPTURE (MSEC)

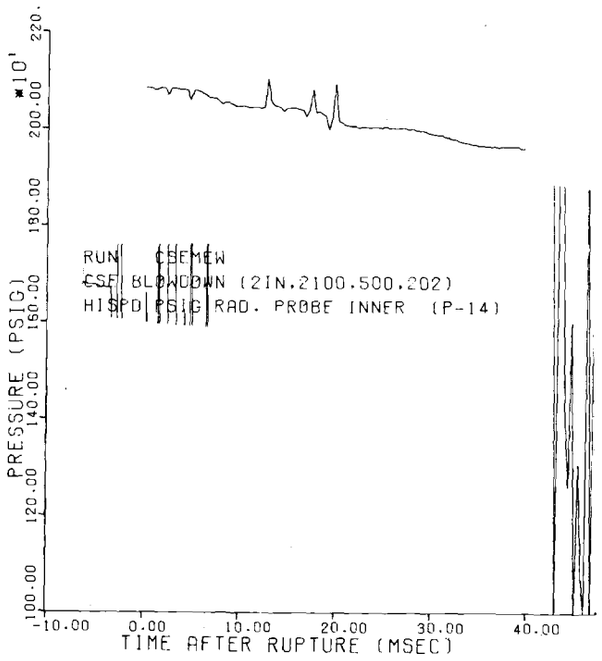
RUN CSEMEW
CSE BLOWDOWN (2IN,2100,500,202)
HISPD PSIG RAD. PROBE INNER (P-14)
PRESSURE (PSIG)
*10'
TIME AFTER RUPTURE (MSEC)

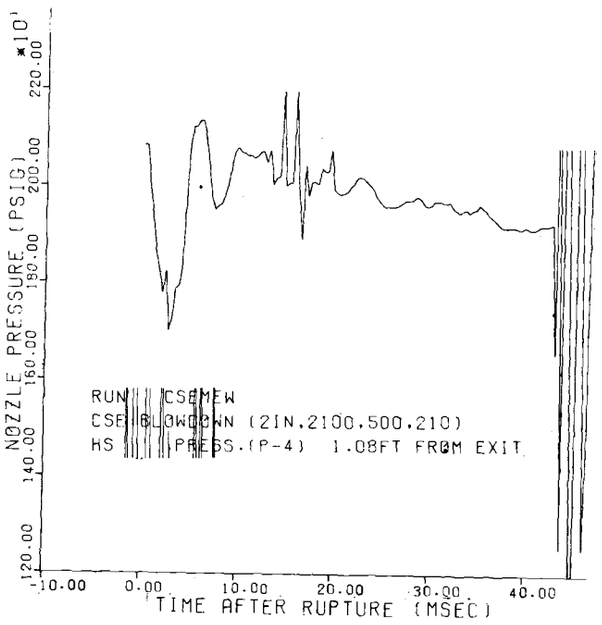
RUN CSEMEW
CSE BLOWDOWN (2IN,2100,500,210)
HS PRESS.(P-4) 1.08FT FROM EXIT
NOZZLE PRESSURE (PSIG)
*10'
TIME AFTER RUPTURE (MSEC)

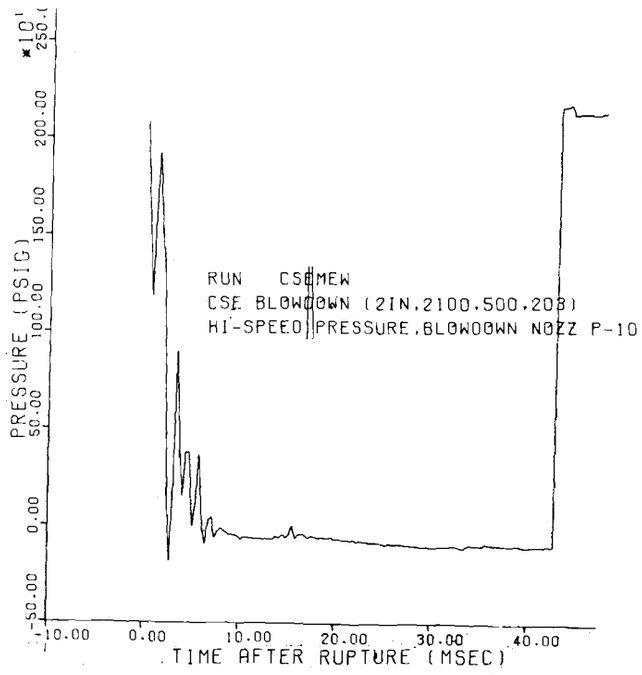
RUN CSEMEW
CSE BLOWDOWN (2IN,2100,500,208)
HI-SPEED PRESSURE,BLOWDOWN NOZZ P-10
PRESSURE (PSIG)
*10'
TIME AFTER RUPTURE (MSEC)

FIGURE B-3.

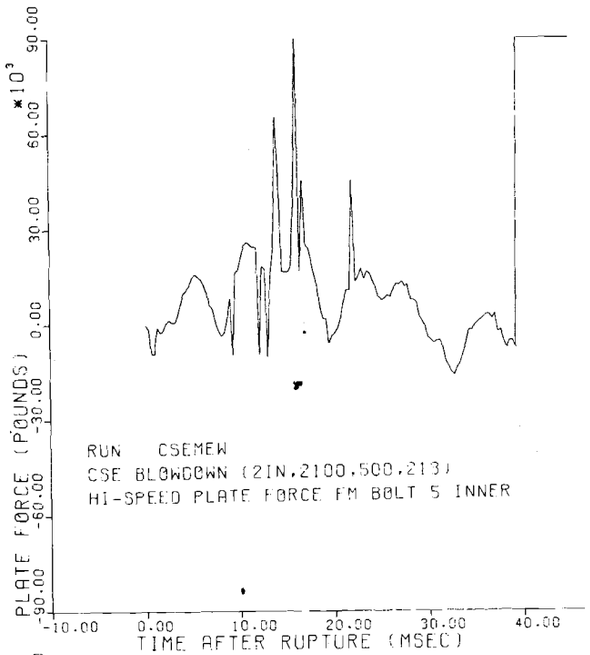
PLATE FORCE (POUNDS)
*10^3
90.00
60.00
30.00
0.00
-30.00
-60.00
-90.00
RUN CSEMEW
CSE BLOWDOWN (2IN,2100,500,213)
HI-SPEED PLATE FORCE FM BOLT 5 INNER
-10.00
0.00
10.00
20.00
30.00
40.00
TIME AFTER RUPTURE (MSEC)

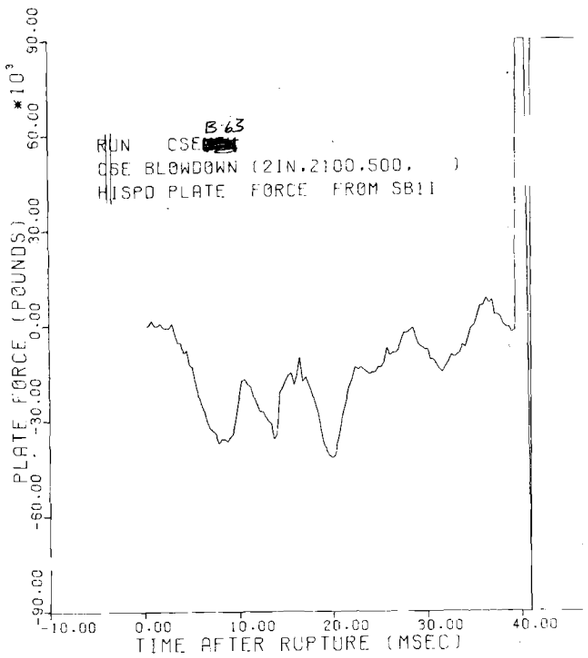
PLATE FORCE (POUNDS)
*10^3
90.00
60.00
30.00
0.00
-30.00
-60.00
-90.00
RUN CSE B-63
CSE BLOWDOWN (2IN,2100,500,)
HISPD PLATE FORCE FROM SB11
-10.00
0.00
10.00
20.00
30.00
40.00
TIME AFTER RUPTURE (MSEC)

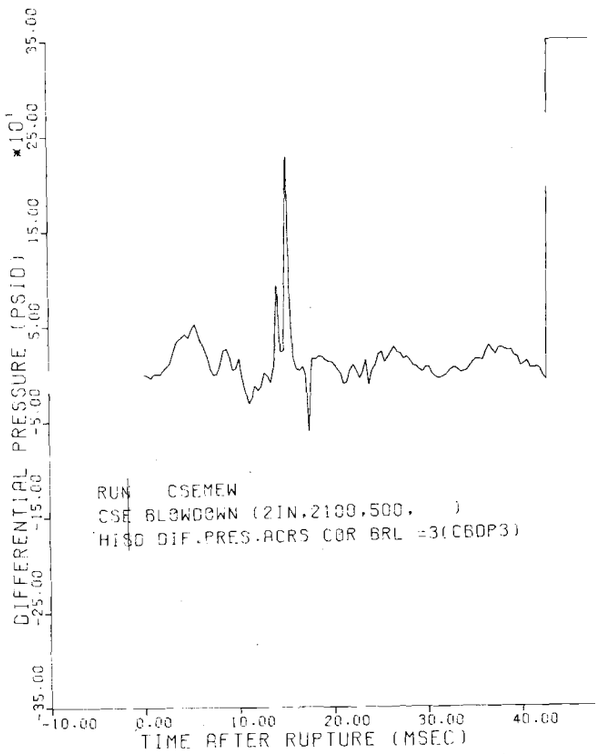
DIFFERENTIAL PRESSURE (PSID)
*10^1
35.00
25.00
15.00
5.00
-5.00
-15.00
-25.00
-35.00
RUN CSEMEW
CSE BLOWDOWN (2IN,2100,500,)
HISD DIF.PRES.ACRS COR BRL =3(CBDP3)
-10.00
0.00
10.00
20.00
30.00
40.00
TIME AFTER RUPTURE (MSEC)

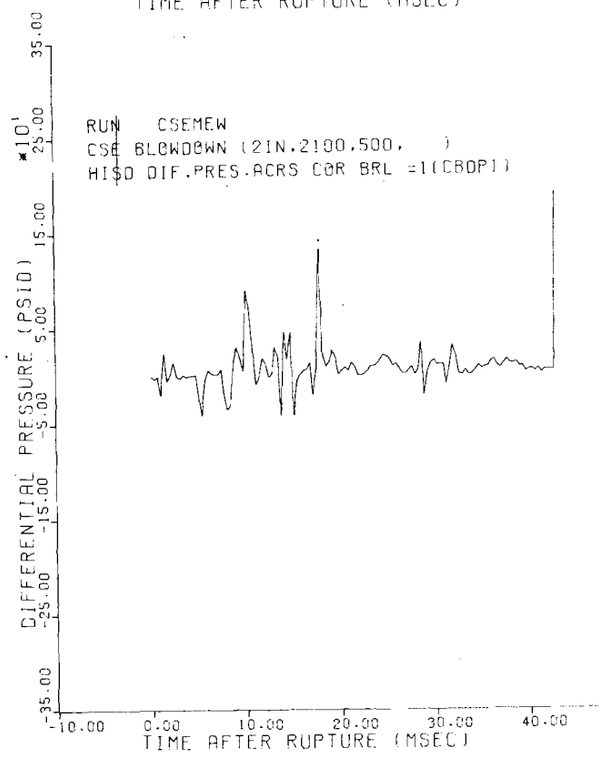
DIFFERENTIAL PRESSURE (PSID)
*10^1
35.00
25.00
15.00
5.00
-5.00
-15.00
-25.00
-35.00
RUN CSEMEW
CSE BLOWDOWN (2IN,2100,500,)
HISD DIF.PRES.ACRS COR BRL =1(CBDP1)
-10.00
0.00
10.00
20.00
30.00
40.00
TIME AFTER RUPTURE (MSEC)

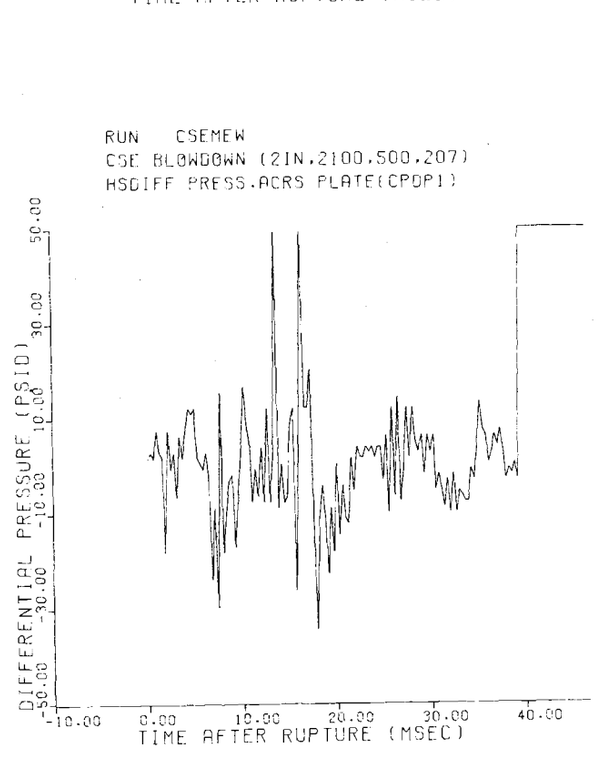
DIFFERENTIAL PRESSURE (PSID)
50.00
30.00
10.00
-10.00
-30.00
-50.00
RUN CSEMEW
CSE BLOWDOWN (2IN,2100,500,207)
HSDIFF PRESS.ACRS PLATE(CPDP1)
-10.00
0.00
10.00
20.00
30.00
40.00
TIME AFTER RUPTURE (MSEC)

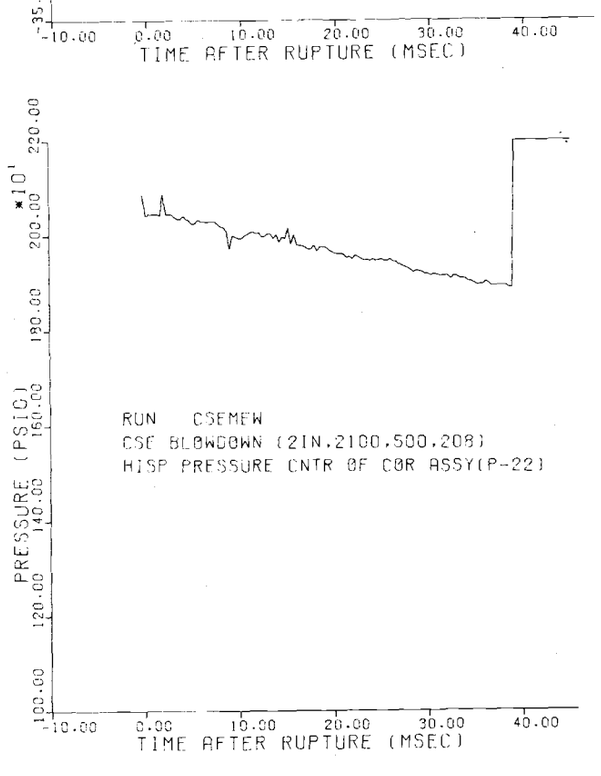
PRESSURE (PSIG)
*10^1
220.00
200.00
180.00
160.00
140.00
120.00
100.00
RUN CSEMEW
CSE BLOWDOWN (2IN,2100,500,208)
HISP PRESSURE CNTR OF COR ASSY(P-22)
-10.00
0.00
10.00
20.00
30.00
40.00
TIME AFTER RUPTURE (MSEC)

FIGURE B-4.

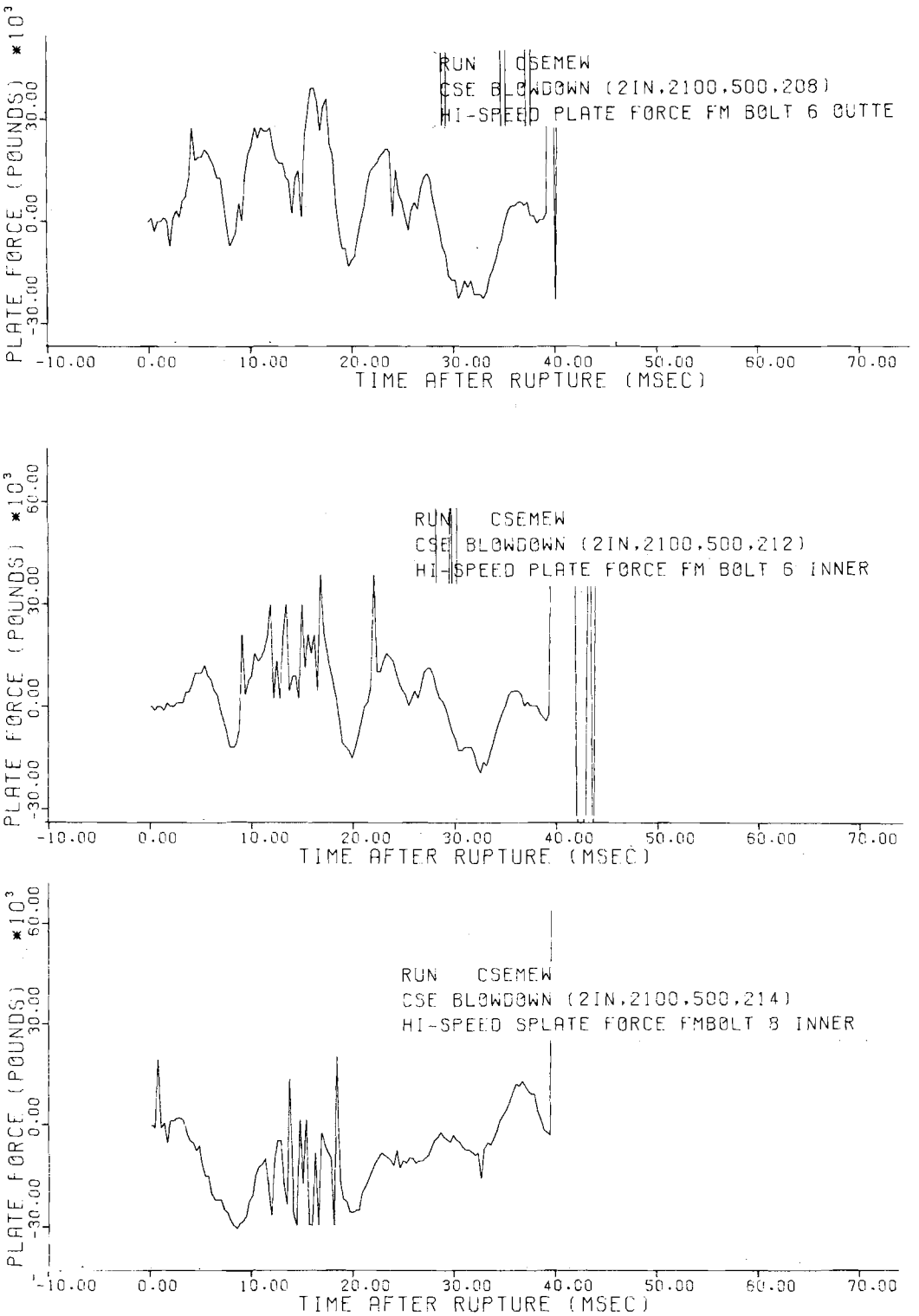
RUN CSEMEW
CSE BLOWDOWN (2IN,2100,500,208)
HI-SPEED PLATE FORCE FM BOLT 6 OUTTE
PLATE FORCE (POUNDS) *10³
30.00
0.00
-30.00
-10.00
0.00
10.00
20.00
30.00
40.00
50.00
60.00
70.00
TIME AFTER RUPTURE (MSEC)
RUN CSEMEW
CSE BLOWDOWN (2IN,2100,500,212)
HI-SPEED PLATE FORCE FM BOLT 6 INNER
PLATE FORCE (POUNDS) *10³
60.00
30.00
0.00
-30.00
TIME AFTER RUPTURE (MSEC)
RUN CSEMEW
CSE BLOWDOWN (2IN,2100,500,214)
HI-SPEED SPLATE FORCE FMBOLT 8 INNER
PLATE FORCE (POUNDS) *10³
TIME AFTER RUPTURE (MSEC)

FIGURE B-5.

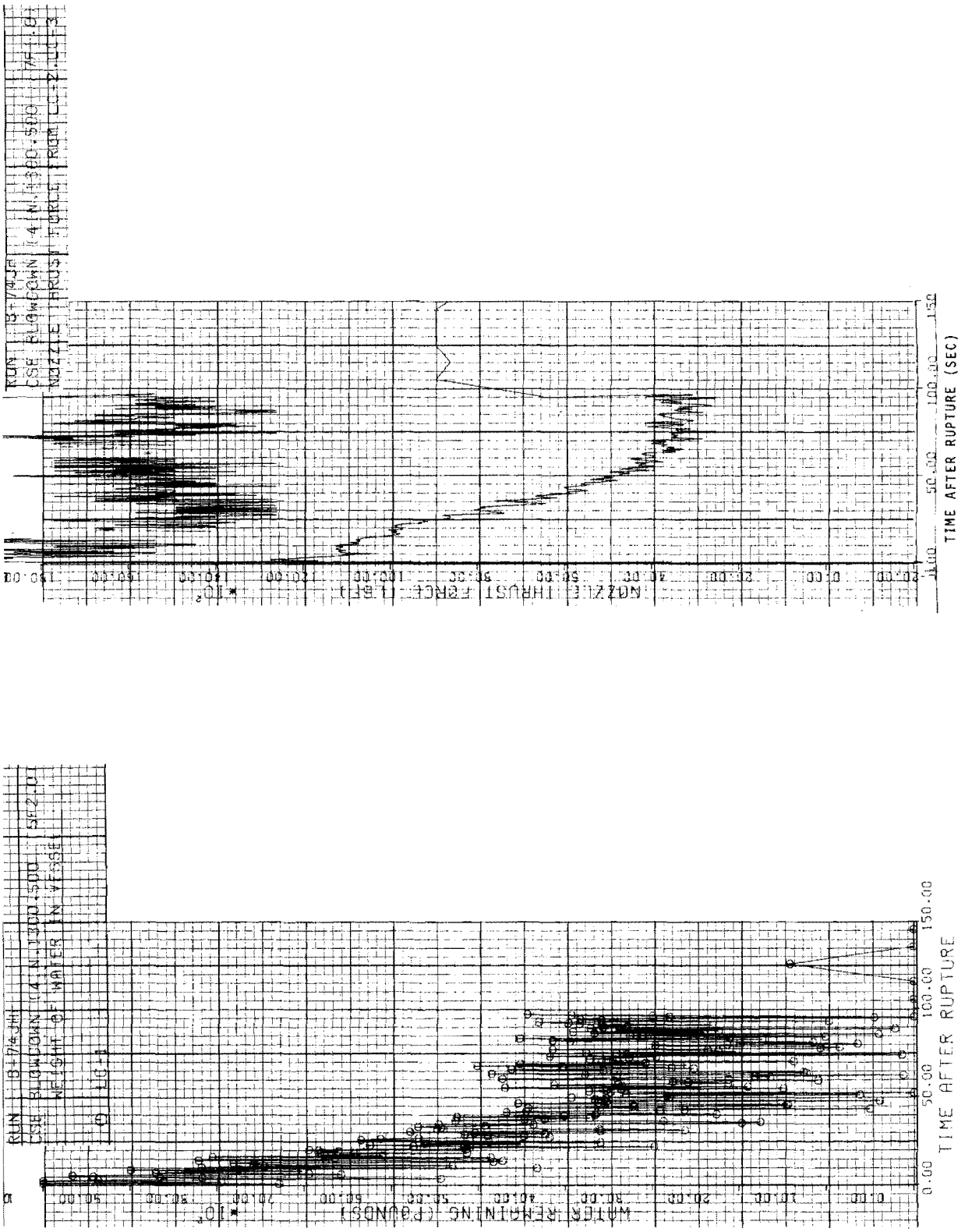
TIME AFTER RUPTURE (SEC)
0.00
50.00
100.00
150.00
TIME AFTER RUPTURE

FIGURE B-6.

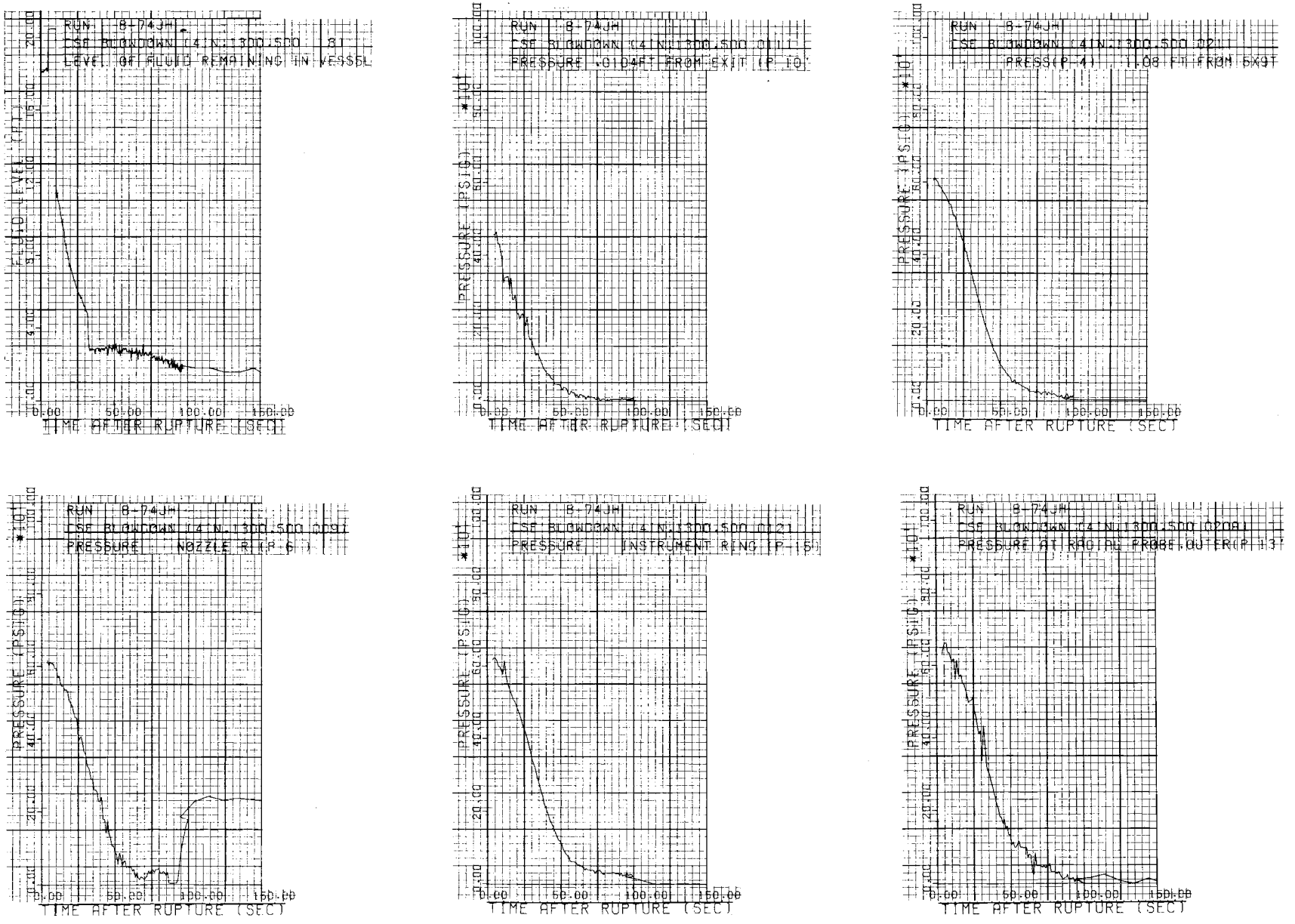
RUN 8-74JM
CSE BLOWDOWN C4 N.1300.500 01
LEVEL OF FLUID REMAINING IN VESSEL
FLUID LEVEL (FT)
TIME AFTER RUPTURE (SEC)
RUN 8-74JM
CSE BLOWDOWN C4 N.1300.500 011
PRESSURE .0104FT FROM EXIT (P 10)
PRESSURE (PSIG) *10
TIME AFTER RUPTURE (SEC)
RUN 8-74JM
CSE BLOWDOWN C4 N.1300.500 021
PRESSURE INSTRUMENT RING (P-15)
PRESSURE (PSIG) *10
TIME AFTER RUPTURE (SEC)
RUN 8-74JM
CSE BLOWDOWN C4 N.1300.500 022
PRESS(P-4) 1.08 FT FROM 6X9T
PRESSURE (PSIG) *10
TIME AFTER RUPTURE (SEC)
RUN 8-74JM
CSE BLOWDOWN C4 N.1300.500 031
PRESSURE NOZZLE R(P-6)
PRESSURE (PSIG) *10
TIME AFTER RUPTURE (SEC)
RUN 8-74JM
CSE BLOWDOWN C4 N.1300.500 0208
PRESSURE AT RAD PR OUTER (P 13)
PRESSURE (PSIG) *10
TIME AFTER RUPTURE (SEC)

FIGURE B-7.

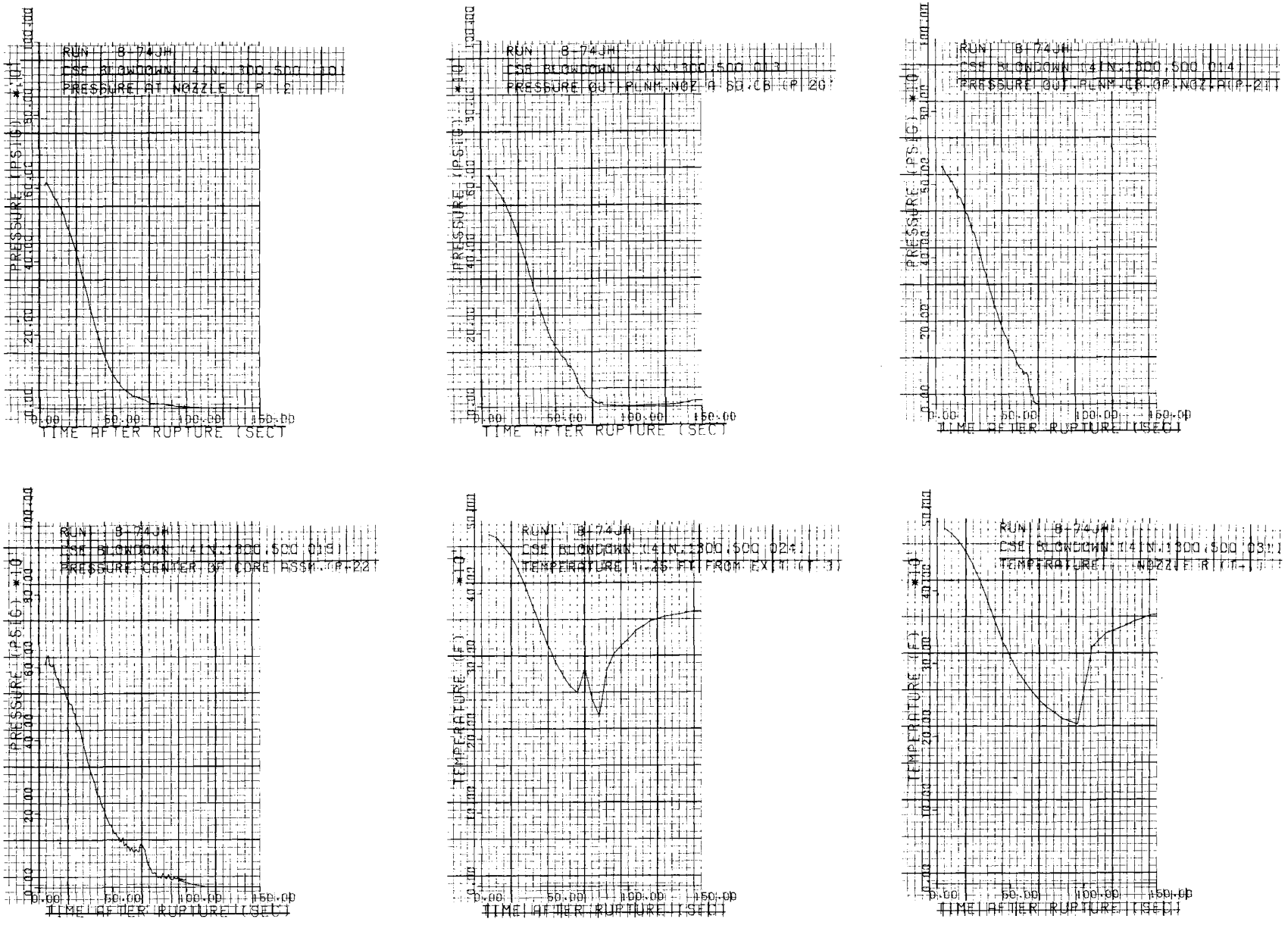
RUN 8-74JH
CSE BLOWDOWN (4IN.1300.500 011)
PRESSURE AT NOZZLE (PSIG) (P-2)
PRESSURE (PSIG)
TIME AFTER RUPTURE (SEC)
RUN 8-74JH
CSE BLOWDOWN (4IN.1300.500 013)
PRESSURE OUT PLNM.NOZ A 50.CB (P-20)
PRESSURE (PSIG)
TIME AFTER RUPTURE (SEC)
RUN 8-74JH
CSE BLOWDOWN (4IN.1300.500 014)
PRESSURE OUT PLNM.CB.OP.NOZZLE A (P-21)
PRESSURE (PSIG)
TIME AFTER RUPTURE (SEC)
RUN 8-74JH
CSE BLOWDOWN (4IN.1300.500 013)
PRESSURE CENTER OF CORE ASSM. (P-22)
PRESSURE (PSIG)
TIME AFTER RUPTURE (SEC)
RUN 8-74JH
CSE BLOWDOWN (4IN.1300.500 021)
TEMPERATURE 1.25 FT FROM EXIT (T-3)
TEMPERATURE (F)
TIME AFTER RUPTURE (SEC)
RUN 8-74JH
CSE BLOWDOWN (4IN.1300.500 031)
TEMPERATURE NOZZLE R (T-
TEMPERATURE (F)
TIME AFTER RUPTURE (SEC)

FIGURE B-8.

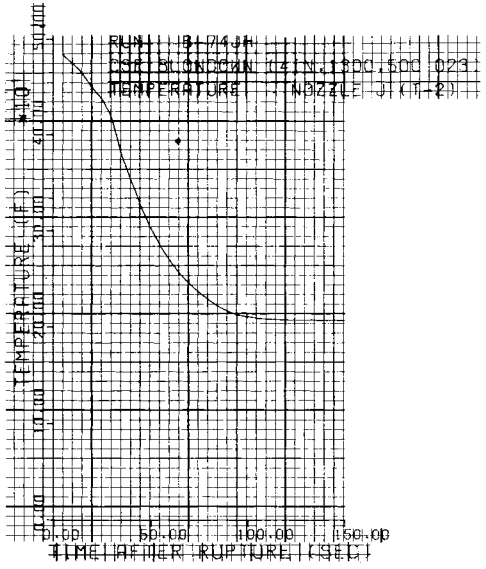
RUN B-74JH
CSE BLOWDOWN (4IN.1300.500 023
TEMPERATURE NOZZLE 1 (T-2)
TEMPERATURE (F)
TIME AFTER RUPTURE (SEC)

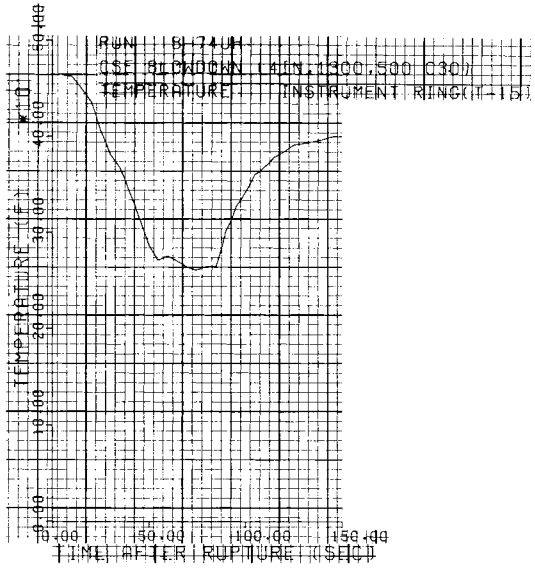
RUN B-74JH
CSE BLOWDOWN (4IN.1300.500 C30)
TEMPERATURE INSTRUMENT RING(T-15)
TEMPERATURE (F)
TIME AFTER RUPTURE (SEC)

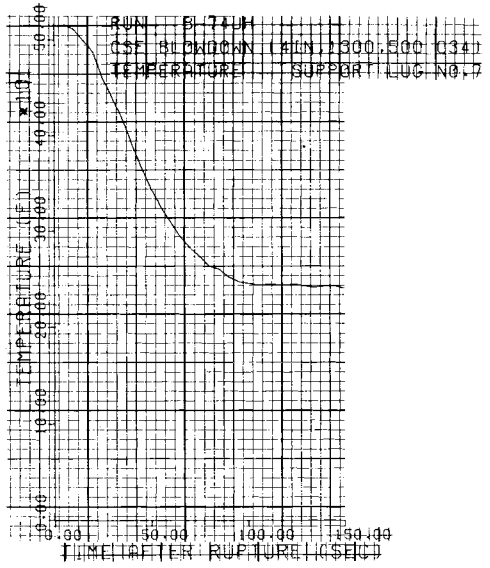
RUN B-74JH
CSE BLOWDOWN (4IN.1300.500 C34)
TEMPERATURE SUPPORT LUG NO.7
TEMPERATURE (F)
TIME AFTER RUPTURE (SEC)

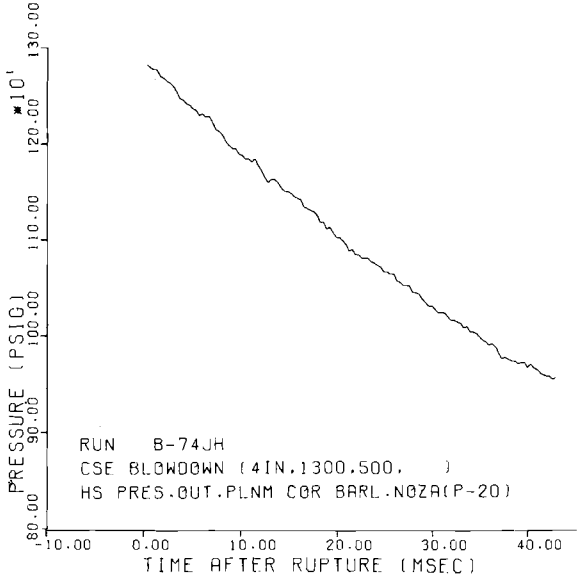
RUN B-74JH
CSE BLOWDOWN (4IN.1300.500.
HS PRES.OUT.PLNM COR BARL.NOZA(P-20)
PRESSURE (PSIG)
TIME AFTER RUPTURE (MSEC)

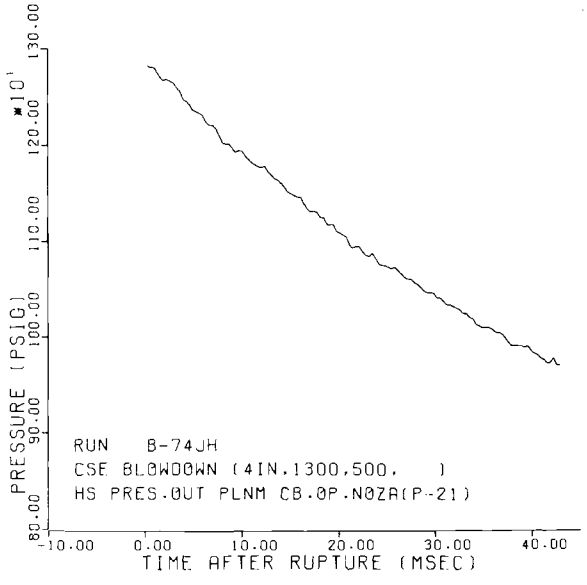
RUN B-74JH
CSE BLOWDOWN (4IN.1300.500.
HS PRES.OUT PLNM CB.0P.NOZA(P-21)
PRESSURE (PSIG)
TIME AFTER RUPTURE (MSEC)

FIGURE B-9.

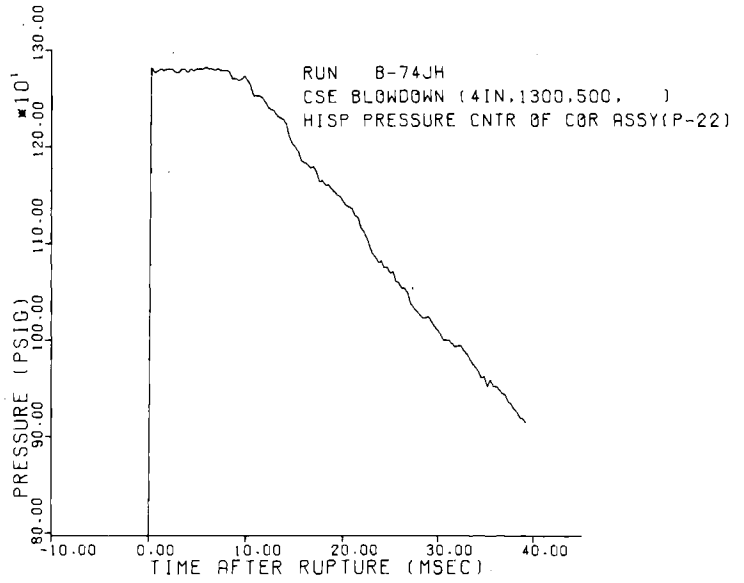
RUN B-74JH
CSE BLOWDOWN (4IN,1300,500,)
HISP PRESSURE CNTR OF COR ASSY(P-22)
PRESSURE (PSIG)
TIME AFTER RUPTURE (MSEC)

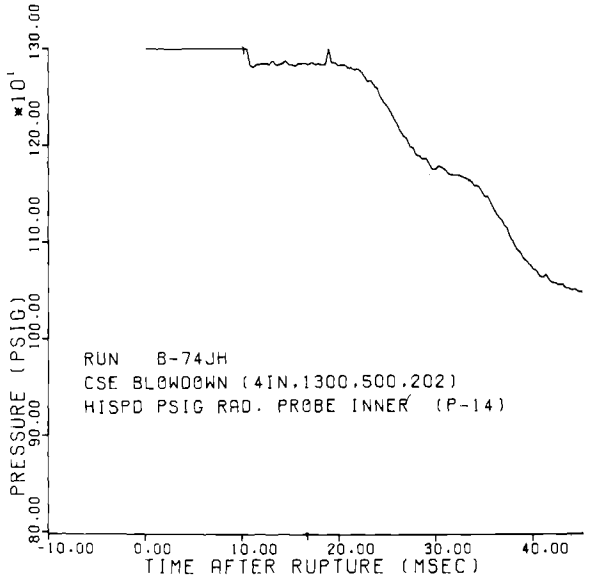
RUN B-74JH
CSE BLOWDOWN (4IN,1300,500,202)
HISPD PSIG RAD. PROBE INNER (P-14)
PRESSURE (PSIG)
TIME AFTER RUPTURE (MSEC)

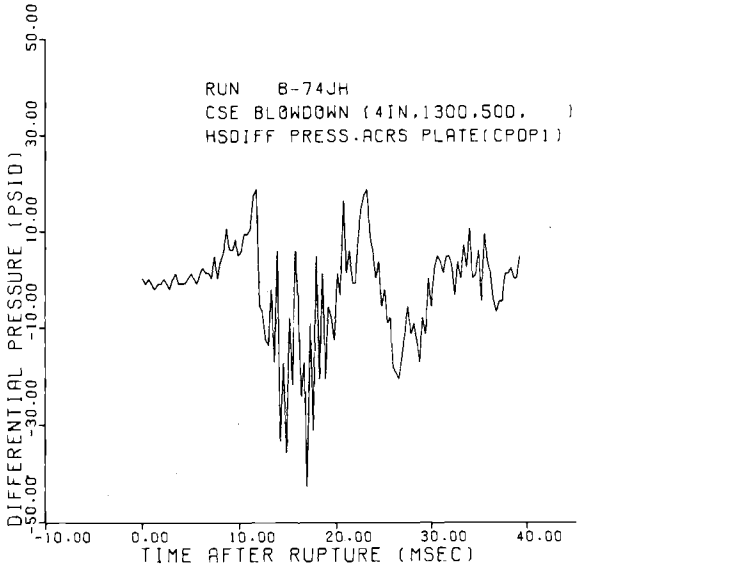
RUN B-74JH
CSE BLOWDOWN (4IN,1300,500,)
HSDIFF PRESS.ACRS PLATE(CPDP1)
DIFFERENTIAL PRESSURE (PSID)
TIME AFTER RUPTURE (MSEC)

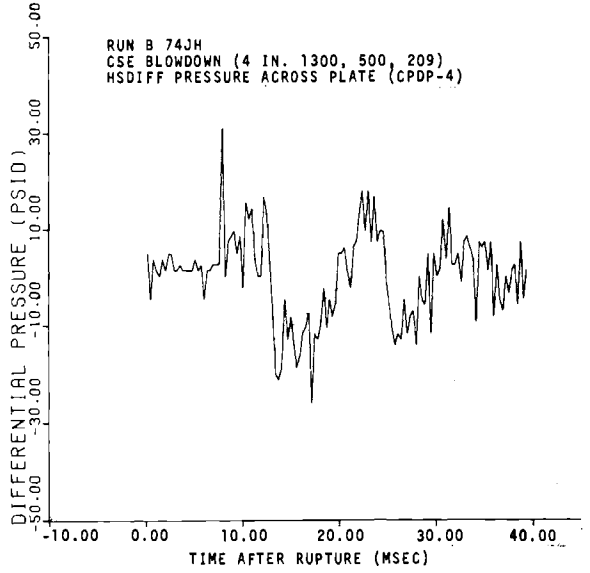
RUN B 74JH
CSE BLOWDOWN (4 IN. 1300, 500, 209)
HSDIFF PRESSURE ACROSS PLATE (CPDP-4)
DIFFERENTIAL PRESSURE (PSID)
TIME AFTER RUPTURE (MSEC)

FIGURE B-10.

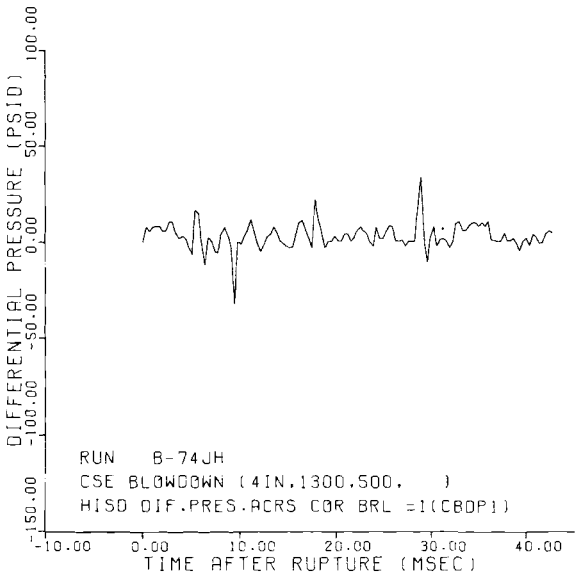
DIFFERENTIAL PRESSURE (PSID)
100.00
50.00
0.00
-100.00
-150.00
-10.00
0.00
10.00
20.00
30.00
40.00
TIME AFTER RUPTURE (MSEC)
RUN B-74JH
CSE BLOWDOWN (4IN,1300,500,)
HISD DIF.PRES.ACRS COR BRL =1(CBDP1)

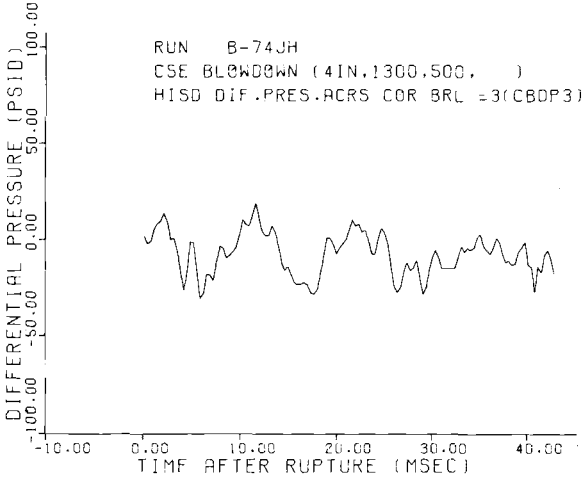
DIFFERENTIAL PRESSURE (PSID)
100.00
50.00
0.00
-50.00
-100.00
-10.00
0.00
10.00
20.00
30.00
40.00
TIME AFTER RUPTURE (MSEC)
RUN B-74JH
CSE BLOWDOWN (4IN,1300,500,)
HISD DIF.PRES.ACRS COR BRL =3(CBDP3)

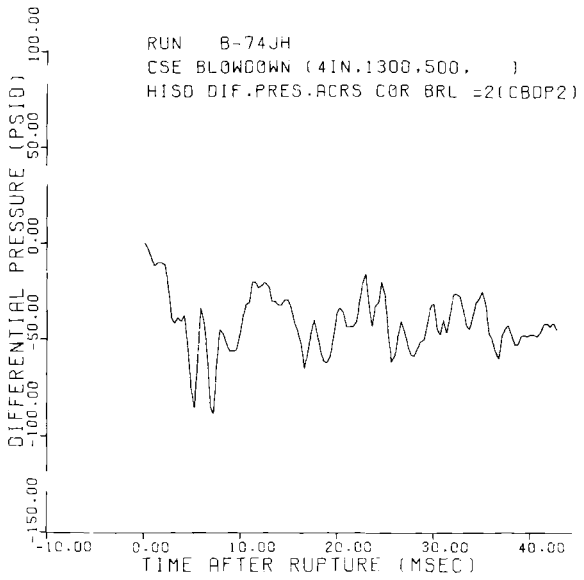
DIFFERENTIAL PRESSURE (PSID)
100.00
50.00
0.00
-100.00
-150.00
-10.00
0.00
10.00
20.00
30.00
40.00
TIME AFTER RUPTURE (MSEC)
RUN B-74JH
CSE BLOWDOWN (4IN,1300,500,)
HISD DIF.PRES.ACRS COR BRL =2(CBDP2)

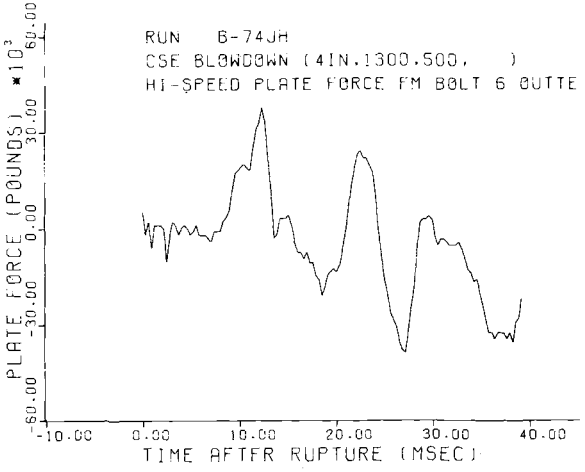
PLATE FORCE (POUNDS) *10³
60.00
30.00
0.00
-30.00
-60.00
-10.00
0.00
10.00
20.00
30.00
40.00
TIME AFTER RUPTURE (MSEC)
RUN B-74JH
CSE BLOWDOWN (4IN,1300,500,)
HI-SPEED PLATE FORCE FM BOLT 6 BUTTE

FIGURE B-11.

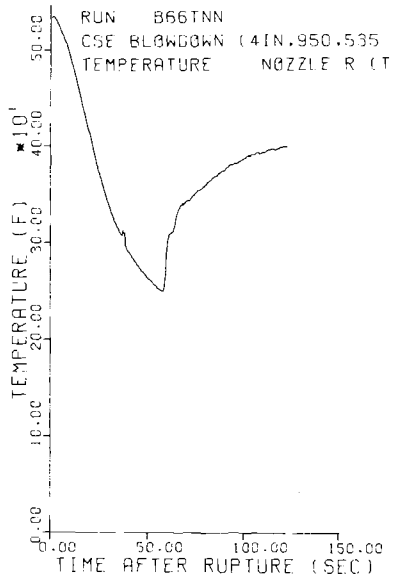
RUN B66TNN
CSE BLOWDOWN (4IN.950.535 031)
TEMPERATURE NOZZLE R (T-1)
TEMPERATURE (F.) *10'
0.00
10.00
20.00
30.00
40.00
50.00
0.00
50.00
100.00
150.00
TIME AFTER RUPTURE (SEC)

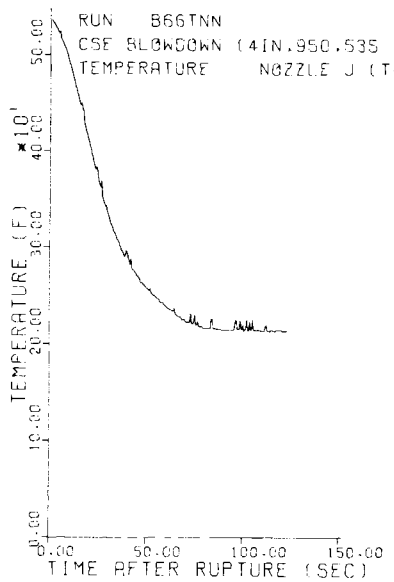
RUN B66TNN
CSE BLOWDOWN (4IN.950.535 023)
TEMPERATURE NOZZLE J (T-2)
TEMPERATURE (F.) *10'
0.00
10.00
20.00
30.00
40.00
50.00
0.00
50.00
100.00
150.00
TIME AFTER RUPTURE (SEC)

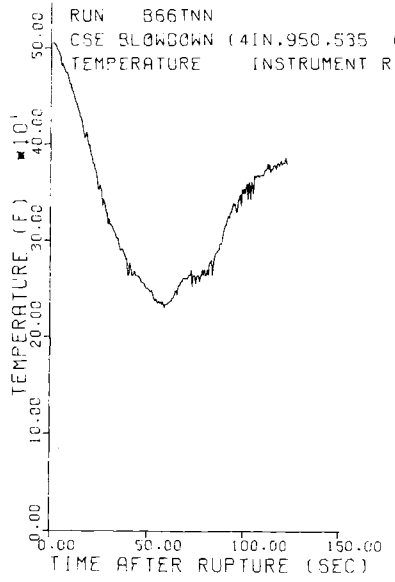
RUN B66TNN
CSE BLOWDOWN (4IN.950.535 030)
TEMPERATURE INSTRUMENT RING(T-15)
TEMPERATURE (F.) *10'
0.00
10.00
20.00
30.00
40.00
50.00
0.00
50.00
100.00
150.00
TIME AFTER RUPTURE (SEC)

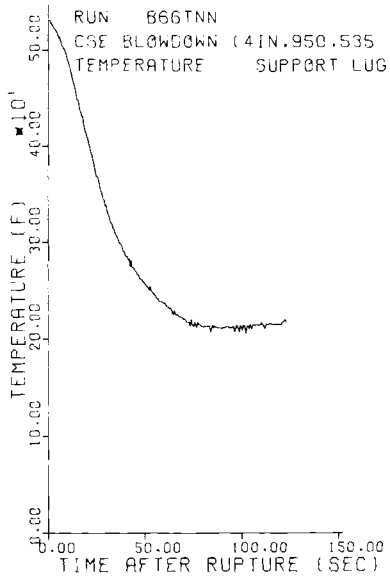
RUN B66TNN
CSE BLOWDOWN (4IN.950.535 034)
TEMPERATURE SUPPORT LUG NO.7
TEMPERATURE (F.) *10'
0.00
10.00
20.00
30.00
40.00
50.00
0.00
50.00
100.00
150.00
TIME AFTER RUPTURE (SEC)

FIGURE B-12.

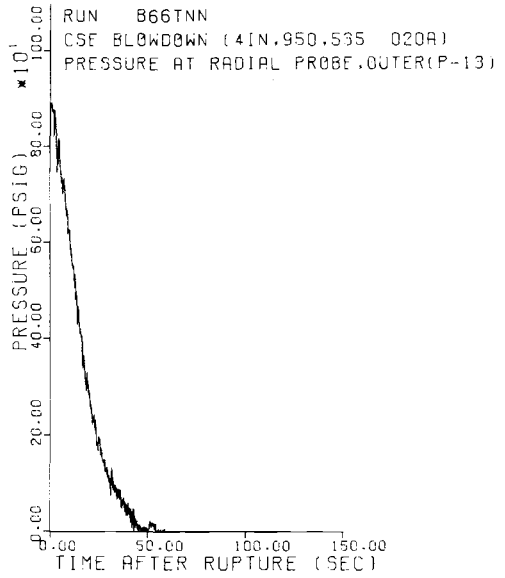
RUN 866TNN
CSE BLOWDOWN (4IN.950.535 020A)
PRESSURE AT RADIAL PROBE.OUTER(P-13)
PRESSURE (PSIG) *10¹
TIME AFTER RUPTURE (SEC)

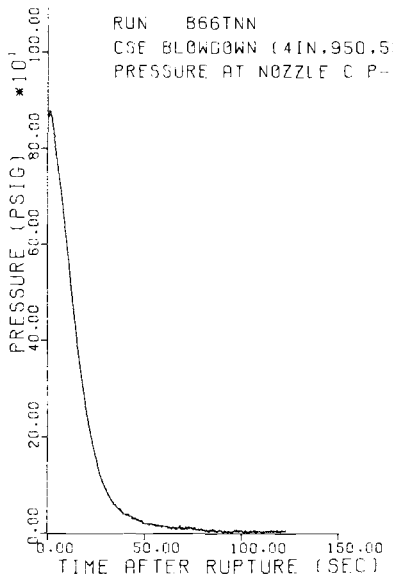
RUN 866TNN
CSE BLOWDOWN (4IN.950.535 110)
PRESSURE AT NOZZLE C P-12
PRESSURE (PSIG) *10¹
TIME AFTER RUPTURE (SEC)

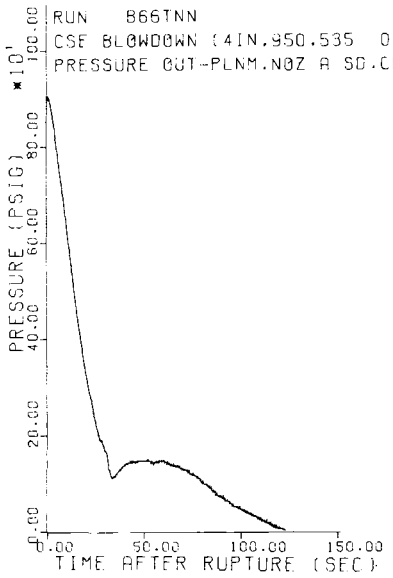
RUN 866TNN
CSE BLOWDOWN (4IN.950.535 013)
PRESSURE OUT-PLNM.NOZ A SD.CB (P-20)
PRESSURE (PSIG) *10¹
TIME AFTER RUPTURE (SEC)

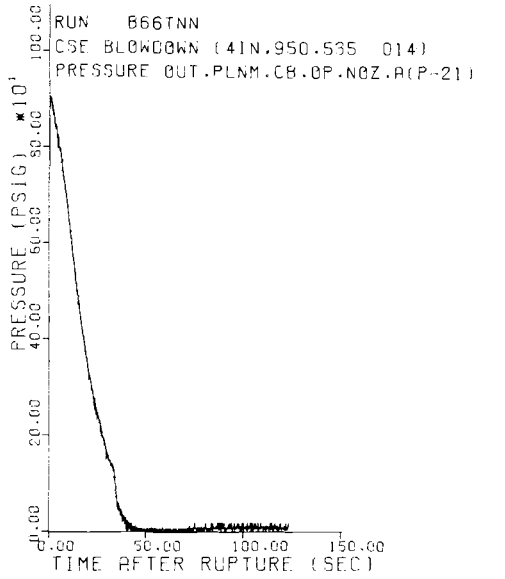
RUN 866TNN
CSE BLOWDOWN (4IN.950.535 014)
PRESSURE OUT.PLNM.CB.OP.NOZ.A(P-21)
PRESSURE (PSIG) *10¹
TIME AFTER RUPTURE (SEC)

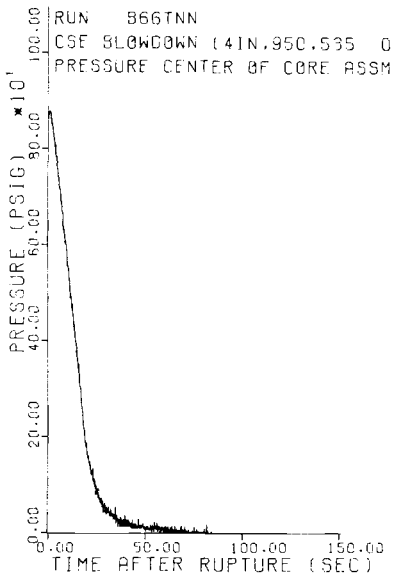
RUN 866TNN
CSE BLOWDOWN (4IN.950.535 015)
PRESSURE CENTER OF CORE ASSM.(P-22)
PRESSURE (PSIG) *10¹
TIME AFTER RUPTURE (SEC)

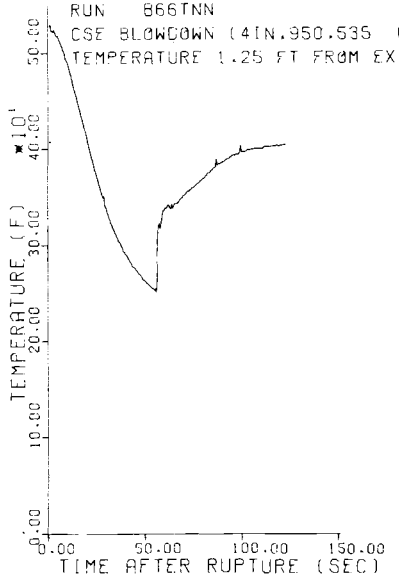
RUN 866TNN
CSE BLOWDOWN (4IN.950.535 024)
TEMPERATURE 1.25 FT FROM EXIT (T-3)
TEMPERATURE (F) *10¹
TIME AFTER RUPTURE (SEC)

FIGURE B-13.

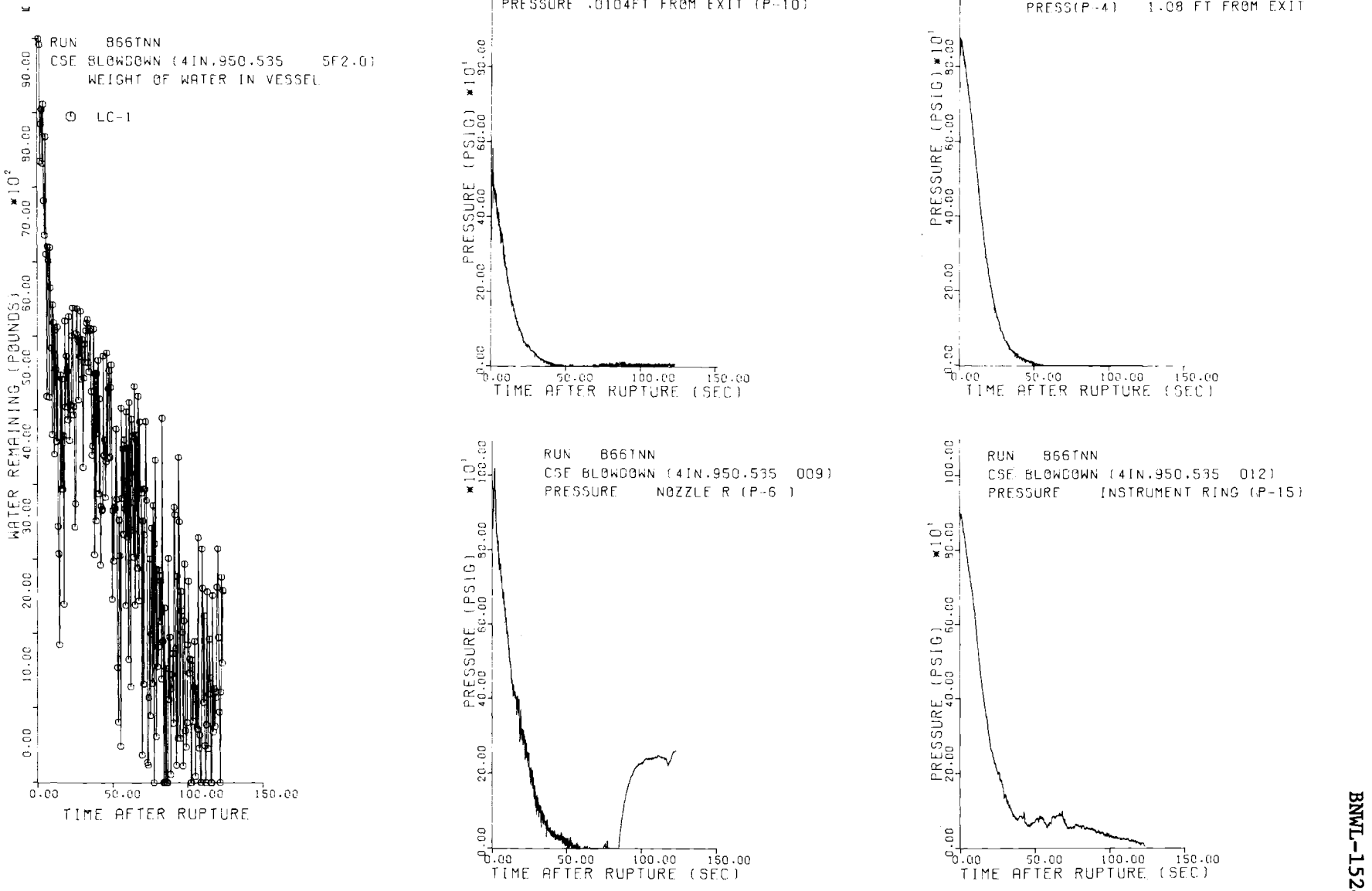
RUN 866TNN
CSE BLOWDOWN (4IN.950.535 5F2.0)
WEIGHT OF WATER IN VESSEL
LC-1
WATER REMAINING (POUNDS) *10²
TIME AFTER RUPTURE
RUN 866TNN
CSE BLOWDOWN (4IN.950.535 011)
PRESSURE .0104FT FROM EXIT (P-10)
PRESSURE (PSIG) *10¹
TIME AFTER RUPTURE (SEC)
RUN 866TNN
CSE BLOWDOWN (4IN.950.535 021)
PRESS(P-4) 1.08 FT FROM EXIT
PRESSURE (PSIG) *10¹
TIME AFTER RUPTURE (SEC)
RUN 866TNN
CSE BLOWDOWN (4IN.950.535 009)
PRESSURE NOZZLE R (P-6)
PRESSURE (PSIG) *10¹
TIME AFTER RUPTURE (SEC)
RUN 866TNN
CSE BLOWDOWN (4IN.950.535 012)
PRESSURE INSTRUMENT RING (P-15)
PRESSURE (PSIG) *10¹
TIME AFTER RUPTURE (SEC)

FIGURE B-14.

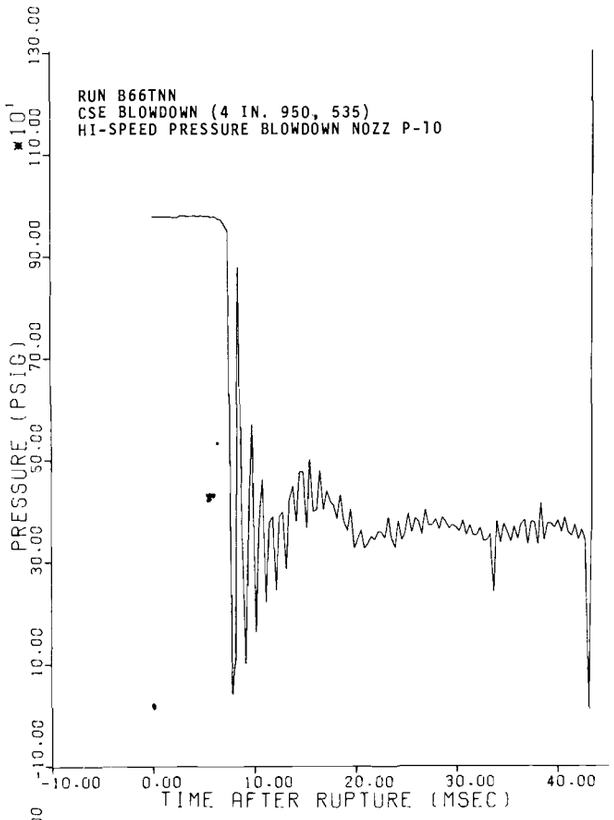
RUN B66TNN
CSE BLOWDOWN (4 IN. 950, 535)
HI-SPEED PRESSURE BLOWDOWN NOZZ P-10
PRESSURE (PSIG)
*10¹
TIME AFTER RUPTURE (MSEC)

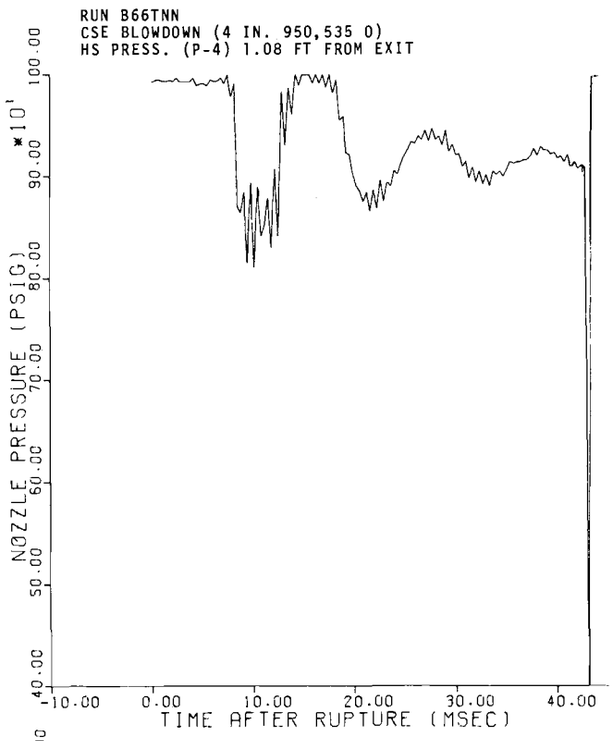
RUN B66TNN
CSE BLOWDOWN (4 IN. 950,535 0)
HS PRESS. (P-4) 1.08 FT FROM EXIT
NOZZLE PRESSURE (PSIG)
*10¹
TIME AFTER RUPTURE (MSEC)

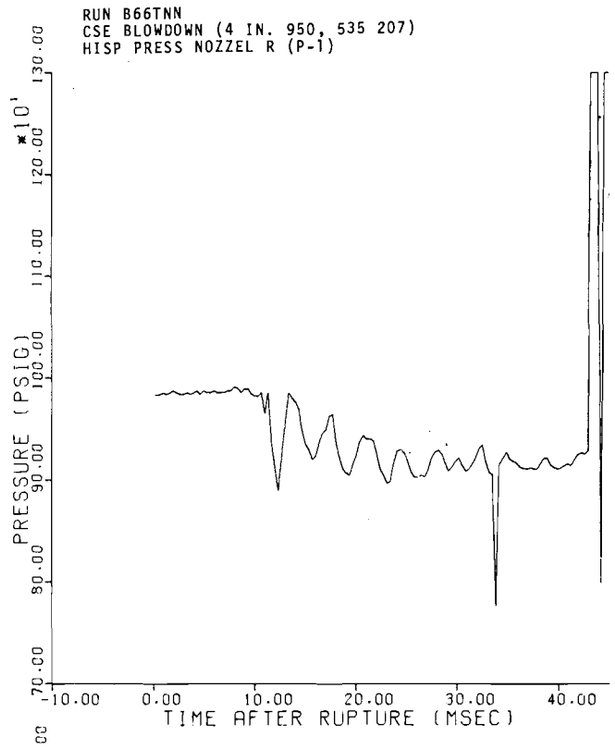
RUN B66TNN
CSE BLOWDOWN (4 IN. 950, 535 207)
HISP PRESS NOZZEL R (P-1)
PRESSURE (PSIG)
*10¹
TIME AFTER RUPTURE (MSEC)

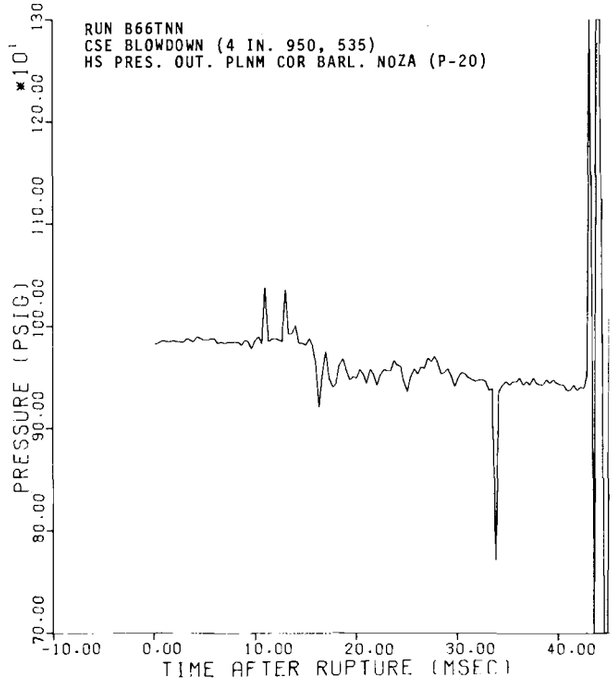
RUN B66TNN
CSE BLOWDOWN (4 IN. 950, 535)
HS PRES. OUT. PLNM COR BARL. NOZA (P-20)
PRESSURE (PSIG)
*10¹
TIME AFTER RUPTURE (MSEC)

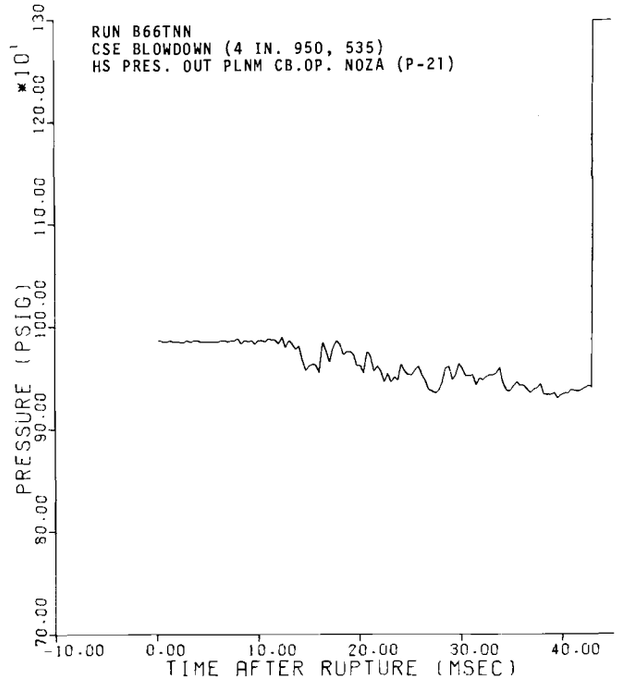
RUN B66TNN
CSE BLOWDOWN (4 IN. 950, 535)
HS PRES. OUT PLNM CB.OP. NOZA (P-21)
PRESSURE (PSIG)
*10¹
TIME AFTER RUPTURE (MSEC)

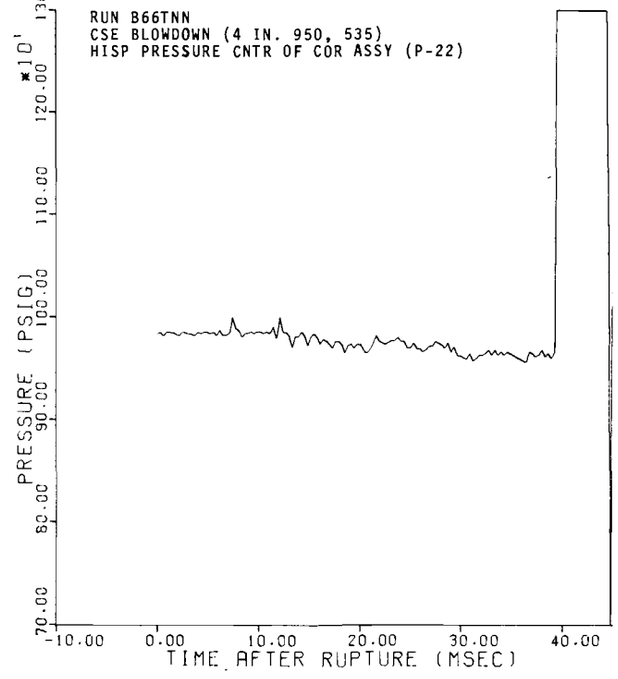
RUN B66TNN
CSE BLOWDOWN (4 IN. 950, 535)
HISP PRESSURE CNTR OF COR ASSY (P-22)
PRESSURE (PSIG)
*10¹
TIME AFTER RUPTURE (MSEC)

FIGURE B-15.

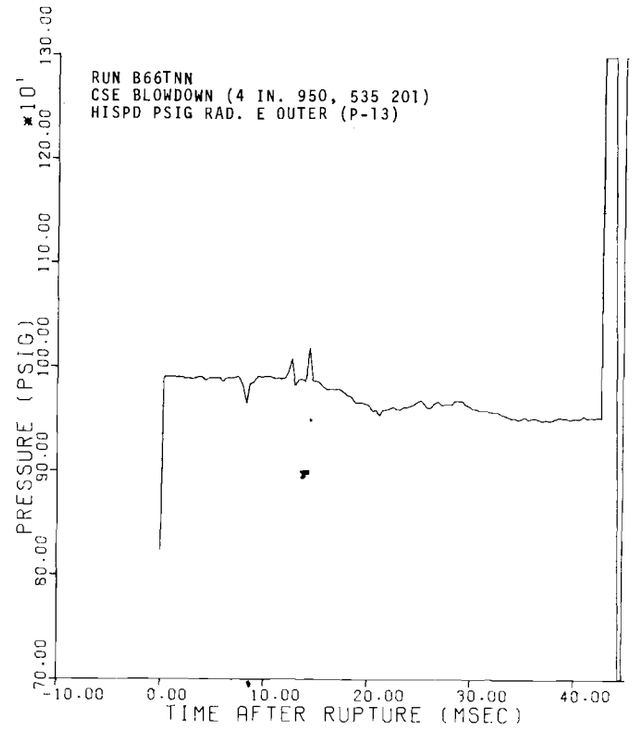
RUN B66TNN
CSE BLOWDOWN (4 IN. 950, 535 201)
HISPD PSIG RAD. E OUTER (P-13)
PRESSURE (PSIG) ×10¹
70.00
80.00
90.00
100.00
110.00
120.00
130.00
-10.00
0.00
10.00
20.00
30.00
40.00
TIME AFTER RUPTURE (MSEC)

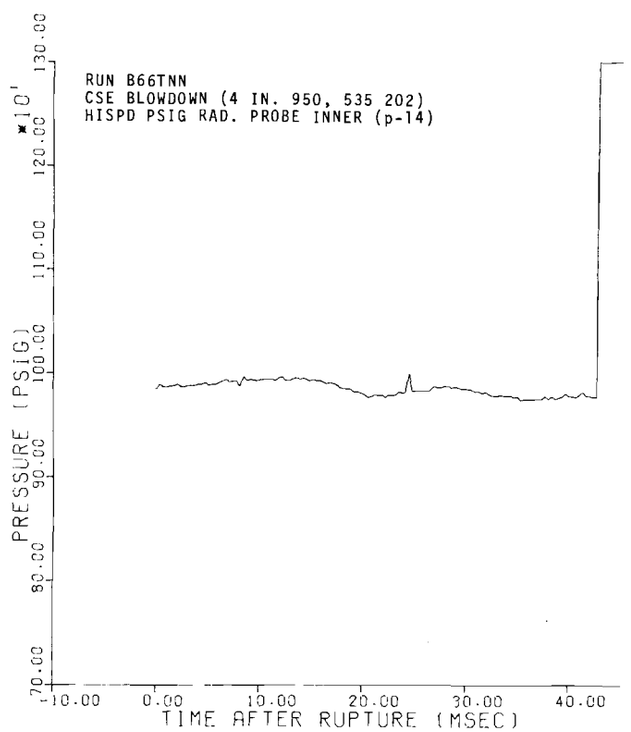
RUN B66TNN
CSE BLOWDOWN (4 IN. 950, 535 202)
HISPD PSIG RAD. PROBE INNER (p-14)
PRESSURE (PSIG) ×10¹
70.00
80.00
90.00
100.00
110.00
120.00
130.00
-10.00
0.00
10.00
20.00
30.00
40.00
TIME AFTER RUPTURE (MSEC)

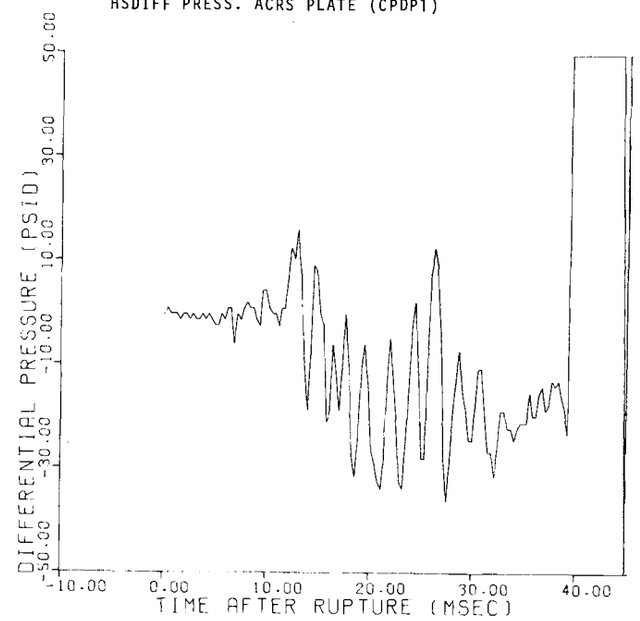
RUN B66TNN
CSE BLOWDOWN (4 IN. 950, 535)
HSDIFF PRESS. ACRS PLATE (CPDP1)
DIFFERENTIAL PRESSURE (PSID)
-50.00
-30.00
-10.00
10.00
30.00
50.00
-10.00
0.00
10.00
20.00
30.00
40.00
TIME AFTER RUPTURE (MSEC)

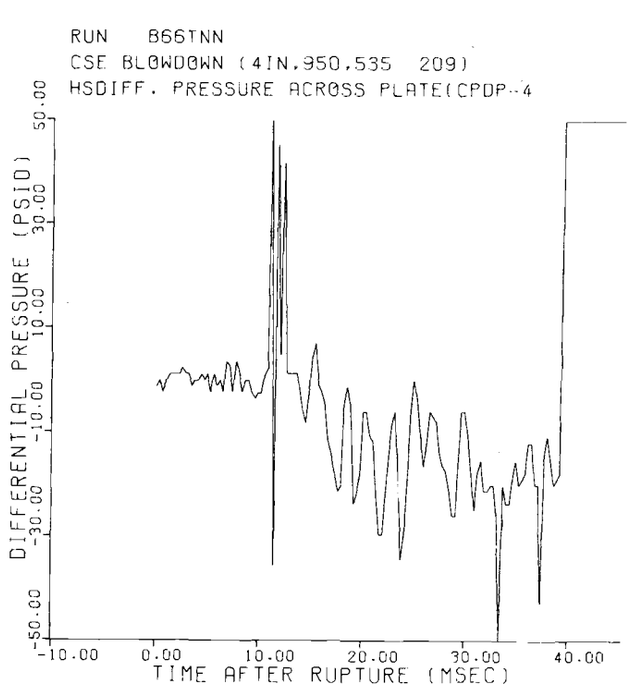
RUN B66TNN
CSE BLOWDOWN (4IN.950,535 209)
HSDIFF. PRESSURE ACROSS PLATE(CPDP-4
DIFFERENTIAL PRESSURE (PSID)
-50.00
-30.00
-10.00
10.00
30.00
50.00
-10.00
0.00
10.00
20.00
30.00
40.00
TIME AFTER RUPTURE (MSEC)

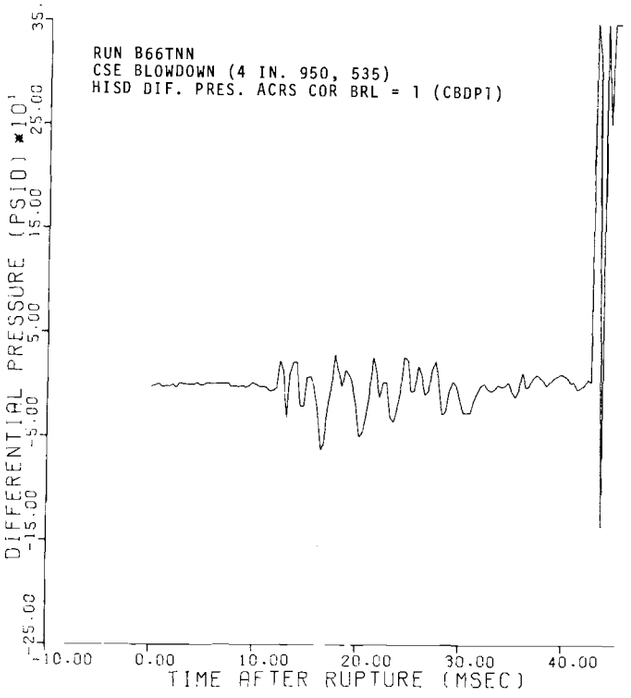
RUN B66TNN
CSE BLOWDOWN (4 IN. 950, 535)
HISD DIF. PRES. ACRS COR BRL = 1 (CBDP1)
DIFFERENTIAL PRESSURE (PSID) ×10¹
-25.00
-15.00
-5.00
5.00
15.00
25.00
35.00
-10.00
0.00
10.00
20.00
30.00
40.00
TIME AFTER RUPTURE (MSEC)

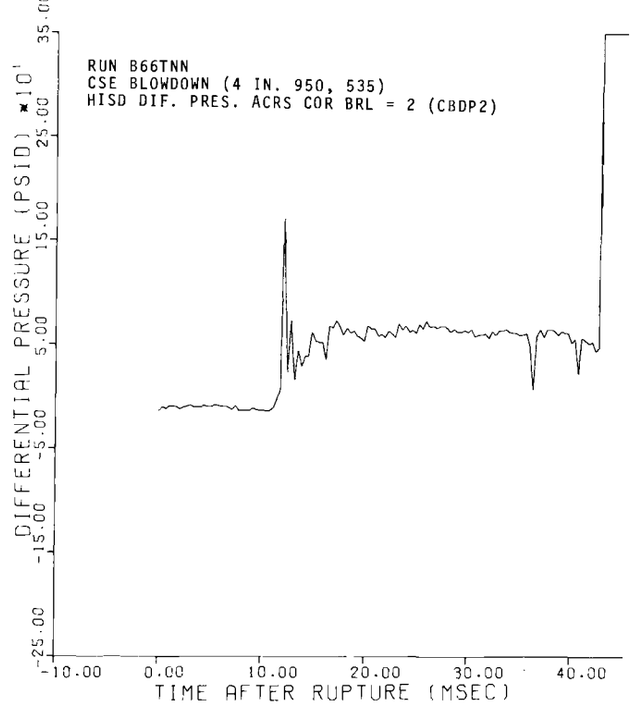
RUN B66TNN
CSE BLOWDOWN (4 IN. 950, 535)
HISD DIF. PRES. ACRS COR BRL = 2 (CBDP2)
DIFFERENTIAL PRESSURE (PSID) ×10¹
-25.00
-15.00
-5.00
5.00
15.00
25.00
35.00
-10.00
0.00
10.00
20.00
30.00
40.00
TIME AFTER RUPTURE (MSEC)

FIGURE B-16.

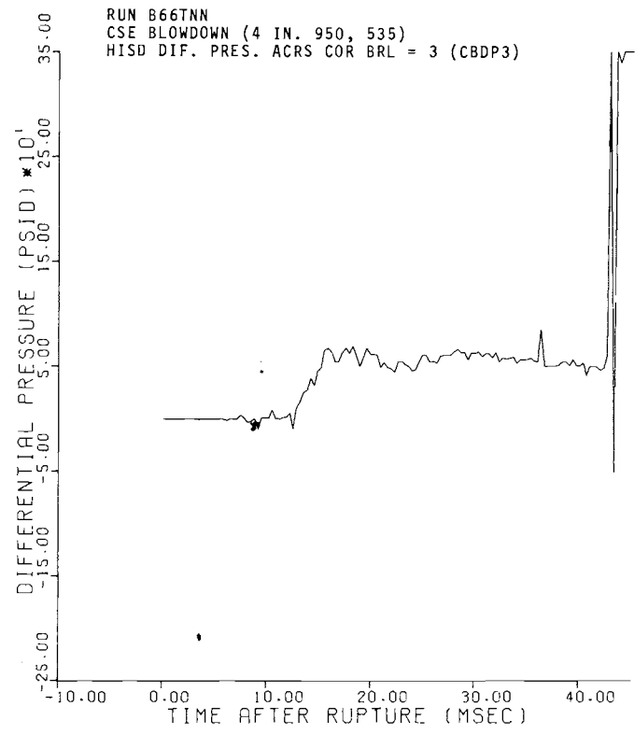
RUN B66TNN
CSE BLOWDOWN (4 IN. 950, 535)
HISD DIF. PRES. ACRS COR BRL = 3 (CBDP3)
DIFFERENTIAL PRESSURE (PSID) *10¹
35.00
25.00
15.00
5.00
-5.00
-15.00
-25.00
-10.00
0.00
10.00
20.00
30.00
40.00
TIME AFTER RUPTURE (MSEC)

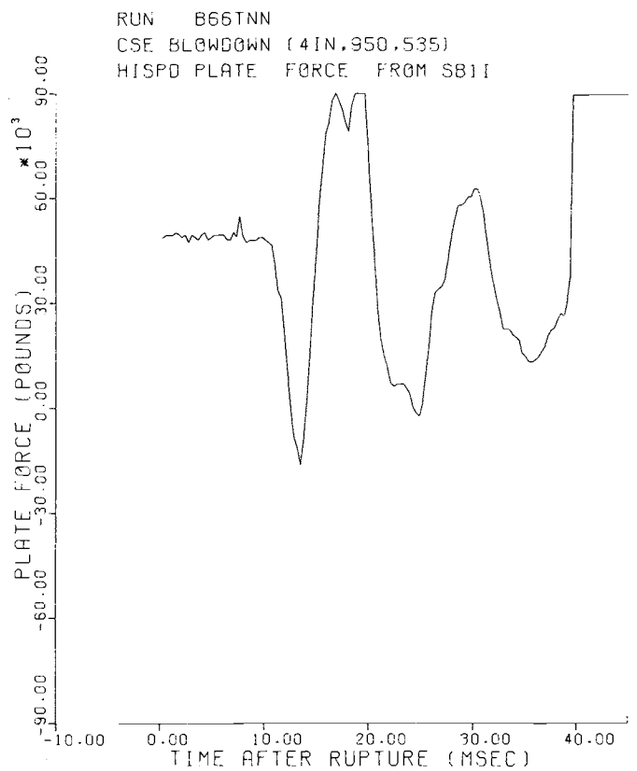
RUN B66TNN
CSE BLOWDOWN (4IN,950,535)
HISPD PLATE FORCE FROM SB11
PLATE FORCE (POUNDS) *10³
90.00
60.00
30.00
0.00
-30.00
-60.00
-90.00
-10.00
0.00
10.00
20.00
30.00
40.00
TIME AFTER RUPTURE (MSEC)

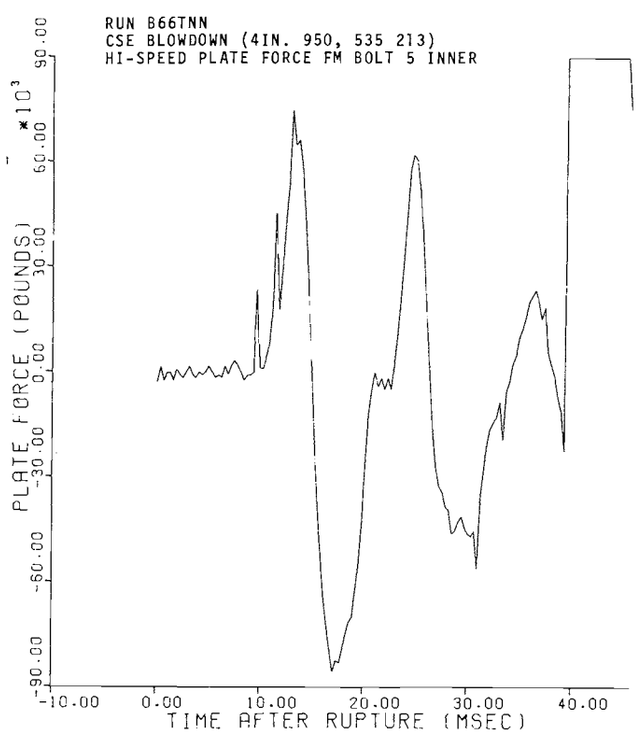
RUN B66TNN
CSE BLOWDOWN (4IN. 950, 535 213)
HI-SPEED PLATE FORCE FM BOLT 5 INNER
PLATE FORCE (POUNDS) *10³
90.00
60.00
30.00
0.00
-30.00
-60.00
-90.00
-10.00
0.00
10.00
20.00
30.00
40.00
TIME AFTER RUPTURE (MSEC)

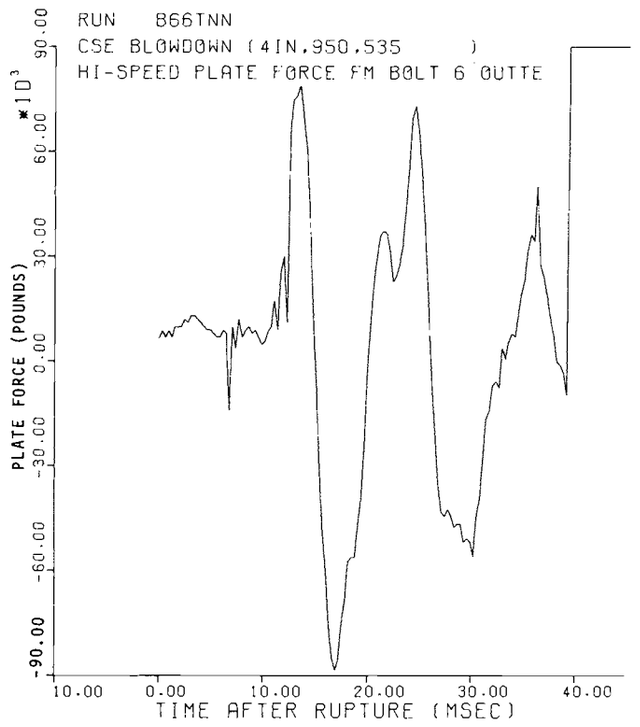
RUN B66TNN
CSE BLOWDOWN (4IN,950,535)
HI-SPEED PLATE FORCE FM BOLT 6 OUTTE
PLATE FORCE (POUNDS) *10³
90.00
60.00
30.00
0.00
-30.00
-60.00
-90.00
10.00
0.00
10.00
20.00
30.00
40.00
TIME AFTER RUPTURE (MSEC)

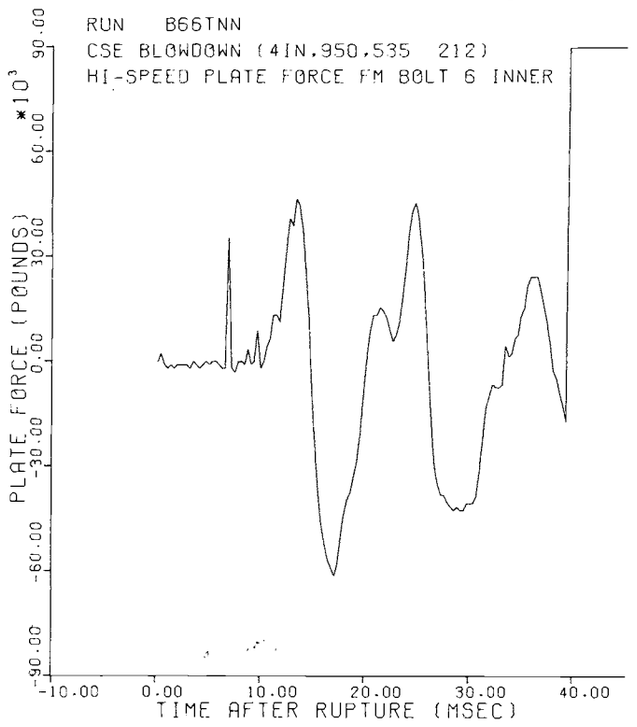
RUN B66TNN
CSE BLOWDOWN (4IN,950,535 212)
HI-SPEED PLATE FORCE FM BOLT 6 INNER
PLATE FORCE (POUNDS) *10³
90.00
60.00
30.00
0.00
-30.00
-60.00
-90.00
-10.00
0.00
10.00
20.00
30.00
40.00
TIME AFTER RUPTURE (MSEC)

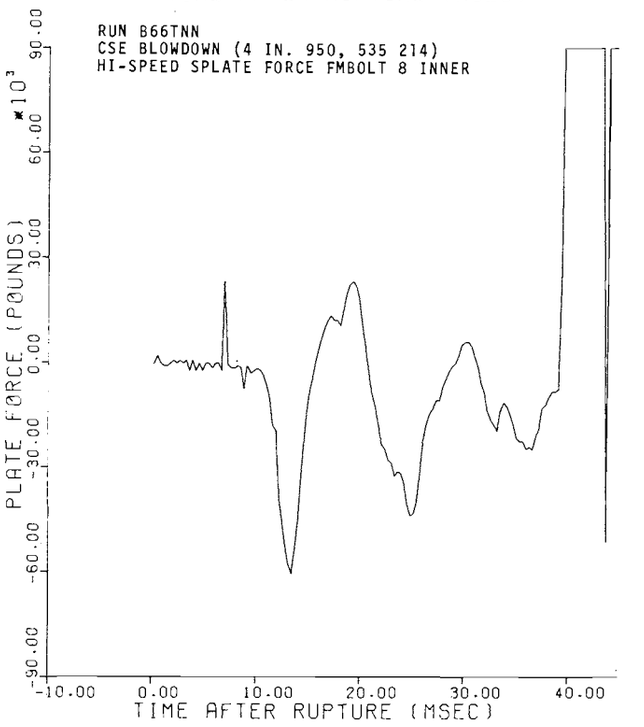
RUN B66TNN
CSE BLOWDOWN (4 IN. 950, 535 214)
HI-SPEED SPLATE FORCE FMBOLT 8 INNER
PLATE FORCE (POUNDS) *10³
90.00
60.00
30.00
0.00
-30.00
-60.00
-90.00
-10.00
0.00
10.00
20.00
30.00
40.00
TIME AFTER RUPTURE (MSEC)

FIGURE B-17.

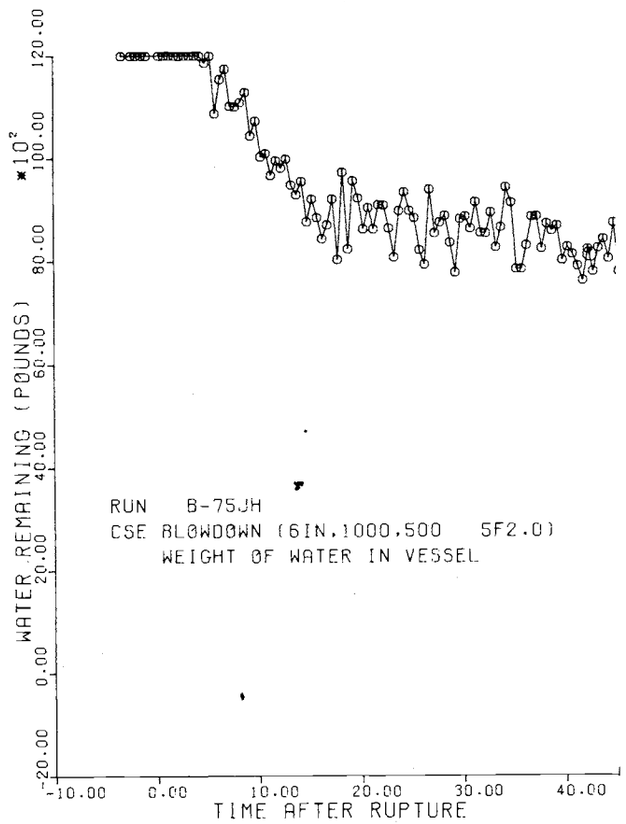
WATER REMAINING (POUNDS)
*10²
120.00
100.00
80.00
60.00
40.00
20.00
0.00
-20.00
-10.00
0.00
10.00
20.00
30.00
40.00
TIME AFTER RUPTURE
RUN B-75JH
CSE BLOWDOWN (6IN,1000,500 5F2.0)
WEIGHT OF WATER IN VESSEL

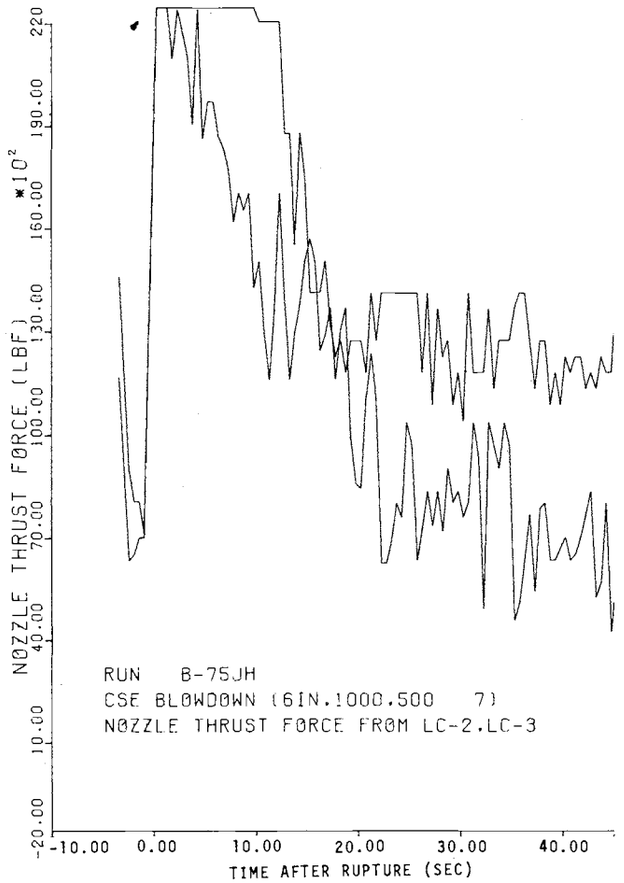
NOZZLE THRUST FORCE (LBF)
*10²
220
190.00
160.00
130.00
100.00
70.00
40.00
10.00
-20.00
-10.00
0.00
10.00
20.00
30.00
40.00
TIME AFTER RUPTURE (SEC)
RUN B-75JH
CSE BLOWDOWN (6IN,1000,500 7)
NOZZLE THRUST FORCE FROM LC-2,LC-3

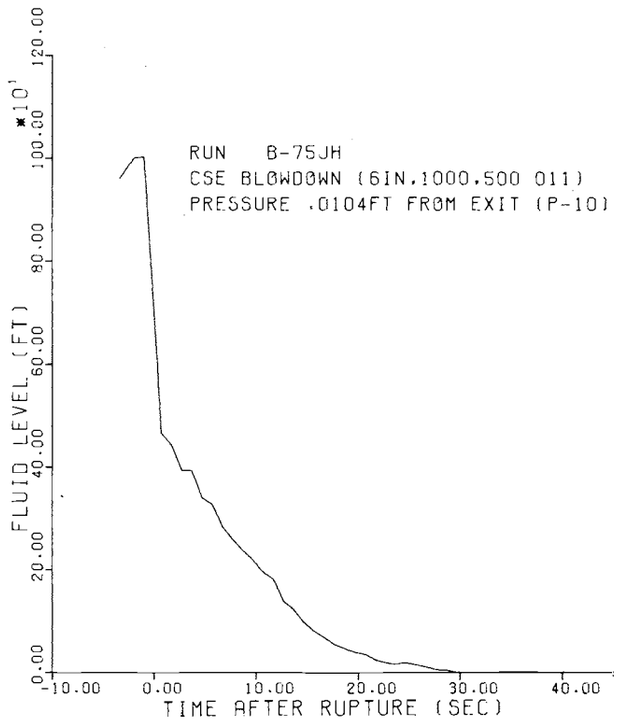
FLUID LEVEL (FT)
*10¹
120.00
100.00
80.00
60.00
40.00
20.00
0.00
-10.00
0.00
10.00
20.00
30.00
40.00
TIME AFTER RUPTURE (SEC)
RUN B-75JH
CSE BLOWDOWN (6IN,1000,500 011)
PRESSURE .0104FT FROM EXIT (P-10)

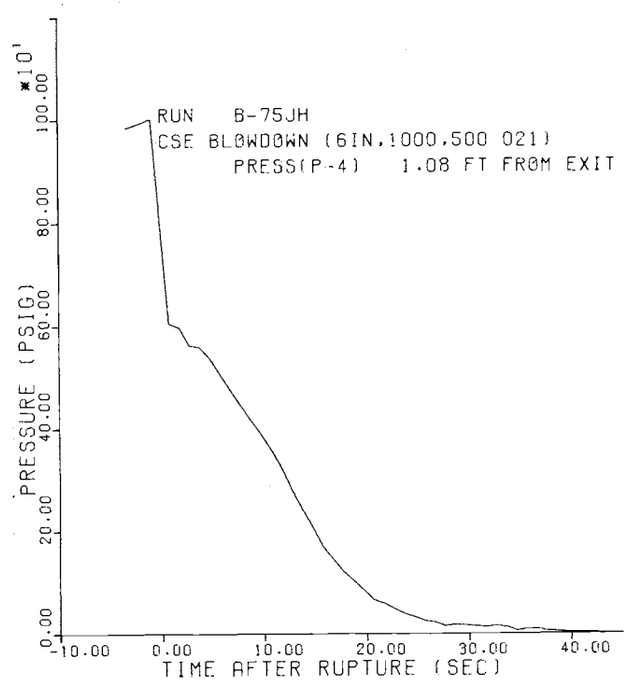
PRESSURE (PSIG)
*10¹
100.00
80.00
60.00
40.00
20.00
0.00
-10.00
0.00
10.00
20.00
30.00
40.00
TIME AFTER RUPTURE (SEC)
RUN B-75JH
CSE BLOWDOWN (6IN,1000,500 021)
PRESS(P-4) 1.08 FT FROM EXIT

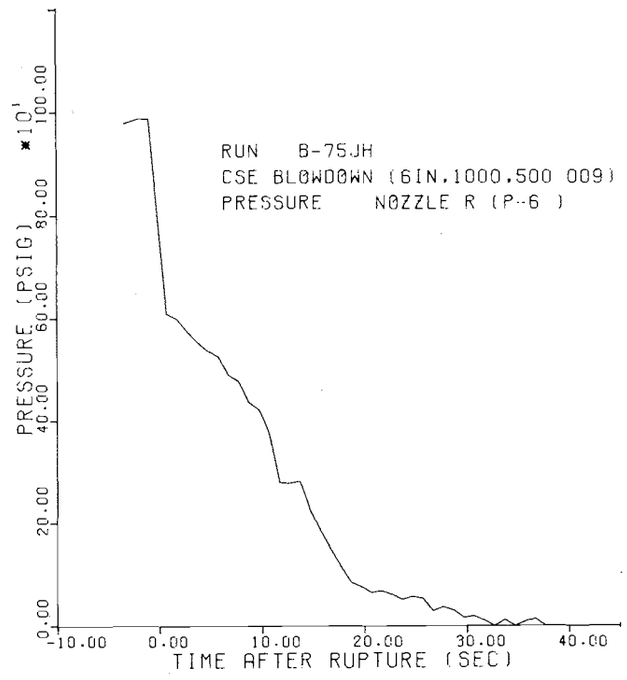
PRESSURE (PSIG)
*10¹
100.00
80.00
60.00
40.00
20.00
0.00
-10.00
0.00
10.00
20.00
30.00
40.00
TIME AFTER RUPTURE (SEC)
RUN B-75JH
CSE BLOWDOWN (6IN,1000,500 009)
PRESSURE NOZZLE R (P-6)

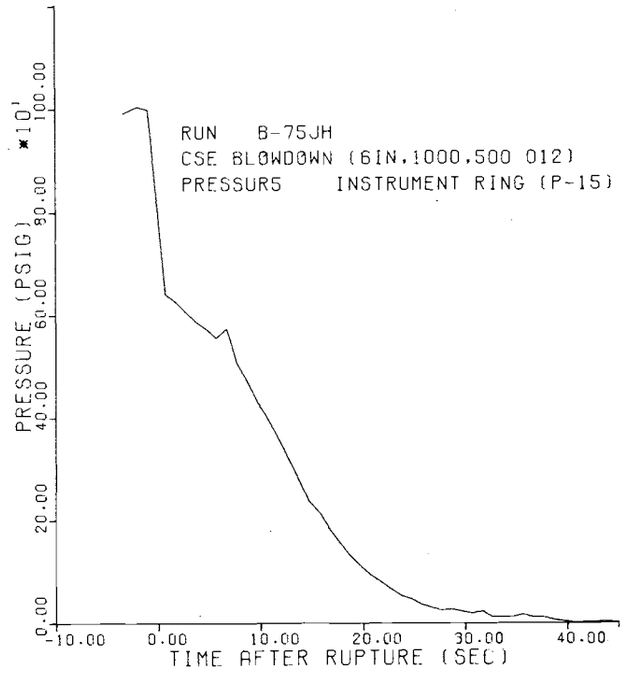
PRESSURE (PSIG)
*10¹
100.00
80.00
60.00
40.00
20.00
0.00
-10.00
0.00
10.00
20.00
30.00
40.00
TIME AFTER RUPTURE (SEC)
RUN B-75JH
CSE BLOWDOWN (6IN,1000,500 012)
PRESSURS INSTRUMENT RING (P-15)

FIGURE B-18.

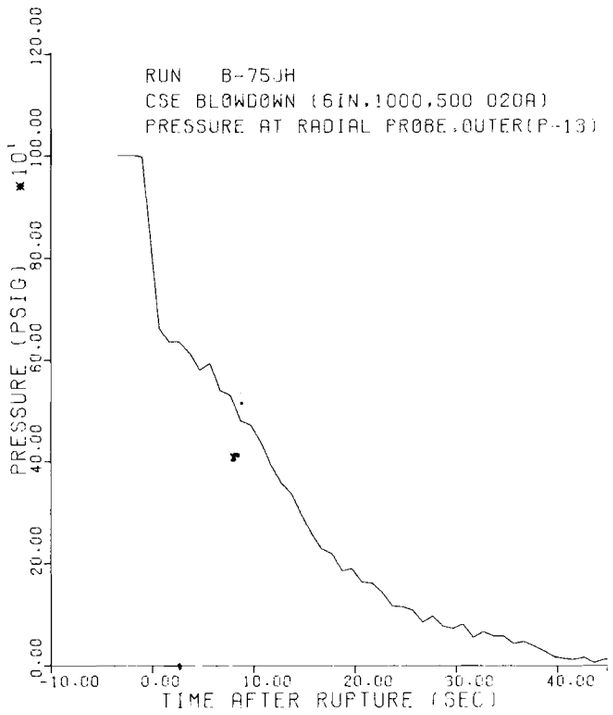
RUN B-75JH
CSE BLOWDOWN (6IN,1000,500 020A)
PRESSURE AT RADIAL PROBE,OUTER(P-13)
PRESSURE (PSIG) *10¹
0.00
20.00
40.00
60.00
80.00
100.00
120.00
-10.00
0.00
10.00
20.00
30.00
40.00
TIME AFTER RUPTURE (SEC)

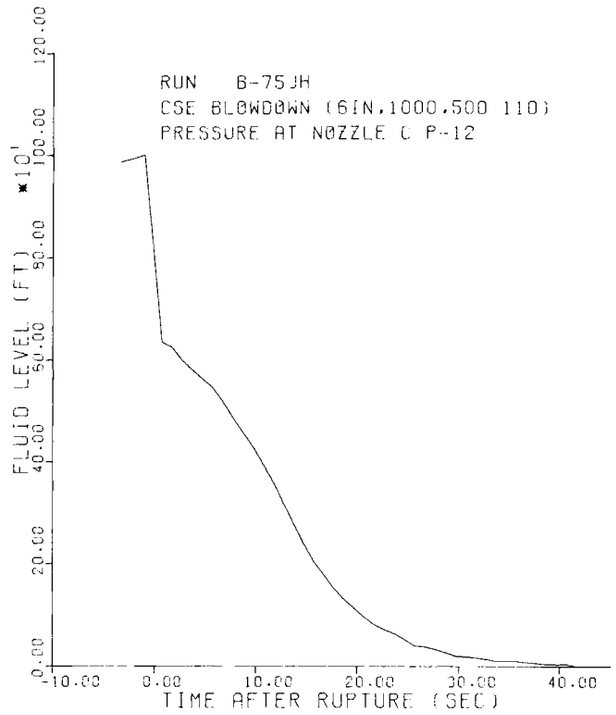
RUN B-75JH
CSE BLOWDOWN (6IN,1000,500 110)
PRESSURE AT NOZZLE C P-12
FLUID LEVEL (FT) *10¹
0.00
20.00
40.00
60.00
80.00
100.00
120.00
-10.00
0.00
10.00
20.00
30.00
40.00
TIME AFTER RUPTURE (SEC)

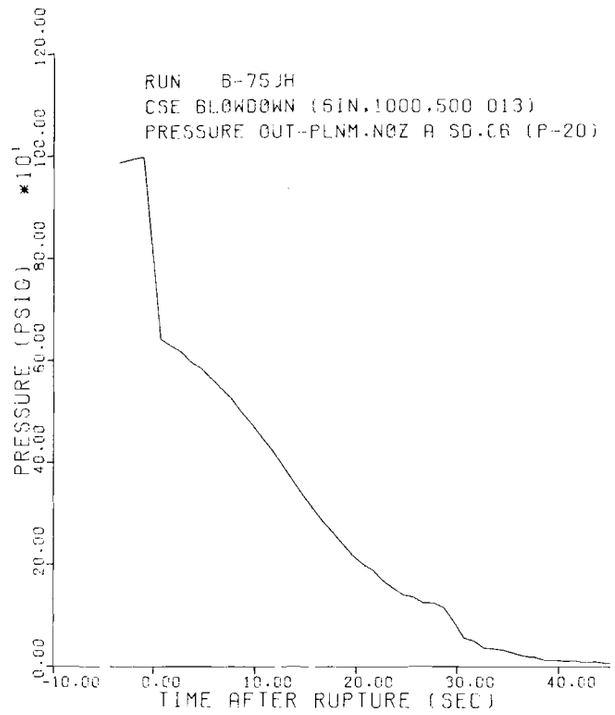
RUN B-75JH
CSE BLOWDOWN (6IN,1000,500 013)
PRESSURE OUT-PLNM,NOZ A SO.C6 (P-20)
PRESSURE (PSIG) *10¹
0.00
20.00
40.00
60.00
80.00
100.00
120.00
-10.00
0.00
10.00
20.00
30.00
40.00
TIME AFTER RUPTURE (SEC)

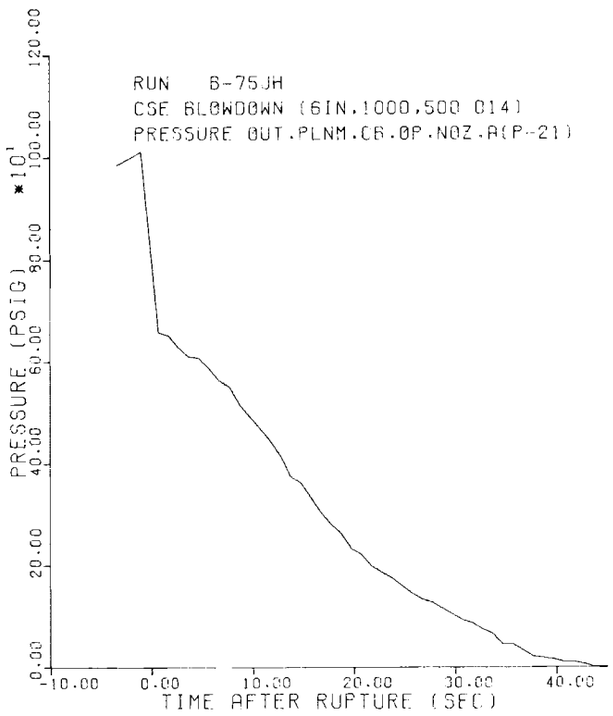
RUN B-75JH
CSE BLOWDOWN (6IN,1000,500 014)
PRESSURE OUT,PLNM,CB,OP,NOZ,A(P-21)
PRESSURE (PSIG) *10¹
0.00
20.00
40.00
60.00
80.00
100.00
120.00
-10.00
0.00
10.00
20.00
30.00
40.00
TIME AFTER RUPTURE (SEC)

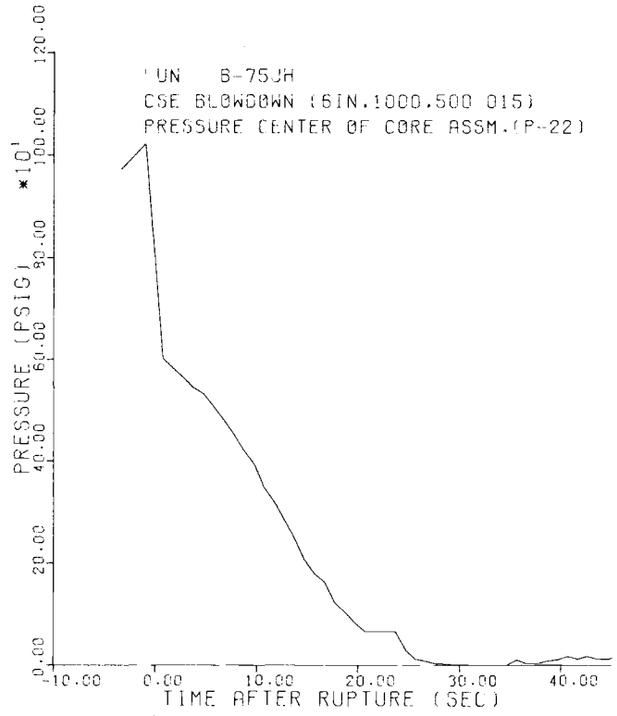
RUN B-75JH
CSE BLOWDOWN (6IN,1000,500 015)
PRESSURE CENTER OF CORE ASSM.(P-22)
PRESSURE (PSIG) *10¹
0.00
20.00
40.00
60.00
80.00
100.00
120.00
-10.00
0.00
10.00
20.00
30.00
40.00
TIME AFTER RUPTURE (SEC)

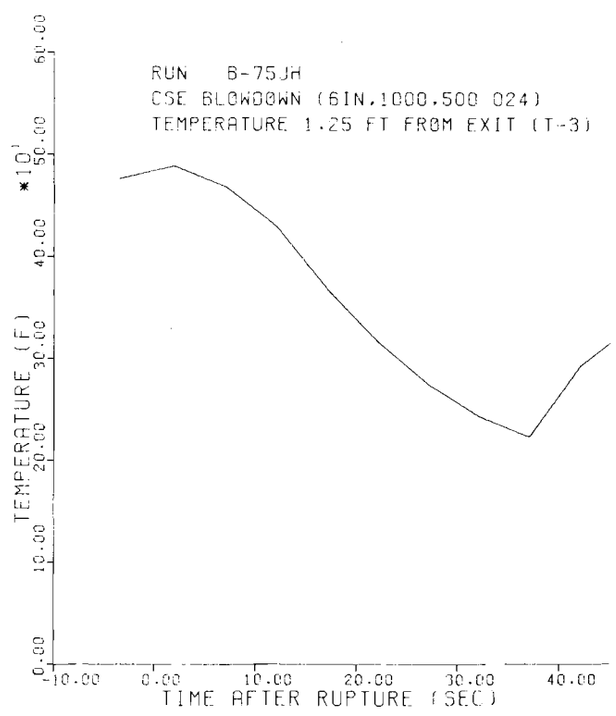
RUN B-75JH
CSE BLOWDOWN (6IN,1000,500 024)
TEMPERATURE 1.25 FT FROM EXIT (T-3)
TEMPERATURE (F) *10¹
0.00
10.00
20.00
30.00
40.00
50.00
60.00
-10.00
0.00
10.00
20.00
30.00
40.00
TIME AFTER RUPTURE (SEC)

FIGURE B-19.

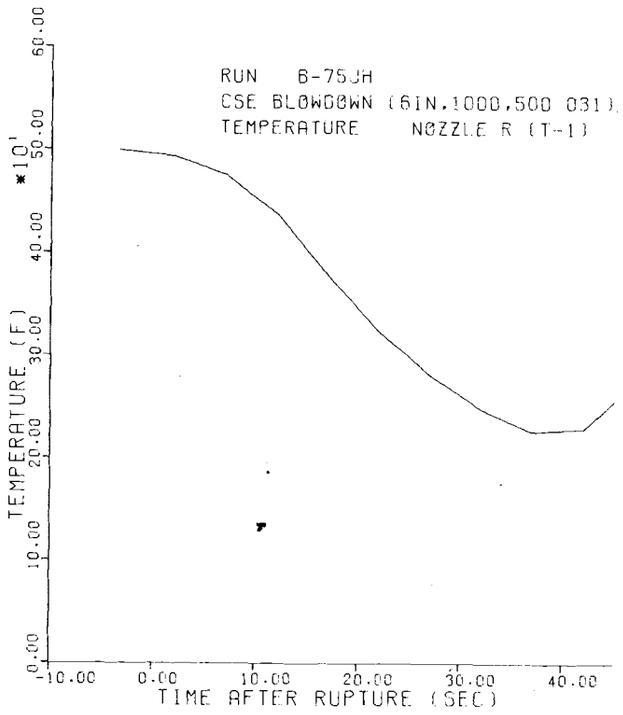
RUN B-75JH
CSE BLOWDOWN (6IN,1000,500 031)
TEMPERATURE NOZZLE R (T-1)
TEMPERATURE (F) *10¹
0.00
10.00
20.00
30.00
40.00
50.00
60.00
-10.00
0.00
10.00
20.00
30.00
40.00
TIME AFTER RUPTURE (SEC)

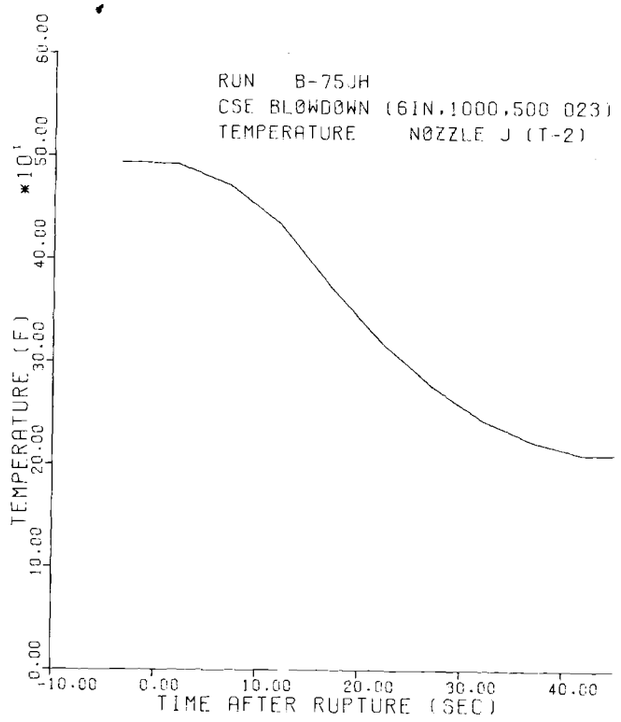
RUN B-75JH
CSE BLOWDOWN (6IN,1000,500 023)
TEMPERATURE NOZZLE J (T-2)
TEMPERATURE (F) *10¹
0.00
10.00
20.00
30.00
40.00
50.00
60.00
-10.00
0.00
10.00
20.00
30.00
40.00
TIME AFTER RUPTURE (SEC)

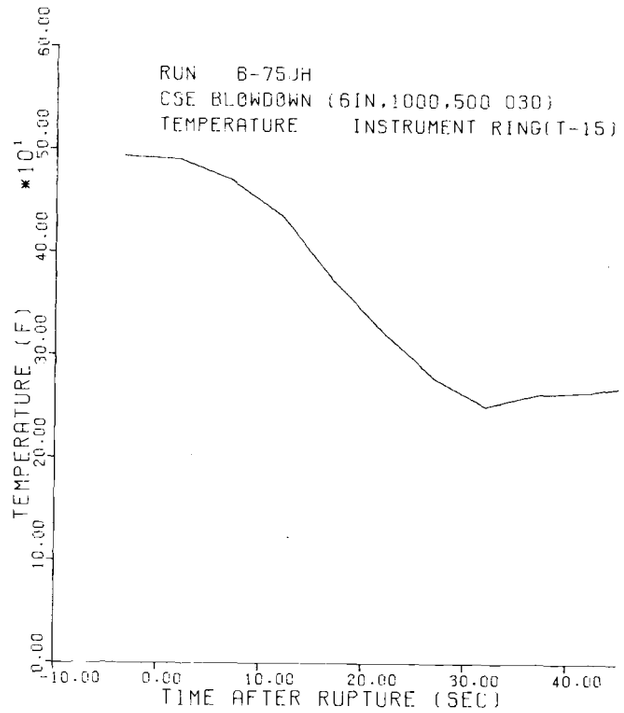
RUN B-75JH
CSE BLOWDOWN (6IN,1000,500 030)
TEMPERATURE INSTRUMENT RING(T-15)
TEMPERATURE (F) *10¹
0.00
10.00
20.00
30.00
40.00
50.00
60.00
-10.00
0.00
10.00
20.00
30.00
40.00
TIME AFTER RUPTURE (SEC)

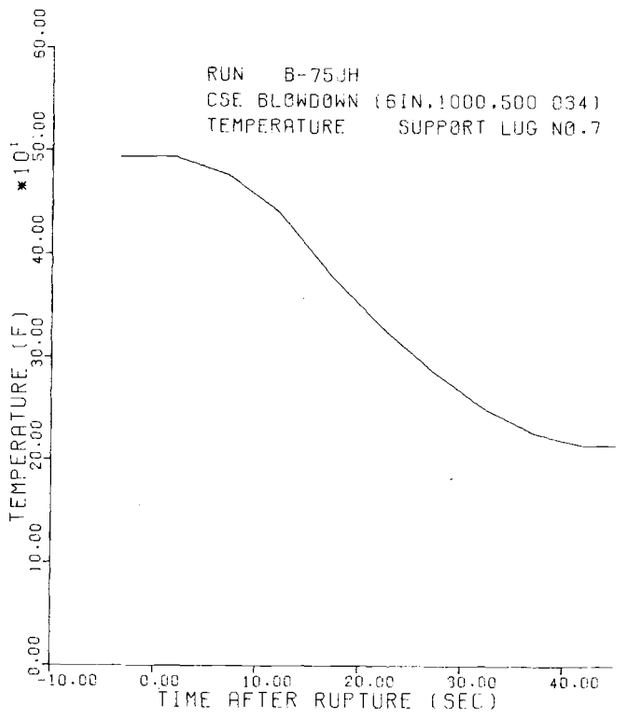
RUN B-75JH
CSE BLOWDOWN (6IN,1000,500 034)
TEMPERATURE SUPPORT LUG NO.7
TEMPERATURE (F) *10¹
0.00
10.00
20.00
30.00
40.00
50.00
60.00
-10.00
0.00
10.00
20.00
30.00
40.00
TIME AFTER RUPTURE (SEC)

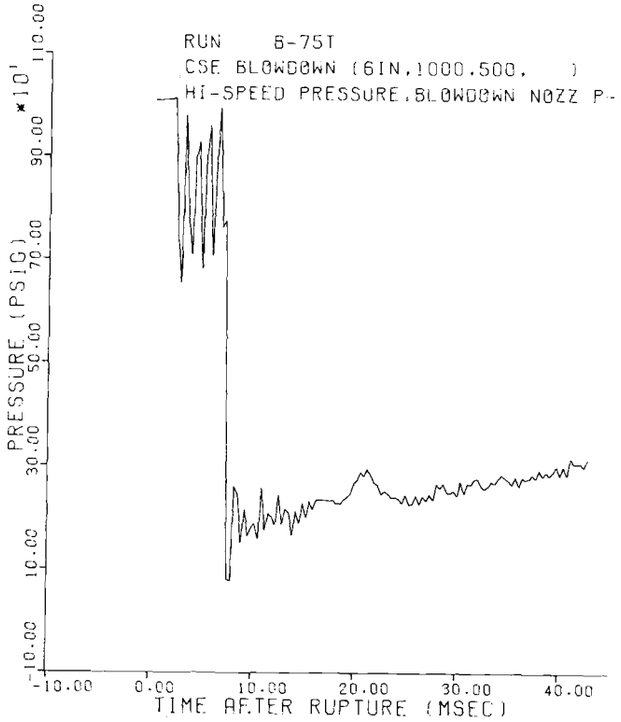
RUN B-75T
CSE BLOWDOWN (6IN,1000,500,)
HI-SPEED PRESSURE,BLOWDOWN NOZZ P-10
PRESSURE (PSIG) *10¹
-10.00
10.00
30.00
50.00
70.00
90.00
110.00
-10.00
0.00
10.00
20.00
30.00
40.00
TIME AFTER RUPTURE (MSEC)

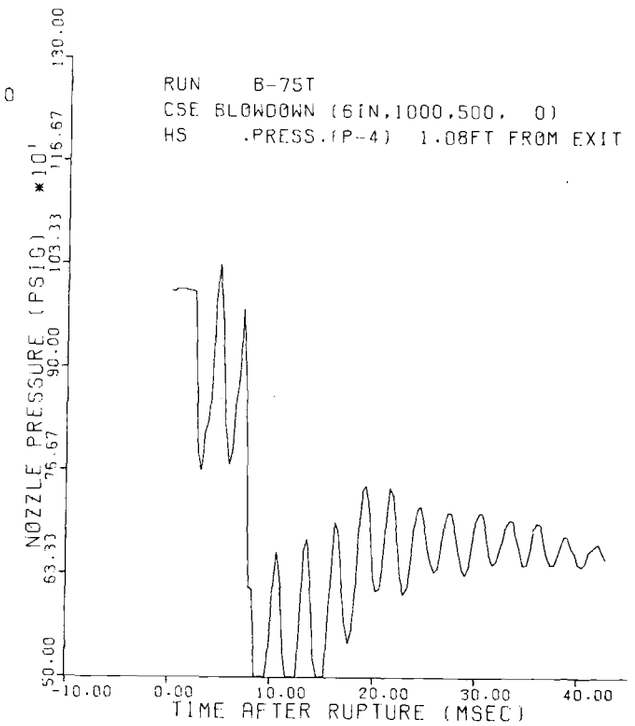
RUN B-75T
CSE BLOWDOWN (6IN,1000,500, 0)
HS .PRESS.(P-4) 1.08FT FROM EXIT
NOZZLE PRESSURE (PSIG) *10¹
50.00
63.33
76.67
90.00
103.33
116.67
130.00
-10.00
0.00
10.00
20.00
30.00
40.00
TIME AFTER RUPTURE (MSEC)

FIGURE B-20.

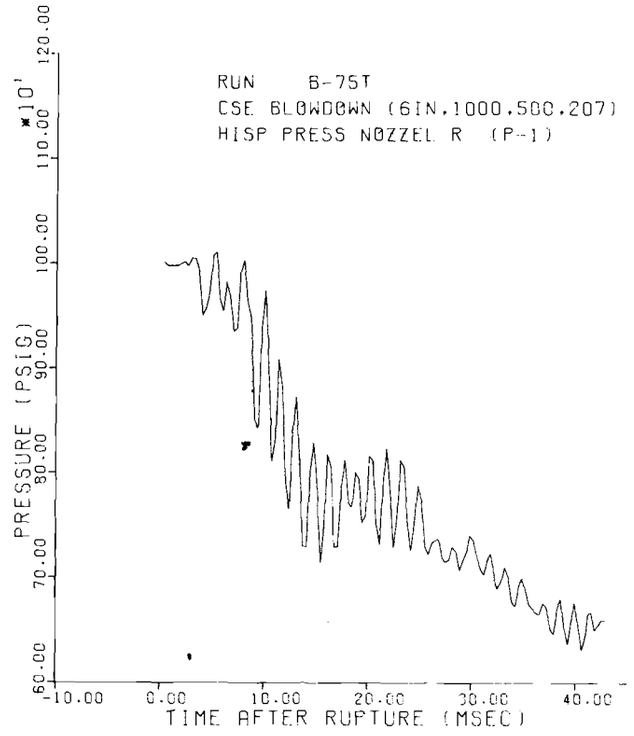
RUN B-75T
CSE BLOWDOWN (6IN,1000,500,207)
HISP PRESS NOZZEL R (P-1)
PRESSURE (PSIG) *10'
TIME AFTER RUPTURE (MSEC)

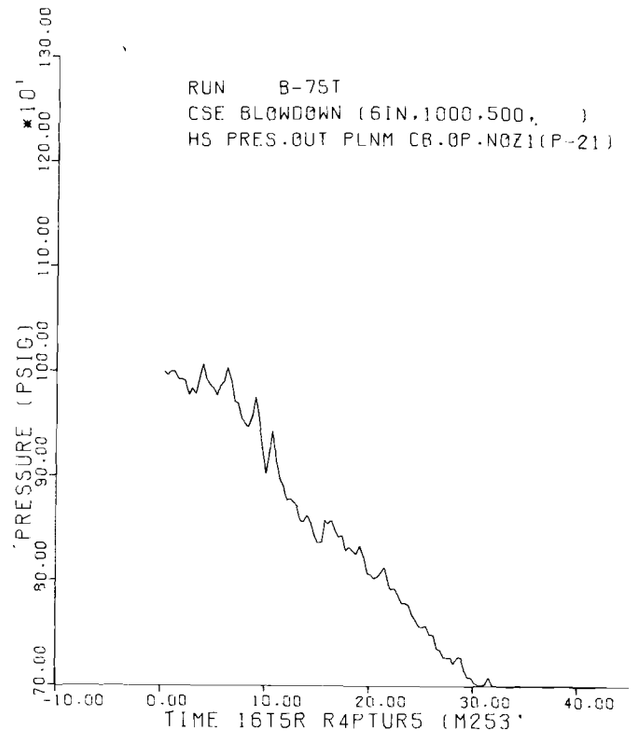
RUN B-75T
CSE BLOWDOWN (6IN,1000,500,)
HS PRES.OUT PLNM CB.OP.NOZ1(P-21)
PRESSURE (PSIG) *10'
TIME AFTER RUPTURE (MSEC)

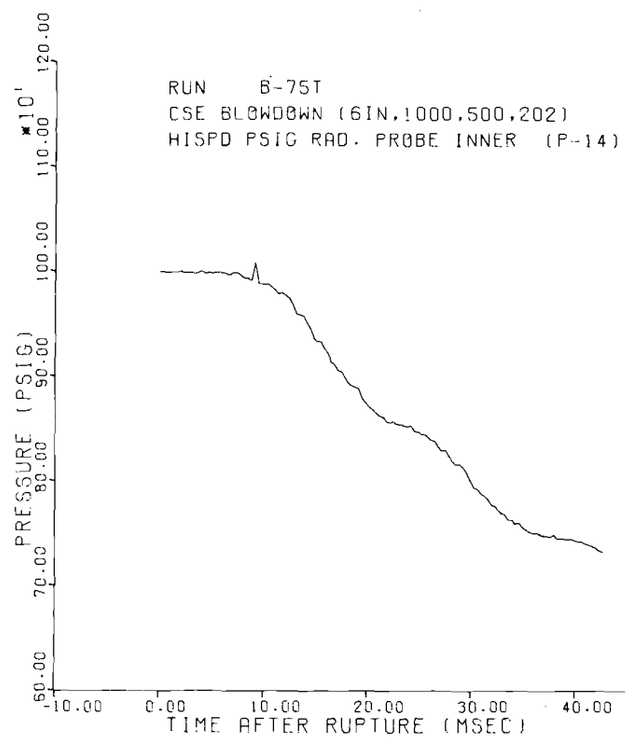
RUN B-75T
CSE BLOWDOWN (6IN,1000,500,202)
HISPD PSIG RAD. PROBE INNER (P-14)
PRESSURE (PSIG) *10'
TIME AFTER RUPTURE (MSEC)

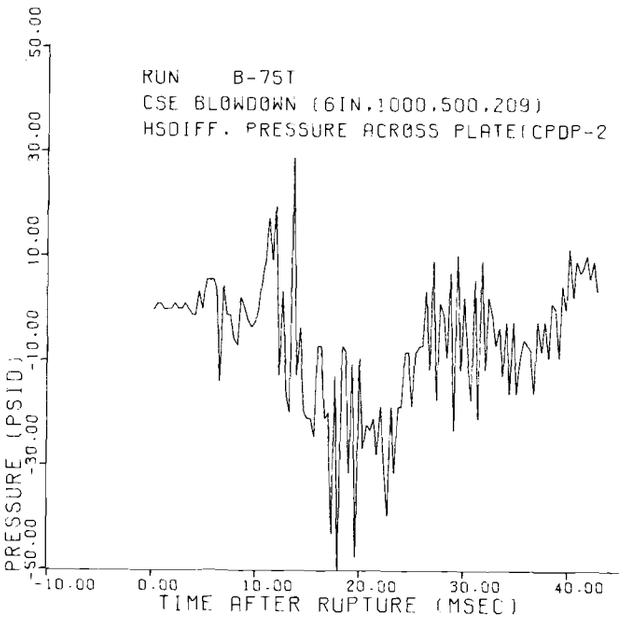
RUN B-75T
CSE BLOWDOWN (6IN,1000,500,209)
HSDIFF. PRESSURE ACROSS PLATE(CPDP-2
PRESSURE (PSID)
TIME AFTER RUPTURE (MSEC)

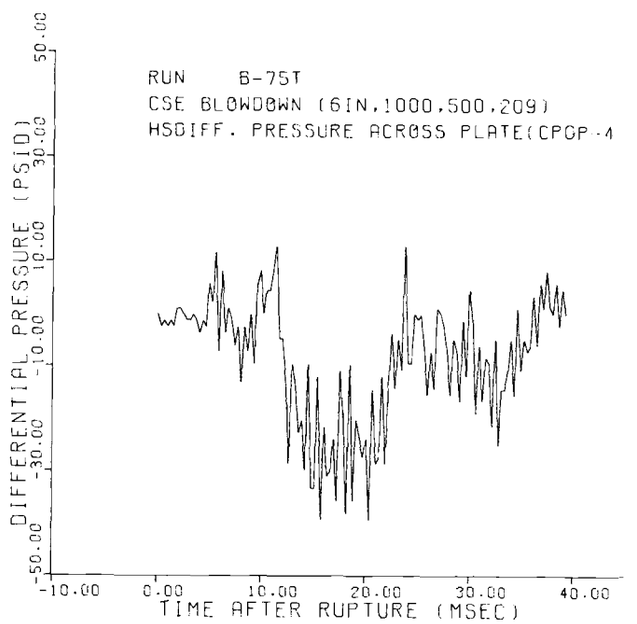
RUN B-75T
CSE BLOWDOWN (6IN,1000,500,209)
HSDIFF. PRESSURE ACROSS PLATE(CPDP-1
DIFFERENTIAL PRESSURE (PSID)
TIME AFTER RUPTURE (MSEC)

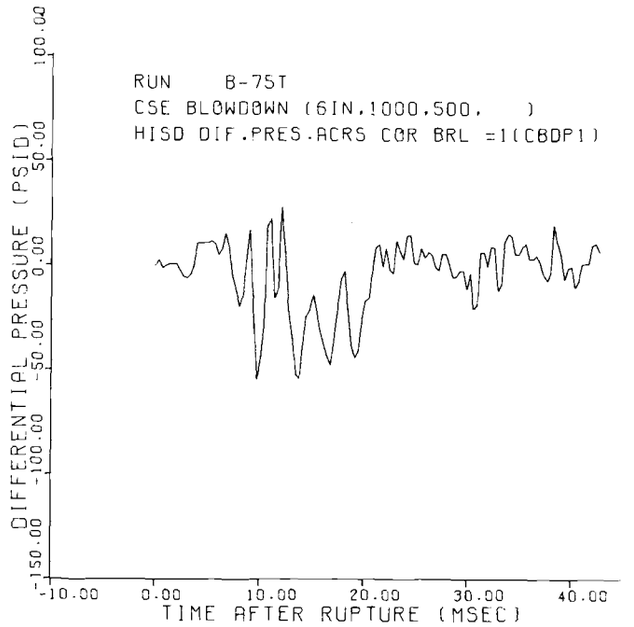
RUN B-75T
CSE BLOWDOWN (6IN,1000,500,)
HISD DIF.PRES.ACRS COR BRL =1(CBDP1)
DIFFERENTIAL PRESSURE (PSID)
TIME AFTER RUPTURE (MSEC)

FIGURE B-21.

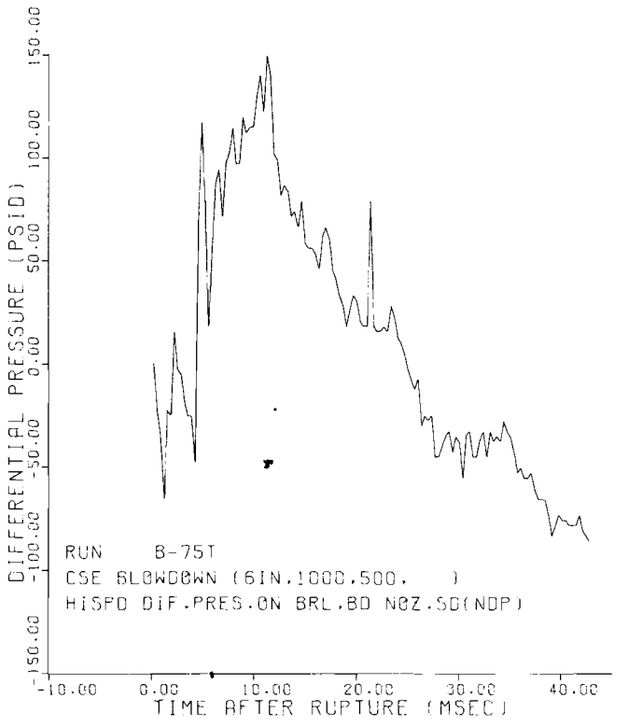
RUN B-75T
CSE BLOWDOWN (6IN,1000,500,)
HiSPD DiF.PRES.ON BRL.BD NOZ.SD(NDP)
DIFFERENTIAL PRESSURE (PSID)
TIME AFTER RUPTURE (MSEC)

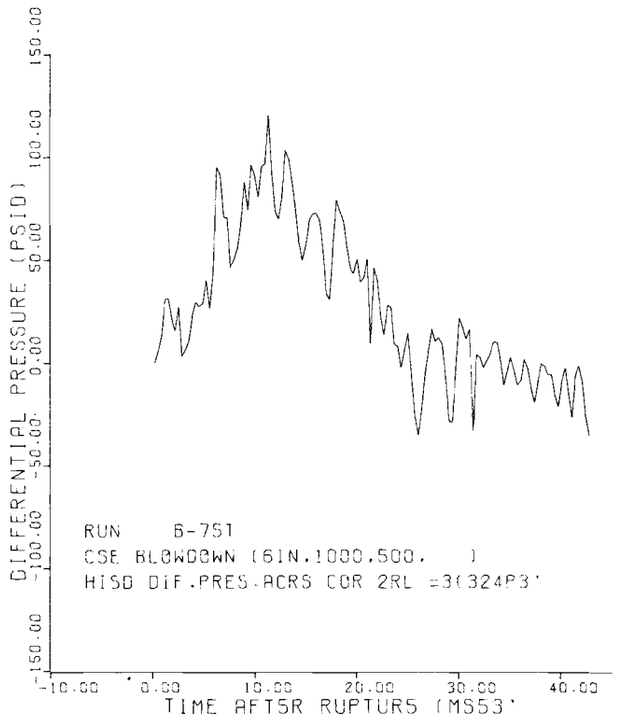
RUN B-75T
CSE BLOWDOWN (6IN,1000,500,)
HiSD DiF.PRES-ACRS COR 2RL =3(324P3'
DIFFERENTIAL PRESSURE (PSID)
TIME AFTER RUPTURE (MSEC)

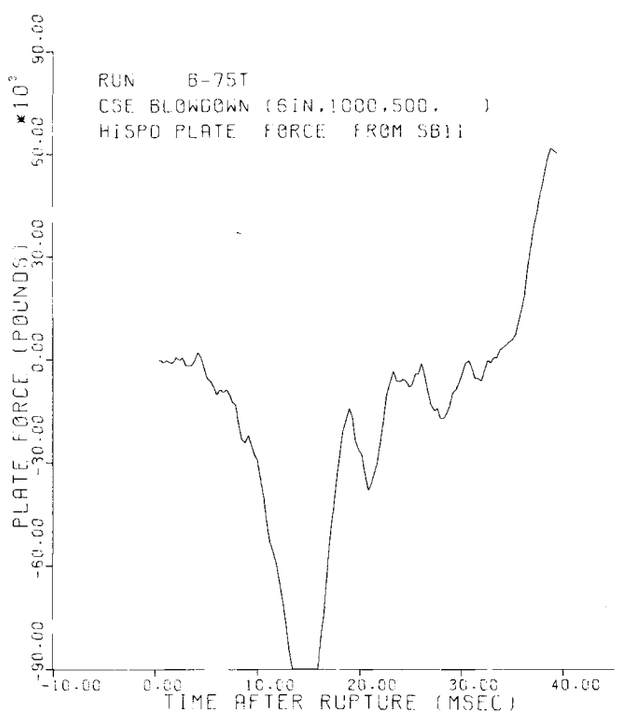
RUN B-75T
CSE BLOWDOWN (6IN,1000,500,)
HiSPD PLATE FORCE FROM SB11
PLATE FORCE (POUNDS)
TIME AFTER RUPTURE (MSEC)

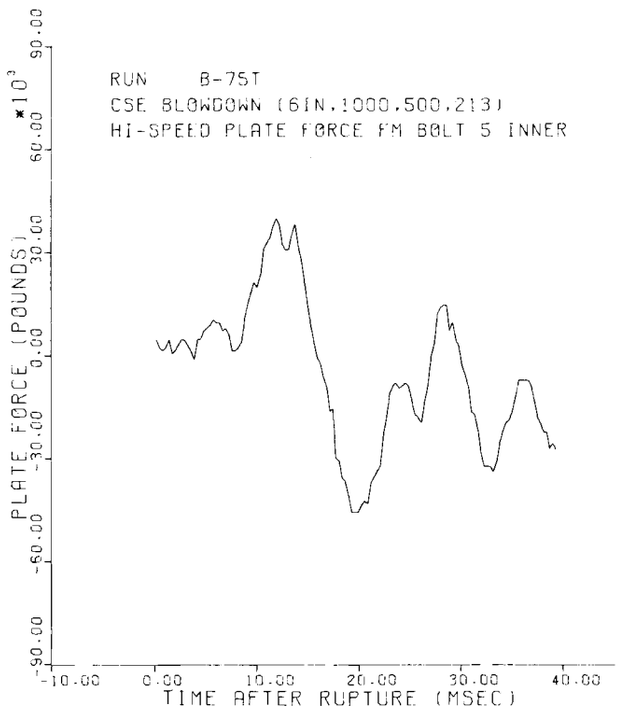
RUN B-75T
CSE BLOWDOWN (6IN,1000,500,213)
HI-SPEED PLATE FORCE FM BOLT 5 INNER
PLATE FORCE (POUNDS)
TIME AFTER RUPTURE (MSEC)

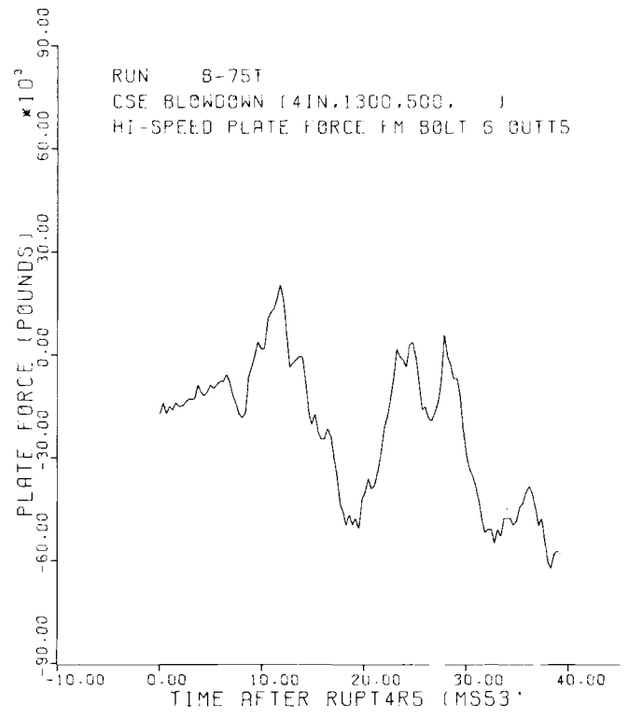
RUN B-75T
CSE BLOWDOWN (4IN,1300,500,)
HI-SPEED PLATE FORCE FM BOLT 6 OUTS
PLATE FORCE (POUNDS)
TIME AFTER RUPTURE (MSEC)

FIGURE B-22.

DISTRIBUTION

No. of Copies

OFFSITE

1 AEC Chicago Operations Office

D. M. Gardiner

1 AEC Chicago Patent Group

G. H. Lee

2 AEC Division of Naval Reactors

R. S. Brodsky

25 AEC Division of Reactor Development and Technology

Assistant Director, Project Management
Chief, Water Projects Branch
Chief, Gas Cooled Projects Branch (2)
Chief, Liquid Metal Projects Branch
Assistant Director, Reactor Technology
Assistant Director, Plant Engineering
Assistant Director, Reactor Engineering
Assistant Director, Nuclear Safety (5)
Chief, Research and Development Branch
H. L. Hamester
R. R. Newton (5)
Environmental and Sanitary Engineering Branch
I. C. Roberts
Assistant Director, Engineering Standards
Assistant Director, Program Analysis
Assistant Director, Army Reactors

16 AEC Division of Reactor Standards

M. Bolotsky
G. Burley
E. G. Case (10)
A. B. Holt
R. Impara
P. Norien
R. Waterfield

215 AEC Division of Technical Information Extension

No. of Copies

5 AEC Library, Washington

Advisory Committee on Reactor Safeguards
F. R. Fraley

Division of Compliance
L. Kornblith, Jr.
J. W. Flora, Region IV

Division of Operational Safety
H. Gilbert

Division of Production
G. B. Pleat

1 AEG - Telefunken
E-213
6 Frankfort/Main 70
AEG - Hochhaus Süd
Germany

Dieter Ewers

1 Aerojet-General Corporation
Idaho Falls, Idaho

W. E. Nyer

1 Aerojet-General Corporation, Sacramento

F. L. Climent

1 American Electric Power Company
2 Broadway
New York, N.Y. 10004

Stephen J. Milioti

10 Argonne National Laboratory

C. E. Dickerman
S. Fistedis
R. O. Ivins
P. Lottes
H. O. Monson
D. Okrent
R. C. Vogel
P. G. Shewmon

LMFBR Program Office

A. Amorosi
L. Baker

No. of Copies

2 Atomics International
H. Morewitz

Liquid Metals Engr. Center
R. W. Dickinson

1 Auburn University
School of Engineering and Engineering Experiment Station
G. H. Nix

4 Babcock & Wilcox Company
Virginia
S. Delicate
D. A. Nitti
R. Wascher
L. R. Weissert - Washington
161 E 42nd Street
New York, New York 10017

6 Battelle Memorial Institute
A. R. Duffy
D. L. Morrison/D. L. Ritzman
S. Paprocki (2)
D. N. Sunderman (2)

1 Battelle Memorial Institute
Frankfurt, Germany
G. Leistner/K. J. Kober

2 Bechtel Corporation
50 Beale Street
San Francisco, California 94119
R. F. Griffin
W. P. Neuendorf

1 Bettis Atomic Power Laboratory
P. O. Box 79
West Mifflin, Pa. 15122
Dr. J. A. Redfield

2 Brookhaven National Laboratory
A. W. Castleman
J. M. Hendri

1 Canoga Park Area Office
R. L. Morgan

No. of Copies	
1	Chalk River Nuclear Laboratories Chalk River, Ontario, Canada Station 3 G. Hake
1	Combustion Engineering M. F. Valerino
1	Consolidated Edison Company 4 Irving Place New York, New York 10003
1	du Pont Company, Aiken (AEC) A. H. Peters
1	du Pont Company, Wilmington (AEC) F. P. Allen for Lombard Squires
1	H. Etherington 84 Lighthouse Drive Jupiter, Florida 33458
1	W. L. Faith 2540 Huntington Drive San Marino, California 91108
3	General Atomic Division (AEC) A. J. Goodjohn (2) R. H. Ball
1	General Electric Company 621 S. W. Alder Street Portland, Oregon 97223 J. E. Grund
8	General Electric Company 175 Curtner Ave. San Jose, California 95125 Fred Moody S. Vandenberg G. E. Wade E. Zebroski P. Bray M. Siegler W. A. Sutherland D. A. Rockwell

No. of Copies	
1	General Electric Company, Cincinnati (AEC) J. F. White
9	Idaho Nuclear Corporation G. O. Bright G. F. Brockett J. A. Buckham S. Forbes (2) C. Haire G. B. Matheny C. M. Slansky N. K. Sowards
2	Idaho Operations Office (AEC) D. Williams
2	IIT Research Institute E. V. Gallagher T. A. Zaker
1	Institute für Reactorsicherheit 5 Köln, Lukasstrasse Germany Heinz G. Seipel
1	Japan Atomic Energy Research Institute Tokai Laboratory, Tokai Ibaragi, Japan Masayoshi Shiba
2	Los Alamos Scientific Laboratory J. H. Russel W. R. Stratton
1	H. G. Mangelsdorf 78 Knollwood Road Short Hills, New Jersey 07078

No. of Copies	
1	MPR Associates, Inc. T. Rockwell, III
1	National Bureau of Standards Gaithersburg, Maryland 20760 C. Muehlhause
1	Naval Ordnance Laboratory J. Proctor
1	North American Carbon, Inc. P. O. Box 19737 Columbus, Ohio 43219 J. Louis Kovach
1	North Carolina State University Raleigh, North Carolina 27607 M. N. Ozisik
1	Nuclear Fuels Service R. P. Wischow
14	Oak Ridge National Laboratory R. E. Adams R. Blanco J. Buchanan W. B. Cottrell (4) D. Ferguson C. E. Miller G. W. Parker L. F. Parsley P. Rittenhouse D. B. Trauger (2)
4	Oak Ridge Operations Office (AEC) D. Cope (2) E. Delaney W. L. Smalley
1	A. A. L*Kelly 2421 West Rowland Avenue Littleton, Colorado 80120

No. of Copies

1 Ontario Water Resources Commission
Water Quality Surveys Branch
Division of Sanitary Engineering
135 St. Clair Avenue West
Toronto 7, Ontario, Canada

W. A. Steggles

1 Oregon State University
Assistant Dean of Engineering
Oregon State University
Corvallis, Oregon 97331

James G. Knudsen

1 The Pennsylvania State University
College of Engineering
101 Hammond Building
University Park, Pennsylvania

N. J. Palladino

2 San Francisco Operations Office
Atomic Energy Commission

Lt. Col. J. B. Radcliffe
C. F. Backlund

1 Sargent & Lundy
Engineers
140 South Dearborn Street
Chicago, Illinois 60603

O. A. Hrynewych

2 Southern Nuclear Engineering, Inc.
P. O. Box 10
Dunedin, Florida 35528

G. Brown
K. E. Roach

1 Stone and Webster Engineering Corp., Boston
255 Franklin
Boston, Massachusetts 02176

L. P. Deackoff

2 TRW Incorporated
TRW Systems Group

D. B. Langmuir
S. M. Zivi

No. of Copies

1 United Engineers & Constructors, Inc.
1401 Arch Street
Philadelphia, Pennsylvania 19105

A. T. Molin

1 United Kingdom Atomic Energy Authority
Authority Health and Safety Branch
Risely Warrington, Lancs
England

A. R. Edwards

2 University of California, Berkeley
Institute of Engineering Research

H. A. Johnson
V. E. Schrock

1 University of Houston
Cullen Boulevard
Houston, Texas 77004

C. W. Zabel, Dir. of Research

1 University of Illinois
Department of Civil Engineering
3129 Civil Engineering Building
Urbana, Illinois 61801

C. P. Siess

1 University of Minnesota
Department of Chemical Engineering
Minneapolis, Minnesota 55455

H. S. Isbin

1 University of Tennessee
606 Dougherty Hall
Knoxville, Tennessee 37916

S. H. Hanauer

1 University of Tokyo
Mechanical Engineering Section
Tokyo, Bunkyo-Ku,
Tokyo, Japan

Prof. Hidao, Uchida

No. of Copies

2 University of Washington

Prof. Wells Moulton
Prof. K. L. Garlid

1 USAEC Scientific Representative
c/o Atomic Energy of Canada, Ltd.
Chalk River, Ontario, Canada

H. J. Reynolds

9 Westinghouse Electric Corporation (AEC)
(APD)

E. Beckjord
S. Fabic
D. Fletcher
H. Graves
F. M. Heck
A. S. Neuls
W. D. Townend
R. A. Wiesemann

(HTD)

A. Lohmeier

1 Yankee Atomic Electric Company
441 Stuart St.
Boston, Massachusetts

John DeVincentis

ONSITE-HANFORD

1 AEC Chicago Patent Group

R. K. Sharp (Richland)

2 RDT Assistant Director for Pacific Northwest Programs

3 AEC Richland Operations Office

A. Brunstad
W. E. Lotz
M. R. Schneller

2 Atlantic Richfield Hanford Company

G. R. Kiel
ARCHO Files

No. of Copies

9 Douglas United Nuclear

J. E. Mecca
N. R. Miller
W. F. Nechodom
R. W. Reid
J. W. Riches
D. L. Renberger
J. R. Spink
R. H. Shoemaker
DUN Files

1 Vitro/HES

A. J. McElfresh

14 WADCO Corporation

J. J. Cadwell
T. T. Claudson
R. L. Junkins
R. D. Leggett
D. P. O'Keefe
H. N. Pederson
G. J. Rogers
D. E. Simpson
J. C. Spanner
N. P. Wilburn (2)
M. E. Witherspoon
J. A. Williams
WADCO Document Control

No. of Copies

51 Battelle-Northwest

F. W. Albaugh
R. T. Allemann (10)
J. M. Batch
S. H. Bush
L. A. Carter
D. L. Condotta
G. J. Dau
F. G. Dawson
R. F. Foster
J. C. Fox
J. J. Fuquay
W. A. Haney
H. Harty
M. M. Hendrickson
J. F. Honstead
P. A. Hutton
R. T. Jaske
B. M. Johnson (2)
H. V. Larson
J. M. Nielson
R. E. Nightingale
D. W. Pearce
L. T. Pedersen
A. M. Platt
D. L. Reid
R. L. Richardson
W. D. Richmond
L. C. Schwendiman
A. M. Sutey
E. E. Voiland
R. G. Wheeler
N. G. Wittenbrock
F. R. Zaloudek
Technical Information Files (5)
Technical Publications (3)